

**Catabolism of Amino Acids by *Fusobacterium* Species**

by

Mohammad Ramezani  
Pharm.D., Mashhad, Iran, 1987

submitted in partial fulfillment of the requirements for  
the degree of Doctor of Philosophy

at

Dalhousie University,  
Halifax, Nova Scotia  
July, 1996

© Copyright by Mohammad Ramezani, 1996



National Library  
of Canada

Acquisitions and  
Bibliographic Services Branch

395 Wellington Street  
Ottawa, Ontario  
K1A 0N4

Bibliothèque nationale  
du Canada

Direction des acquisitions et  
des services bibliographiques

395, rue Wellington  
Ottawa (Ontario)  
K1A 0N4

*Your file* *Votre référence*

*Our file* *Notre référence*

**The author has granted an irrevocable non-exclusive licence allowing the National Library of Canada to reproduce, loan, distribute or sell copies of his/her thesis by any means and in any form or format, making this thesis available to interested persons.**

**L'auteur a accordé une licence irrévocable et non exclusive permettant à la Bibliothèque nationale du Canada de reproduire, prêter, distribuer ou vendre des copies de sa thèse de quelque manière et sous quelque forme que ce soit pour mettre des exemplaires de cette thèse à la disposition des personnes intéressées.**

**The author retains ownership of the copyright in his/her thesis. Neither the thesis nor substantial extracts from it may be printed or otherwise reproduced without his/her permission.**

**L'auteur conserve la propriété du droit d'auteur qui protège sa thèse. Ni la thèse ni des extraits substantiels de celle-ci ne doivent être imprimés ou autrement reproduits sans son autorisation.**

ISBN 0-612-15901-9

**Canada**

Name Mohammad Ramezani

Dissertation Abstracts International is arranged by broad, general subject categories. Please select the one subject which most nearly describes the content of your dissertation. Enter the corresponding four-digit code in the spaces provided.

CHEMISTRY  
SUBJECT TERM

1490 U.M.I.  
SUBJECT CODE

**Subject Categories**

**THE HUMANITIES AND SOCIAL SCIENCES**

**COMMUNICATIONS AND THE ARTS**

Architecture ..... 0729  
Art History ..... 0377  
Cinema ..... 0900  
Dance ..... 0378  
Fine Arts ..... 0357  
Information Science ..... 0723  
Journalism ..... 0391  
Library Science ..... 0399  
Mass Communications ..... 0708  
Music ..... 0413  
Speech Communication ..... 0459  
Theater ..... 0465

**EDUCATION**

General ..... 0515  
Administration ..... 0514  
Adult and Continuing ..... 0516  
Agricultural ..... 0517  
Art ..... 0273  
Bilingual and Multicultural ..... 0282  
Business ..... 0688  
Community College ..... 0275  
Curriculum and Instruction ..... 0727  
Early Childhood ..... 0518  
Elementary ..... 0524  
Finance ..... 0277  
Guidance and Counseling ..... 0519  
Health ..... 0680  
Higher ..... 0745  
History of ..... 0520  
Home Economics ..... 0278  
Industrial ..... 0521  
Language and Literature ..... 0279  
Mathematics ..... 0280  
Music ..... 0522  
Philosophy of ..... 0998  
Physical ..... 0523

Psychology ..... 0525  
Reading ..... 0535  
Religious ..... 0527  
Sciences ..... 0714  
Secondary ..... 0533  
Social Sciences ..... 0534  
Sociology of ..... 0340  
Special ..... 0529  
Teacher Training ..... 0530  
Technology ..... 0710  
Tests and Measurements ..... 0288  
Vocational ..... 0747

**LANGUAGE, LITERATURE AND LINGUISTICS**

Language  
General ..... 0679  
Ancient ..... 0289  
Linguistics ..... 0290  
Modern ..... 0291  
Literature  
General ..... 0401  
Classical ..... 0294  
Comparative ..... 0295  
Medieval ..... 0297  
Modern ..... 0298  
African ..... 0316  
American ..... 0591  
Asian ..... 0305  
Canadian (English) ..... 0352  
Canadian (French) ..... 0355  
English ..... 0593  
Germanic ..... 0311  
Latin American ..... 0312  
Middle Eastern ..... 0315  
Romance ..... 0313  
Slavic and East European ..... 0314

**PHILOSOPHY, RELIGION AND THEOLOGY**

Philosophy ..... 0422  
Religion  
General ..... 0318  
Biblical Studies ..... 0321  
Clergy ..... 0319  
History of ..... 0320  
Philosophy of ..... 0322  
Theology ..... 0469

**SOCIAL SCIENCES**

American Studies ..... 0323  
Anthropology  
Archaeology ..... 0324  
Cultural ..... 0326  
Physical ..... 0327  
Business Administration  
General ..... 0310  
Accounting ..... 0272  
Banking ..... 0770  
Management ..... 0454  
Marketing ..... 0338  
Canadian Studies ..... 0385  
Economics  
General ..... 0501  
Agricultural ..... 0503  
Commerce-Business ..... 0505  
Finance ..... 0508  
History ..... 0509  
Labor ..... 0510  
Theory ..... 0511  
Folklore ..... 0358  
Geography ..... 0346  
Gerontology ..... 0351  
History  
General ..... 0578

Ancient ..... 0579  
Medieval ..... 0581  
Modern ..... 0582  
Black ..... 0328  
African ..... 0331  
Asia, Australia and Oceania ..... 0332  
Canadian ..... 0334  
European ..... 0335  
Latin American ..... 0336  
Middle Eastern ..... 0333  
United States ..... 0337  
History of Science ..... 0585  
Law ..... 0398  
Political Science  
General ..... 0615  
International Law and Relations ..... 0616  
Public Administration ..... 0617  
Recreation ..... 0814  
Social Work ..... 0452  
Sociology  
General ..... 0626  
Criminology and Penology ..... 0627  
Demography ..... 0938  
Ethnic and Racial Studies ..... 0631  
Individual and Family Studies ..... 0628  
Industrial and Labor Relations ..... 0629  
Public and Social Welfare ..... 0630  
Social Structure and Development ..... 0700  
Theory and Methods ..... 0344  
Transportation ..... 0709  
Urban and Regional Planning ..... 0999  
Women's Studies ..... 0453

**THE SCIENCES AND ENGINEERING**

**BIOLOGICAL SCIENCES**

Agriculture  
General ..... 0473  
Agronomy ..... 0285  
Animal Culture and Nutrition ..... 0475  
Animal Pathology ..... 0476  
Food Science and Technology ..... 0359  
Forestry and Wildlife ..... 0478  
Plant Culture ..... 0479  
Plant Pathology ..... 0480  
Plant Physiology ..... 0817  
Range Management ..... 0777  
Wood Technology ..... 0746  
Biology  
General ..... 0306  
Anatomy ..... 0287  
Biostatistics ..... 0308  
Botany ..... 0309  
Cell ..... 0379  
Ecology ..... 0329  
Entomology ..... 0353  
Genetics ..... 0369  
Limnology ..... 0793  
Microbiology ..... 0410  
Molecular ..... 0307  
Neuroscience ..... 0317  
Oceanography ..... 0416  
Physiology ..... 0433  
Radiation ..... 0821  
Veterinary Science ..... 0778  
Zoology ..... 0472  
Biophysics  
General ..... 0786  
Medical ..... 0760

**EARTH SCIENCES**

Biogeochemistry ..... 0425  
Geochemistry ..... 0996

Geodesy ..... 0370  
Geology ..... 0372  
Geophysics ..... 0373  
Hydrology ..... 0388  
Mineralogy ..... 0411  
Paleobotany ..... 0345  
Paleoecology ..... 0426  
Paleontology ..... 0418  
Paleozoology ..... 0985  
Palynology ..... 0427  
Physical Geography ..... 0368  
Physical Oceanography ..... 0415

**HEALTH AND ENVIRONMENTAL SCIENCES**

Environmental Sciences ..... 0768  
Health Sciences  
General ..... 0566  
Audiology ..... 0300  
Chemotherapy ..... 0992  
Dentistry ..... 0567  
Education ..... 0350  
Hospital Management ..... 0769  
Human Development ..... 0758  
Immunology ..... 0982  
Medicine and Surgery ..... 0564  
Mental Health ..... 0347  
Nursing ..... 0569  
Nutrition ..... 0570  
Obstetrics and Gynecology ..... 0380  
Occupational Health and Therapy ..... 0354  
Ophthalmology ..... 0381  
Pathology ..... 0571  
Pharmacology ..... 0419  
Pharmacy ..... 0572  
Physical Therapy ..... 0382  
Public Health ..... 0573  
Radiology ..... 0574  
Recreation ..... 0575

Speech Pathology ..... 0460  
Toxicology ..... 0383  
Home Economics ..... 0386

**PHYSICAL SCIENCES**

Pure Sciences  
Chemistry  
General ..... 0485  
Agricultural ..... 0749  
Analytical ..... 0486  
Biochemistry ..... 0487  
Inorganic ..... 0488  
Nuclear ..... 0738  
Organic ..... 0490  
Pharmaceutical ..... 0491  
Physical ..... 0494  
Polymer ..... 0495  
Radiation ..... 0754  
Mathematics ..... 0405  
Physics  
General ..... 0605  
Acoustics ..... 0986  
Astronomy and Astrophysics ..... 0606  
Atmospheric Science ..... 0608  
Atomic ..... 0748  
Electronics and Electricity ..... 0607  
Elementary Particles and High Energy ..... 0798  
Fluid and Plasma ..... 0759  
Molecular ..... 0609  
Nuclear ..... 0610  
Optics ..... 0752  
Radiation ..... 0756  
Solid State ..... 0611  
Statistics ..... 0463  
Applied Sciences  
Applied Mechanics ..... 0346  
Computer Science ..... 0984

Engineering  
General ..... 0537  
Aerospace ..... 0538  
Agricultural ..... 0539  
Automotive ..... 0540  
Biomedical ..... 0541  
Chemical ..... 0542  
Civil ..... 0543  
Electronics and Electrical ..... 0544  
Heat and Thermodynamics ..... 0348  
Hydraulic ..... 0545  
Industrial ..... 0546  
Marine ..... 0547  
Materials Science ..... 0794  
Mechanical ..... 0548  
Metallurgy ..... 0743  
Mining ..... 0551  
Nuclear ..... 0552  
Packaging ..... 0549  
Petroleum ..... 0765  
Sanitary and Municipal ..... 0554  
System Science ..... 0790  
Geotechnology ..... 0428  
Operations Research ..... 0796  
Plastics Technology ..... 0795  
Textile Technology ..... 0994

**PSYCHOLOGY**

General ..... 0621  
Behavioral ..... 0384  
Clinical ..... 0622  
Developmental ..... 0620  
Experimental ..... 0623  
Industrial ..... 0624  
Personality ..... 0625  
Physiological ..... 0989  
Psychobiology ..... 0349  
Psychometrics ..... 0632  
Social ..... 0451



## Table of Contents

List of Tables	viii
List of Figures	ix
Abstract	xiii
Abbreviations and Symbols	xiv
Acknowledgments	xvii
Chapter 1 Introduction	1
1.1 Uptake of Amino Acids by <i>Fusobacterium</i> Species	2
1.2 Preparation of Optically Pure Amino Acids	4
1.2.1 Enzymatic Methods	5
1.3 Glutamate Catabolism	14
1.3.1 Acetate and Butyrate Interconversion	15
1.3.2 The Methylaspartate Pathway	18
1.3.3 The Hydroxyglutarate Pathway	23
1.3.4 The Aminobutyrate Pathway	29
1.3.5 Distribution of Glutamate Pathways Among Anaerobic Bacteria	32
1.4 Outline of Thesis and Literature Discrepancies	34
Chapter 2 Results: Stereochemical Aspects of Amino Acid Uptake	38
2.1 Uptake of D- and L-Amino Acids by <i>Fusobacterium</i> Species	38
2.2 Preparation of D-Amino Acids from Racemic Mixtures	45

2.2.1	D-Amino Acid Preparation by <i>F. nucleatum</i> Cultures Growing on Peptone Medium	45
2.2.2	D-Amino Acid Preparation by Bacterial Resuspension	47
Chapter 3	Results: Examination of the Pathways of Glutamic Acid Catabolism in <i>Fusobacterium</i> Species Using Isotopically-Labelled Substrates	66
3.1	General Approach	66
3.2	Catabolism of <sup>13</sup> C-Labelled L-Glutamates by <i>F. nucleatum</i>	68
3.2.1	Metabolism of <sup>2</sup> H- and <sup>13</sup> C-Labelled Acetate by <i>F. nucleatum</i>	74
3.3	Catabolism of <sup>13</sup> C-Labelled Glutamic Acids by <i>F. varium</i>	79
3.3.1	Metabolism of <sup>2</sup> H- and <sup>13</sup> C-Labelled Acetate by <i>F. varium</i>	84
3.4	Detection and Partial Purification of Enzymes in the Methylaspartate Pathway	86
3.5	Detection and Partial Purification of Glutamate Racemase	92
Chapter 4	Discussion	100
4.1	Amino Acid Uptake by <i>Fusobacterium</i> Species	99
4.2	Preparation of D-Amino Acids	106
4.3	Conversion of Acetate to Butyrate	112
4.4	Glutamate Catabolism in <i>F. nucleatum</i>	115
4.5	Glutamate Catabolism in <i>F. varium</i>	117

4.6	Conclusions and Future Work . . . . .	124
Chapter 5	Experimental . . . . .	128
5.1	Materials . . . . .	128
5.2	General Methods . . . . .	129
5.3	Microorganisms . . . . .	130
5.4	Media . . . . .	131
5.5	Analysis of Amino Acids . . . . .	132
5.6	Stereochemical Aspects of Amino Acid Uptake . . . . .	136
5.6.1	Survey of Amino Acid Uptake from Peptone Medium by <i>F. nucleatum</i> and <i>F. varium</i> . . . . .	136
5.6.2	Preparation of D-Glutamate by <i>F. nucleatum</i> Growing on Peptone Medium . . . . .	136
5.6.3	Amino Acid Uptake by Resuspensions of <i>F. nucleatum</i> and <i>F. varium</i> . . . . .	137
5.6.4	Preparation of D-Amino Acids by Resuspensions of <i>F. nucleatum</i> . . . . .	138
5.7	Feeding Experiments Using Isotopically Labelled Substrates . . . . .	139
5.7.1	Culture Conditions . . . . .	139
5.7.2	Formation and Isolation of 4-Bromophenacyl Acetate and Butyrate . . . . .	140
5.7.3	Isotopic Analysis . . . . .	142

5.8	Preparation and Partial Purification of <i>F. varium</i>	
	cell-free Extracts . . . . .	143
5.9	Enzyme Assays . . . . .	145
5.9.1	General Conditions . . . . .	145
5.9.2	Catabolism of D- and L-Glutamate . . . . .	145
5.9.3	Glutamate Mutase and 3-Methylaspartase . . . . .	145
5.9.4	Glutamate Racemase . . . . .	146
5.9.5	Glutamate Dehydrogenase . . . . .	147
5.9.6	D-Amino Acid Transaminase . . . . .	148
	References . . . . .	149

## List of Tables

1.	Proposed intermediates in three pathways of glutamate catabolism . . . . .	15
2.	Uptake of amino acids with acidic, basic or polar side-chain substituents . . . . .	39
3.	Uptake of amino acids with aromatic and hydrophobic side chains . . . . .	40
4.	Isotopic feeding experiments in <i>F. nucleatum</i> . . . . .	70
5.	Incorporation of L-[ <sup>13</sup> C]glutamic acids into acetic and butyric acids by <i>F. nucleatum</i> . . . . .	72
6.	Incorporation of labelled acetic acids into butyric acid by <i>F. nucleatum</i> . . . . .	76
7.	Isotopic feeding experiments in <i>F. varium</i> . . . . .	80
8.	Incorporation of [ <sup>13</sup> C]glutamic acids into acetic and butyric acids by <i>F. varium</i> . . . . .	81
9.	Yield of acetate and butyrate isolated from a culture supplemented with D-glutamate . . . . .	83
10.	Incorporation of labelled acetic acids into butyric acid by <i>F. varium</i> . . . . .	85
11.	Stereochemistry of the amino acids assimilated by fusobacteria . . .	101

## List of Figures

1.	Examples of substances containing D-amino acid subunits . . . . .	4
2.	Preparation of D-amino acids using a multi-enzyme system . . . . .	7
3.	Reaction sequence for the enzymatic conversion of DL-methionine to L-methionine: a, D-amino acid oxidase; b, catalase; c, leucine dehydrogenase; d, formate dehydrogenase . . .	9
4.	Resolution of <i>p</i> -hydroxyphenylglycine using acylase . . . . .	11
5.	Preparation of D-amino acids from racemic amino acid amides . . . . .	12
6.	D-Amino acid preparation using L-hydantoin derivatives of amino acids . . . . .	13
7.	Interconversion of acetate and butyrate in anaerobic microorganisms . . . . .	16
8.	Glutamate catabolism <i>via</i> the methylaspartate pathway . . . . .	18
9.	Glutamate catabolism <i>via</i> the hydroxyglutarate pathway . . . . .	24
10.	Proposed radical mechanism for the dehydratase from <i>A. fermentans</i> . . . . .	28
11.	Hypothetical mechanism for the <i>syn</i> -dehydration of ( <i>R</i> )-2-hydroxyglutaryl-CoA to ( <i>E</i> )-glutaconyl-CoA by the dehydratase from <i>F. nucleatum</i> . . . . .	28
12.	Glutamate catabolism <i>via</i> the aminobutyrate pathway . . . . .	30
13.	Uptake of D- and L-amino acids by <i>F. nucleatum</i> . . . . .	41
14.	Uptake of D- and L-amino acids by <i>F. varium</i> . . . . .	42
15.	Effect of increasing the concentration of DL-glutamate on L-glutamate uptake by <i>F. nucleatum</i> in peptone medium . . . . .	48
16.	Effect of inoculum size on the rate of L-glutamate degradation by <i>F. nucleatum</i> in peptone medium . . . . .	48

17.	Effect of stirring on the rate of L-amino acid degradation in resuspension buffer containing either 270 mM DL-glutamate (A) or 340 mM DL-serine (B) . . . . .	50
18.	Effect of increasing the concentration of DL-glutamate on L-glutamate degradation by <i>F. nucleatum</i> in resuspension buffer . . . . .	51
19.	Effect of increasing the concentration of DL-serine on L-serine degradation by <i>F. nucleatum</i> in resuspension buffer at low concentrations of DL-serine analyzed by normal hplc (A) and at high concentrations of DL-serine analyzed by chiral hplc (B) . . . . .	53
20.	L-Arginine degradation by <i>F. varium</i> in resuspension buffer. The initial concentrations of DL-arginine were 100 (A), 200 (B), and 300 (C) mM . . . . .	54
21.	Hplc chromatograms of DL-arginine (300 mM) incubated with <i>F. varium</i> in resuspension buffer . . . . .	55
22.	Effect of increasing the cell density on the rate of L-glutamate uptake by <i>F. nucleatum</i> in resuspension buffer at high concentrations of DL-glutamate (480 mM) . . . . .	57
23.	Effect of increasing cell the density on the rate of L-glutamate degradation by <i>F. nucleatum</i> in resuspension buffer at 250 mM (A) and 175 mM (B) . . . . .	58
24.	Effect of increasing the cell density on the rate of L-serine degradation by <i>F. nucleatum</i> in resuspension buffer containing 800 mM DL-serine . . . . .	59
25.	Effect of consecutive resuspensions on the ability of <i>F. nucleatum</i> to degrade L-serine in resuspension buffer containing 800 mM DL-serine . . . . .	60
26.	<sup>1</sup> H- and <sup>13</sup> C-nmr spectra of the residue from glutamic acid catabolism. The peaks in <sup>13</sup> C-nmr spectrum are labelled as A, acetate and B, butyrate . . . . .	61
27.	<sup>1</sup> H- and <sup>13</sup> C-nmr spectra of residue from serine catabolism. The peaks in <sup>13</sup> C-nmr spectrum are labelled as A, acetate; B, butyrate; and L, lactate . . . . .	63

28.	Effect of sodium acetate and butyrate on the rate of L-glutamate degradation by <i>F. nucleatum</i> resuspended in buffer containing 175 mM DL-glutamate . . . . .	64
29.	Incorporation patterns of the carbon atoms of glutamate into acetate and butyrate by three different pathways. The numbers correspond to the carbon atoms of glutamate . . . . .	67
30.	Isolation of the metabolic end-products (acetic and butyric acids) as <i>p</i> -bromophenacyl esters . . . . .	69
31.	<sup>13</sup> C-Nmr spectra of <i>p</i> -bromophenacyl acetate: (A) isolated from a culture of <i>F. nucleatum</i> supplemented with L-[4- <sup>13</sup> C]glutamate and (B) a natural abundance sample . . . . .	73
32.	<sup>13</sup> C-Nmr spectra of <i>p</i> -bromophenacyl butyrate: (A) isolated from a culture of <i>F. nucleatum</i> supplemented with L-[4- <sup>13</sup> C]glutamate and (B) a natural abundance sample . . . . .	75
33.	<sup>13</sup> C-Nmr (A) and <sup>2</sup> H-nmr (B) spectra of <i>p</i> -bromophenacyl butyrate isolated from cultures of <i>F. nucleatum</i> supplemented with [1,2- <sup>13</sup> C <sub>2</sub> ] acetate and [ <sup>2</sup> H <sub>3</sub> ]acetate, respectively . . . . .	77
34.	Catabolism of D- and L-glutamate by a crude cell-free extract of <i>F. varium</i> . . . . .	86
35.	<sup>13</sup> C-Nmr spectra of a cell-free extract of <i>F. varium</i> incubated with L-[4- <sup>13</sup> C]glutamate . . . . .	88
36.	Hplc chromatograms of crude cell-free extract (A) and charcoal-treated cell-free extract (B) of <i>F. varium</i> incubated with mesaconate for 5 min . . . . .	89
37.	Formation of β-methylaspartate and glutamate from mesaconate by crude cell-free extract (A) and charcoal treated cell-free extract (B) of <i>F. varium</i> detected by hplc . . . . .	90
38.	Standard curve relating molecular mass to the elution volume from a Sephadex G-150 column . . . . .	92
39.	Chromatograms of the products from the incubation of mesaconate with methylaspartase eluted from Sephadex G-150 column (A), the standard sample (B), and the mixture of standard and incubation samples analyzed (C) by chiral hplc . . . . .	93

40.	Racemization of either D- or L-glutamate by a charcoal treated, partially purified cell-free extract of <i>F. varium</i> . . . . .	95
41.	Racemization of D-glutamate (bottom) and L-glutamate (top) by a charcoal treated, partially purified cell-free extract of <i>F. varium</i> grown on either D- (■) or L-glutamate (●) . . . . .	97
42.	Effect of addition of cofactors on the rate and degree of racemization by a charcoal treated, partially purified cell-free extract of <i>F. varium</i> . . . . .	98
43.	<sup>1</sup> H-Nmr spectra of the products from the racemization of D-glutamate in D <sub>2</sub> O. Spectrum C was recorded while the residual water signal was saturated . . . . .	99
44.	Proposed route for serine catabolism in <i>F. nucleatum</i> . . . . .	107

## Abstract

The uptake and metabolism of stereoisomers of amino acids were investigated in *Fusobacterium nucleatum*, an oral bacterium associated with oral infections, and *Fusobacterium varium*, an inhabitant of the gastrointestinal tract.

*F. nucleatum* assimilated both isomers of glutamine, histidine and lysine, but only the L-isomers of glutamic acid and serine. In *F. varium*, the L-isomers of arginine and histidine were selectively taken up, along with both isomers of 3-aminobutyric acid, glutamic acid, lysine and serine. Although amino acids are major sources of energy for fusobacteria, the catabolism of D-amino acids has not been investigated previously.

The preferential uptake of L-amino acids was employed to prepare gram quantities of D-amino acids. Conditions were optimized for the preparation of D-glutamate and D-serine from their racemic mixtures by *F. nucleatum*. Recoveries of 70-80% were obtained, and the products had enantiomeric excesses >99%. Furthermore, it was demonstrated that D-arginine and D-histidine could be prepared under similar conditions by *F. varium*.

The occurrence of three distinct pathways for the bacterial catabolism of glutamate to acetate, butyrate, NH<sub>3</sub> and CO<sub>2</sub> was investigated in *F. nucleatum* and *F. varium* using isotopically labelled substrates and enzyme assays. The acidic end-products (acetate and butyrate) were converted to *p*-bromophenacyl esters and separated prior to the determination of isotopic enrichments by nmr spectroscopy and mass spectrometry.

The nonincorporation of label from L-[5-<sup>13</sup>C]glutamate and a major incorporation of <sup>13</sup>C into C-1 of acetate and butyrate from L-[1-<sup>13</sup>C]glutamate indicated that the hydroxyglutarate pathway predominated and that participation of the aminobutyrate route was insignificant in *F. nucleatum*. The possible presence of the methylaspartate pathway was ruled out by the incorporation of label from L-[4-<sup>13</sup>C]glutamate into only C-2 of acetate and C-4 and C-2 of butyrate. Incorporation of [1,2-<sup>13</sup>C<sub>2</sub>]- and [<sup>2</sup>H<sub>3</sub>]acetate confirmed that the minor labelling of a second site in butyrate was due to the synthesis of butyrate from acetate produced by the hydroxyglutarate pathway.

In *F. varium*, label was incorporated into C-1 of acetate and equally into C-1 and C-3 of butyrate from both L-[1-<sup>13</sup>C]- and L-[4-<sup>13</sup>C]glutamate, and unenriched carboxylic acids were isolated from the cultures supplemented with L-[5-<sup>13</sup>C]glutamate. Only the methylaspartate pathway is supported by these results, in contrast to an earlier suggestion that the three pathways operated simultaneously in *F. varium*. D-[3-<sup>13</sup>C]Glutamate was also catabolized by the methylaspartate pathway, ruling out differential metabolism of the glutamate enantiomers as the source of this discrepancy. In the cell-free extracts of *F. varium*, the metabolism of D- and L-glutamate and the formation of these amino acids from mesaconate was followed by hplc and nmr. A glutamate racemase was detected and partially purified from these extracts.

## Abbreviations and Symbols

$[\alpha]_D$	optical rotation at the D line of sodium
$\nu_{\max}$	wavenumbers at absorption maximum
Arg	arginine
°C	degree celsius
(d)	doublet
Da	dalton
(dd)	doublet of doublets
cpm	counts per minute
EC	enzyme classification number
ee	enantiomeric excess
FMN	flavin mononucleotide
$\times g$	gravitational force
Gln	glutamine
<i>glr</i>	glutamate racemase gene
Glu	glutamic acid
h	hours
His	histidine
Hz	Hertz
hplc	high performance liquid chromatography
I.D.	inner diameter
<i>in vacuo</i>	in vacuum

ir	infrared
J	coupling constant
lit.	literature
Lys	lysine
M <sup>+</sup>	molecular ion
<i>m/z</i>	mass to charge ratio
min	minutes
NAD <sup>+</sup>	nicotinamide adenine dinucleotide
NADH	nicotinamide adenine dinucleotide (reduced form)
NADP	nicotinamide adenine dinucleotide phosphate
nmr	nuclear magnetic resonance
O.D.	outer diameter
opa	<i>o</i> -phthalaldehyde
ppm	parts per million
(q)	quartet
R <sub>f</sub>	retention factor
rpm	revolutions per minute
s	seconds
(s)	singlet
Ser	serine
(t)	triplet
tic	thin layer chromatography

uv	ultraviolet
v/v	volume/volume
w/v	weight/volume
m/v	mass/volume

## Acknowledgments

I wish to express my sincere thanks to my supervisor Dr. Robert White for his advice and guidance during my studies. I would like to thank members, past and present of the White group, particularly Ratika Seth and Amanda Doherty-Kirby for their help with the initial feeding experiment in *F. nucleatum*. I am also grateful for the assistance of Dr. J.S. Grossert and Dr. J.-H. Kim for supplying mass spectra, the Atlantic Regional Magnetic Resonance centre for the use of their nmr facilities, and the Institute of Marine Biosciences, NRC, for access to the polarimeter. Special thanks to Dr. Song F. Lee, Dr. David E. Mahoney, and Dr. D. Cunningham in the Faculty of Dentistry for providing facilities for culturing microorganisms.

I would like to acknowledge the financial support from the Ministry of Health and Medical Education, Islamic Republic of Iran, the Innovations in Chemistry Fund, and Dalhousie University.

✎ Finally, I thank my family for many years of support and patience.

Most of all, I would like to thank my wife Homa for her support and encouragement during the past four years.

## Chapter 1

### Introduction

The first life on earth is believed to have existed in an environment without oxygen. According to the evidence of microfossils formed in sedimentary deposits in Australia and the presence of stromatolites (fossilized bacterial mats or colonies of bacteria embedded within minerals), the first anaerobic bacteria appeared approximately  $3.5 \times 10^9$  years ago (1).

Generally speaking, anaerobic bacteria are divided into two major groups: a) obligate anaerobes that cannot grow in the presence of oxygen and b) facultative anaerobes that grow in an atmosphere with or without oxygen. However, other nonanaerobic bacteria such as microphilic and carboxyphilic organisms can be mistakenly categorized into these groups. Microphilic bacteria need less oxygen than that normally present in air, while carboxyphilic bacteria grow in a higher concentration of  $\text{CO}_2$ . Obligate anaerobes which display different sensitivities to oxygen are either aerotolerant or aerosensitive (1).

Anaerobic bacteria in man and animals are widely distributed over the oral cavity, the gastrointestinal tract, and the female genital tract (1). The site of colonization depends on the availability of nutrients (2). A wide variety of substrates are metabolized by anaerobic bacteria; amino acids are a major energy source for some anaerobes, particularly species of *Fusobacterium*. The common end-products of amino acid catabolism are ammonia,  $\text{CO}_2$ ,  $\text{H}_2$ , and short-chain fatty acids, such as acetic and butyric acids (3).

### 1.1 Uptake of Amino Acids by *Fusobacterium* Species

Amino acids are transported into the bacterial cells *via* three mechanisms, namely, free diffusion, facilitated diffusion, and active transport. While free diffusion requires water-filled pores in the membrane, the facilitated diffusion and active transport mechanisms involve carrier proteins. In addition, active transport is coupled with the free energy of a chemical reaction taking place in the transport region (4). Carrier proteins are substrate specific; carriers specific for the basic amino acids, glutamine and leucine-isoleucine-valine have been isolated from *E. coli* (5). The stereochemistry of carrier proteins has also been reported. For example, L-glutamate uptake is inhibited by D-glutamate in *E. coli* (6).

Most investigations of amino acid uptake by *Fusobacterium* species have focused on the fermentation patterns of amino acids among different strains of *Fusobacterium nucleatum*, as this species is most commonly encountered in oral infections (7).

These studies have demonstrated that glutamic acid, histidine, lysine and serine are utilized by most strains of *F. nucleatum*, whereas asparagine, aspartic acid, cysteine, glutamine, methionine, threonine and tyrosine are metabolized by some other strains. Most hydrophobic and aromatic amino acids are metabolized poorly or not at all (8-13).

The fermentation of amino acids by other species of fusobacteria has been investigated to a lesser extent. In four species of *Fusobacterium varium*, high levels of arginine, asparagine, cysteine, glutamate and serine were utilized,

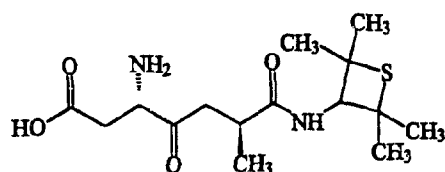
whereas lower concentrations of aspartic acid, histidine, lysine and threonine were taken up. The *F. varium* strains (14), like those of *F. nucleatum*, did not metabolize hydrophobic and aromatic amino acids to any extent.

Clinical isolates of *Fusobacterium* species utilized smaller numbers of amino acids at lower levels than the reference strains (11). However, subculturing fresh isolates of *F. nucleatum* over four months increased their ability to degrade amino acids, to levels comparable to those of reference strains (15). Bakken *et al.* (10) suggested that differences in amino acid uptake profiles by different groups of investigators could be explained by either strain variations or the fact that the cells studied were from different growth phases.

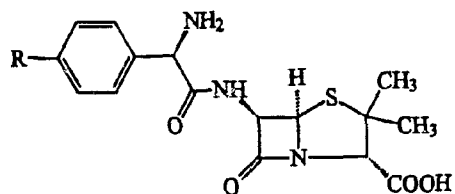
The most striking feature in most of these studies on amino acid uptake by anaerobic bacteria, in general, and by fusobacteria in particular is the lack of attention to the stereochemistry of the amino acids used. In many cases, the stereochemistry of the amino acids was not defined and in others racemic mixtures of amino acids were used, most likely due to the unavailability of the L-isomers. To the best of our knowledge, there is no report on the stereoselective uptake of amino acids by anaerobic bacteria. Studies on the stereoselective uptake of amino acids would provide a comparison of the catabolic activities towards D- and L-amino acids within different species of anaerobic bacteria. Furthermore, it could be useful for the taxonomic classification of anaerobic bacteria.

PyroGlu-His-Trp-Ser-Tyr-D-Ser (Bu<sup>1</sup>)-Leu-Arg-Pro-NHEt

Buserlin



Alitame



R = H Ampicillin

R = OH Amoxycillin

**Figure 1** Examples of substances containing D-amino acid subunits.

## 1.2 Preparation of Optically Pure Amino Acids

There is an increasing demand for amino acids in optically pure forms. Most L-amino acids are produced in large quantities by fermentation (16). In recent years, D-amino acids are becoming increasingly important as chiral building blocks for the synthesis of optically active pharmaceuticals and dietary supplements (Figure 1). For example, protection against proteolytic enzymes is achieved by incorporating D-serine into peptides such as the prostate cancer drug buserlin, and D-alanine into alitame, a new sweetener introduced by Pfizer company. The non-proteinogenic D-amino acids D-phenylglycine and its *p*-hydroxy derivative are required for the semisynthesis of the  $\beta$ -lactam antibiotics ampicillin and

amoxicillin (17).

Several different methods have been used over the years to obtain optically pure amino acids. In the classical approach, the racemic amino acid is synthesized and the pure enantiomers are obtained from the racemate by direct crystallization or by crystallization of diastereomeric salts. For example, L-glutamate has been obtained on a large scale by direct crystallization of its racemate (17).

More recently, several methods for the asymmetric synthesis of amino acids have been developed and applied to the synthesis of many different amino acids (18). For example, a transition metal catalyst containing chiral ligands was used to hydrogenate a prochiral compound in the commercial production of 3,4-dihydroxy-L-phenylalanine (L-DOPA) (19).

### 1.2.1 Enzymatic Methods

In these systems, an enzyme or group of enzymes or intact cells, mainly bacteria, containing appropriate enzymes are employed to either synthesize an amino acid from an unrelated substrate or to enantioselectively attack only one of the enantiomers of the racemic amino acid or its derivatives. The most common reactions that are catalyzed by enzymes are oxidation, reduction, transamination and hydration.

The large-scale production of amino acids was first accomplished by fermentation processes, and L-glutamic acid was the first amino acid produced using *Corynebacterium glutamicum*. Fermentation processes are still in use for

industrial production of L-glutamate (350,000 tons per annum) (20), L-lysine (180,000 tons per annum) (21) and are alternative methods for the production of other L-amino acids such as L-arginine, L-histidine, L-threonine, L-valine, L-glutamine, L-isoleucine, and L-proline (16).

Immobilized cells of *Escherichia coli* containing aspartase convert fumarate to L-aspartate on a commercial scale (22). L-Alanine is produced on a large scale by immobilized cells of *Pseudomonas dacunhae*, a bacterium containing L-aspartate- $\beta$ -decarboxylase (EC 4.1.1.12) that decarboxylates L-aspartate to L-alanine (22). The production of D-alanine from glycerol by cultures of *Corynebacterium fascians* has also been reported (23).

Isolated enzymes and multi-enzyme systems are used for production of optically pure amino acids. Nakajima *et al.* (24) have used D-amino acid transaminase (EC 2.6.1.21) to convert 2-oxoacids to their corresponding D-amino acids. The 2-oxoglutarate needed for the transamination was produced *in situ* by a combination of glutamate racemase (EC 5.1.1.3), glutamate dehydrogenase (E.C. 1.4.1.2) and formate dehydrogenase (EC 1.2.1.2). The reaction sequence is shown in Figure 2. This method was successfully applied to the preparation of a series of D-amino acids. However, attempts to make D-serine and aromatic amino acids failed.

Another example is the synthesis of L-alanine and L-leucine using alanine or leucine dehydrogenase (EC 1.4.1.9) in combination with a dehydrogenase which regenerates the NADH needed for the oxidative deamination reaction (25).

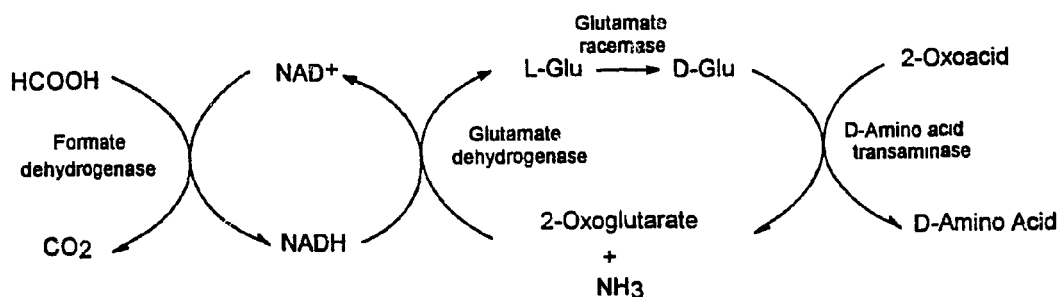


**Figure 2.** Preparation of D-amino acids using a multi-enzyme system.

The use of microorganisms for the preparation of enantiomerically pure compounds from their racemic mixtures dates back to mid 19th century when Pasteur obtained (-)-tartaric acid by brewer's yeast fermentation of the racemic mixture (26).

This approach has been used to prepare enantiomerically pure amino acids by exploiting the catabolic activity of bacteria towards only one of the enantiomers in the racemate. The unreacted enantiomer is subsequently separated from the reaction mixture or culture. For most cases, the D-amino acid product of the reaction is more valuable than the racemate.

The production of D-aspartate and L-alanine from DL-aspartate using immobilized cells of *P. dacunhae* which contain L-aspartate- $\beta$ -decarboxylase has been commercialized (27).

An extensive screening program for yeasts with L-alanine degrading activity,

selected *Candida maltosa* for the production of D-alanine from its racemic mixture. The yeast processed high concentrations of DL-alanine, *i.e.*, 200 g/L and yielded 90 g/L of enantiomerically pure D-alanine. *C. maltosa* was also found to have the ability to assimilate the L-isomers of arginine, aspartate, glutamate, proline and serine and could potentially be used for the production of these D-amino acids (28). Similarly, *Pseudomonas putida* has been used for the small scale preparation of D- $\alpha$ -amino adipic acid from the DL-mixture (29).

*Lactobacillus brevis* contains both glutamate racemase (EC 5.1.1.3) and glutamate decarboxylase (EC 4.1.1.15) activities. Yagasaki *et al.* have exploited this organism to prepare D-glutamate from the much cheaper L-glutamate. L-Glutamate was racemized by incubation with the bacterium at pH 8.5, the optimum pH for glutamate racemase. By lowering the pH to 4.0, glutamate decarboxylase became active, and the residual L-glutamate decarboxylated to form 4-aminobutyrate, which was easily separated from the D-glutamate in the culture medium (30). Since the *Lactobacillus* was not suitable for an industrial process due to poor growth, the gene coding for glutamate racemase was cloned into *E. coli*, and another strain of *E. coli* with a high glutamate decarboxylase activity was identified. Thus, a process was developed in which L-glutamate was converted to a racemic mixture by the recombinant *E. coli* and decarboxylated by addition of the second *E. coli* strain. The system worked at 100 g/L of L-glutamate to give 50 g/L of enantiomerically pure D-glutamate (31).

Similar processes have employed isolated enzymes. For example, D-

histidine and histamine have been prepared from the racemic mixture using commercially available histidine decarboxylase (EC 4.1.1.22) (32). By using a multi-enzyme system, D-methionine in the racemate has been converted to its L-isomer, thereby providing a total conversion of DL-methionine to L-methionine (Figure 3). The D-amino acid oxidase (EC 1.4.3.3) converted D-methionine to the corresponding 2-oxoacid which is reaminated to L-methionine by leucine dehydrogenase (EC 1.4.1.9). Catalase (EC 1.11.1.6) removes the hydrogen peroxide while NADH is regenerated by formate dehydrogenase (EC 1.2.1.2) (33).

Enzymes have also been successfully applied to the preparation of optically pure amino acids from racemic derivatives of amino acids. Aminoacylases,

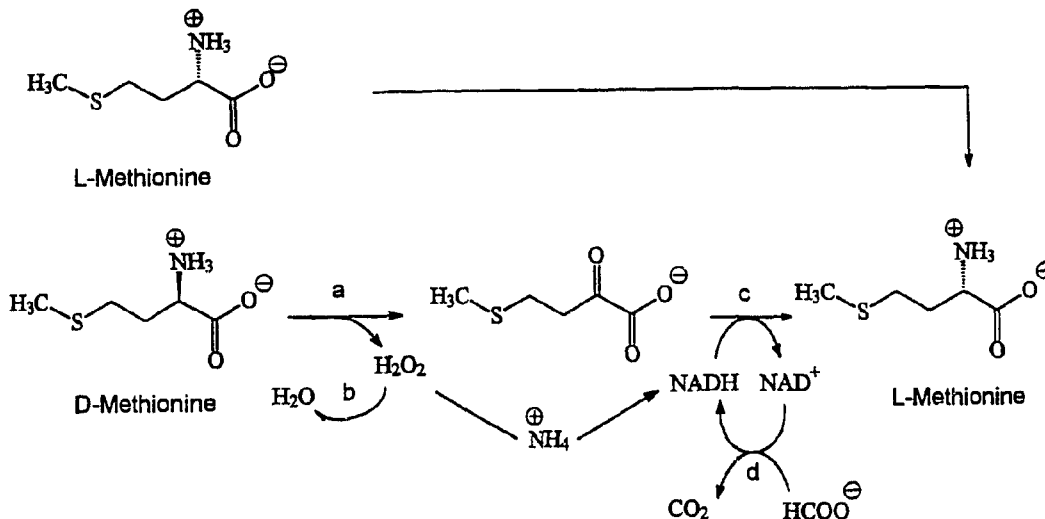


**Figure 3.** Reaction sequence for the enzymatic conversion of DL-methionine to L-methionine: a, D-amino acid oxidase; b, catalase; c, leucine dehydrogenase; d, formate dehydrogenase.

amidases and hydantoinases are the most common enzymes employed in these kinetic processes, either as the purified enzyme or as intact microorganism.

Over the years, aminoacylases (EC 3.5.1.14) have been commonly used for the resolution of *N*-acyl derivatives of amino acids, and the first industrial application of an immobilized enzyme used aminoacylase purified from *Aspergillus oryzae* for the production of variety of L-amino acids. In this method, the enzyme deacylates the L-isomer, which is isolated from the reaction mixture, and the remaining D-amino acid is racemized and reused. L-Methionine, L-phenylalanine and L-valine have been prepared from their racemic mixtures in commercial quantities using this method (22), and the production of L-methionine from *N*-acetyl-DL-methionine has been reported (34). D-Phenylglycine and D-*p*-hydroxyphenylglycine were prepared from their racemic mixtures by incubating penicillin G acylase with these substrates in the presence of mandelic acid methyl ester. The L-isomer was acylated and the D-isomer did not react (Figure 4). A complete recovery of the D-isomer from the racemic mixture was obtained (35).

Amidases (EC 3.5.1.4) are able to stereospecifically convert amide derivatives of amino acids to their corresponding amino acids. Considering the fact that the DL-amino acid amides are intermediates in the Strecker synthesis of amino acids, they are readily available. A broad screening program resulted in identifying *Pseudomonas putida* as a source of a useful amidase. The enzyme is specific for the L-isomer of amino acid amides; the desired D-amino acid amide remaining in the reaction is separated and hydrolyzed to the corresponding D-amino acid. The

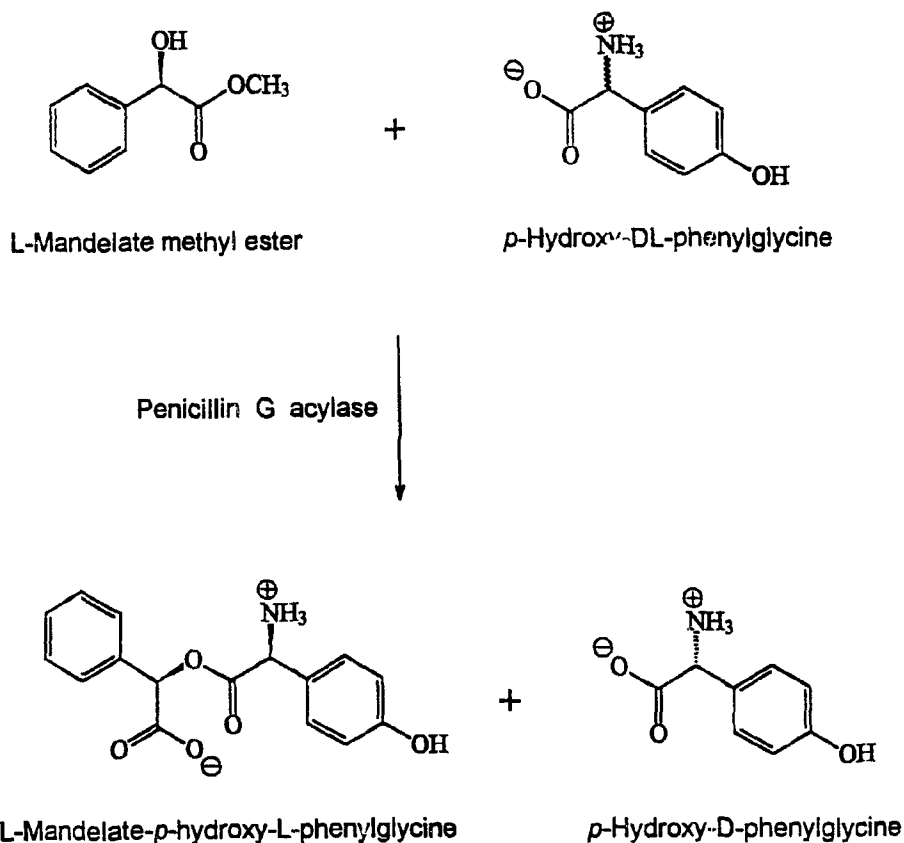


**Figure 4.** Resolution of *p*-hydroxyphenylglycine using acylase.

L-amino acid recovered is racemized chemically and reused (Figure 5). The method was commercialized for the preparation of several amino acids in 1987 (17). D-Alanine has also been produced from DL-alaninamide using *Arthrobacter sp.* cells which contain a D-amidase. The culture medium containing 210 g/L of the DL-alaninamide yielded 105 g/L of D-alanine with over 99% enantiomeric excess (36).

The major drawback to using aminoacylases and amidases is that the maximum yield is 50%. To increase this yield, the undesired enantiomer must be



corresponding amino acids, either chemically or enzymatically (Figure 6). The L-hydantoin derivative left in the reaction mixture can be racemized *in situ* and reprocessed in the system. This allows the system to work continuously and the yield of the D-amino acid could be as high as 100%. The use of organisms containing both D-specific hydantoinase and carbamoylase (EC 3.5.1.77) activities has resulted in production of large scale of D-amino acids such as D-phenylglycine and its *p*-hydroxy derivative (17). Recently, the genes coding for the hydantoinase

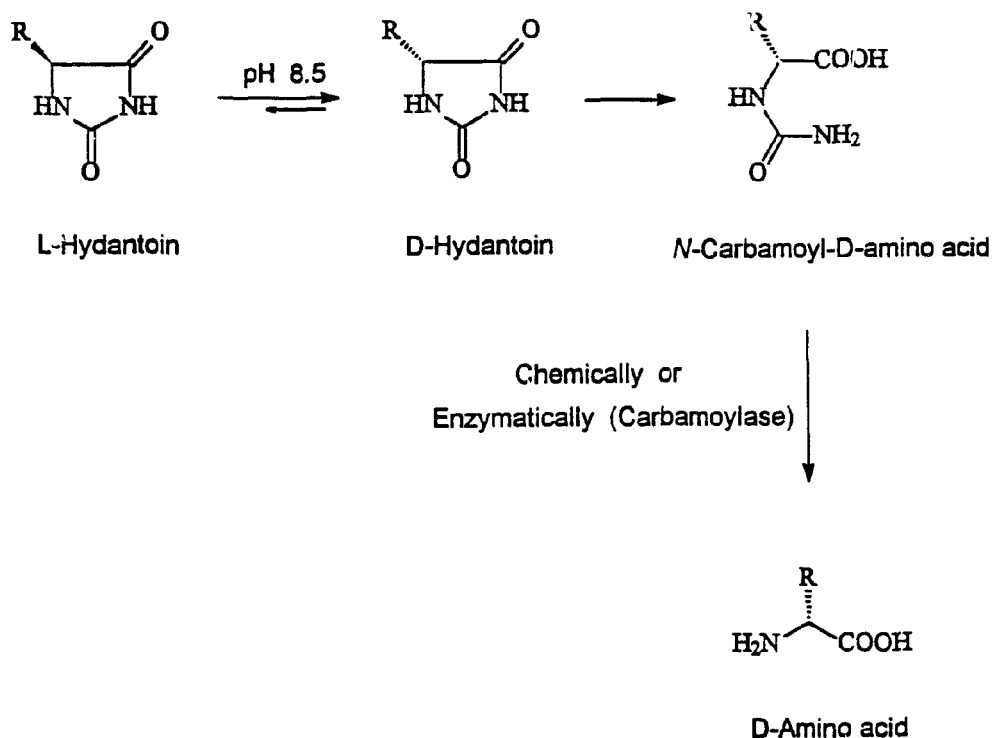


**Figure 6.** D-Amino acid preparation using L-hydantoin derivatives of amino acids.

and carbamoylase enzymes have been cloned into either *E. coli* or *Bacillus subtilis* and used for the production of D-amino acids (37). Among bacteria containing both D-hydantoinase and carbamoylase activities are *Agrobacterium sp. I-671* (38) and *Flavobacter sp. DSM 7330* (39). Both bacteria have been used for production of D-amino acids. Also, the preparation of D-citrulline from the hydantoin derivative of L-citrulline using whole cells of *Agrobacterium radiobacter* was reported. The hydantoin derivative of L-citrulline readily racemizes at the pH of the culture (pH 8.4) (40). A series of D-amino acids were prepared using commercially available D-hydantoinases followed by chemical conversion of the *N*-carbamoyl-D-amino acids to their corresponding D-amino acids (41).

### 1.3 Glutamate Catabolism

The investigation of catabolic pathways of various amino acids used by anaerobic bacteria has been of interest to many scientists for the past half of this century. One of the most interesting areas has been the identification of the metabolic pathway(s) by which glutamate is degraded. This investigation was stimulated by the fact that anaerobes produce one mole of CO<sub>2</sub> per mole of glutamate degraded whereas aerobes produce 3 moles of CO<sub>2</sub> per mole of glutamate *via* the tricarboxylic acid cycle (42). Based on results obtained from the degradation of isotopically labelled compounds and the identification and purification of enzymes, three distinct pathways for the catabolism of glutamate to acetate and butyrate have been proposed (Table 1). The evidence in support of

the individual routes is described in subsequent sections.

### 1.3.1 Acetate and Butyrate Interconversion

The final steps of all the glutamate degradation pathways involve the interconversion of acetate and butyrate *via* crotonyl-CoA (Figure 7). The details of the experiments establishing these enzyme-catalyzed reactions are described below, and an understanding of this pathway (*i.e.*, Figure 7) is needed to interpret the isotopic results obtained from studies of glutamate catabolism.

Table 1. Proposed intermediates in three pathways of glutamate catabolism.

Pathway	Intermediates
Methylaspartate (Figure 8)	$\beta$ -Methylaspartate, Mesaconate, L-Citramalate, Pyruvate
Hydroxyglutarate (Figure 9)	2-Oxoglutarate, ( <i>R</i> )-2-Hydroxyglutarate, ( <i>E</i> )-Glutaconate, Glutaconyl-CoA, Crotonyl-CoA
Aminobutyrate (Figure 12)	4-Aminobutyrate, Succinic semialdehyde, 4-Hydroxybutyrate, 4-Hydroxybutyrate-CoA, Vinylacetyl-CoA, Crotonyl-CoA

In an early investigation on the mechanism of the formation of acetate from CO<sub>2</sub> by *Butyrobacterium rettgeri*, glucose was fermented in the presence of [1-

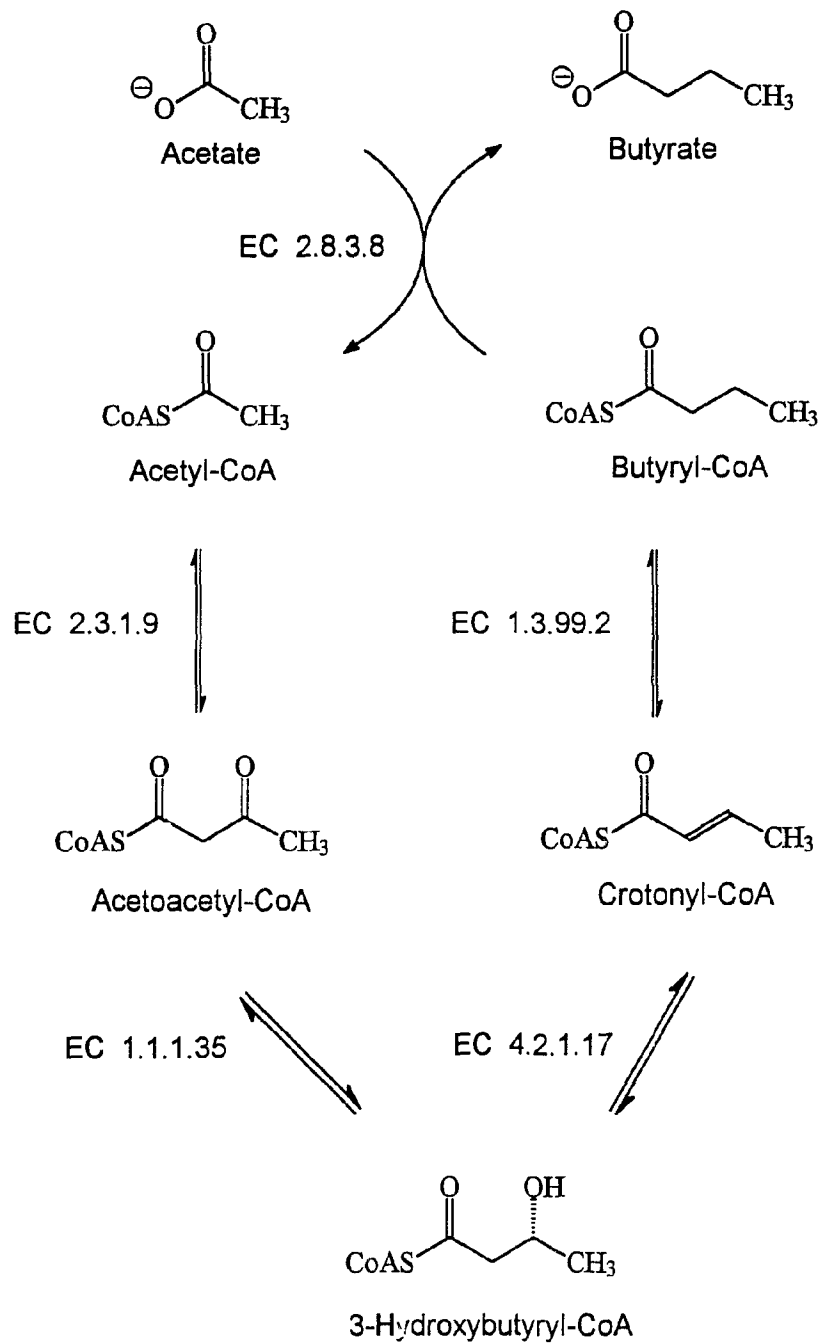


**Figure 7.** Interconversion of acetate and butyrate in anaerobic microorganisms.

$^{14}\text{C}$ ]acetate and  $[2\text{-}^{14}\text{C}]$ acetate, and a high level of radioactivity was recovered in butyrate. However, the location of isotope in butyrate was not determined (43). The first demonstration of intact incorporation of acetate into butyrate was made when  $[1\text{-}^{13}\text{C}]$ acetate was coadministered with starch to the culture of *Clostridium acetobutylicum*; C-1 and C-3 of butyrate and butanol were enriched equally (44). Subsequently, the incorporation of  $^{13}\text{C}$ -labelled ethanol and acetate into butyrate and caproate was demonstrated in *Clostridium kluyveri* (45). Furthermore, in an investigation of succinate catabolism to acetate and butyrate by *C. kluyveri*,  $[1,4\text{-}^{13}\text{C}_2]$ succinate was degraded to  $[1\text{-}^{13}\text{C}]$ acetate,  $[2\text{-}^{13}\text{C}]$ acetate and fully-labelled butyrate. The butyrate was enriched equally at C-1,4 and C-2,3. However, the enrichment in C-1,4 was four times that in C-2,3, indicating formation of butyrate either directly from succinyl-CoA or from two acetate molecules (46). The sequence of reactions leading to incorporation of label from carboxyl group of succinate into C-4 of butyrate are, reduction, dehydration and reduction. Consequently, the acetate formed from butyrate labelled at C-4 would be labelled at C-2.

Five major enzymic activities are involved in the interconversion of acetate and butyrate (Figure 7) including butyryl-CoA:acetate CoA-transferase (EC 2.8.3.8), acetylCoA:acetylCoA acetyltransferase (thiolase) (EC 2.3.1.9), hydroxybutyryl-CoA dehydrogenase (EC 1.1.1.35), crotonase (EC 4.2.1.17) and butyryl-CoA dehydrogenase (EC 1.3.99.2). Activities associated with these enzymes have been detected in *C. kluyveri* (44), *Peptostreptococcus asacharoliticus* (47) and *F.*

*nucleatum* (48), and most of the enzymes have been purified and characterized (49).

### 1.3.2 The Methylaspartate Pathway

The methylaspartate pathway (Figure 8) was the first pathway of glutamate catabolism discovered in anaerobic bacteria, and the initial evidence was obtained from isotopic feeding experiments in *Clostridium tetanomorphum* (42). Radioactivity from L-[5-<sup>14</sup>C]glutamate was recovered in CO<sub>2</sub>, whereas most of the radioactivity

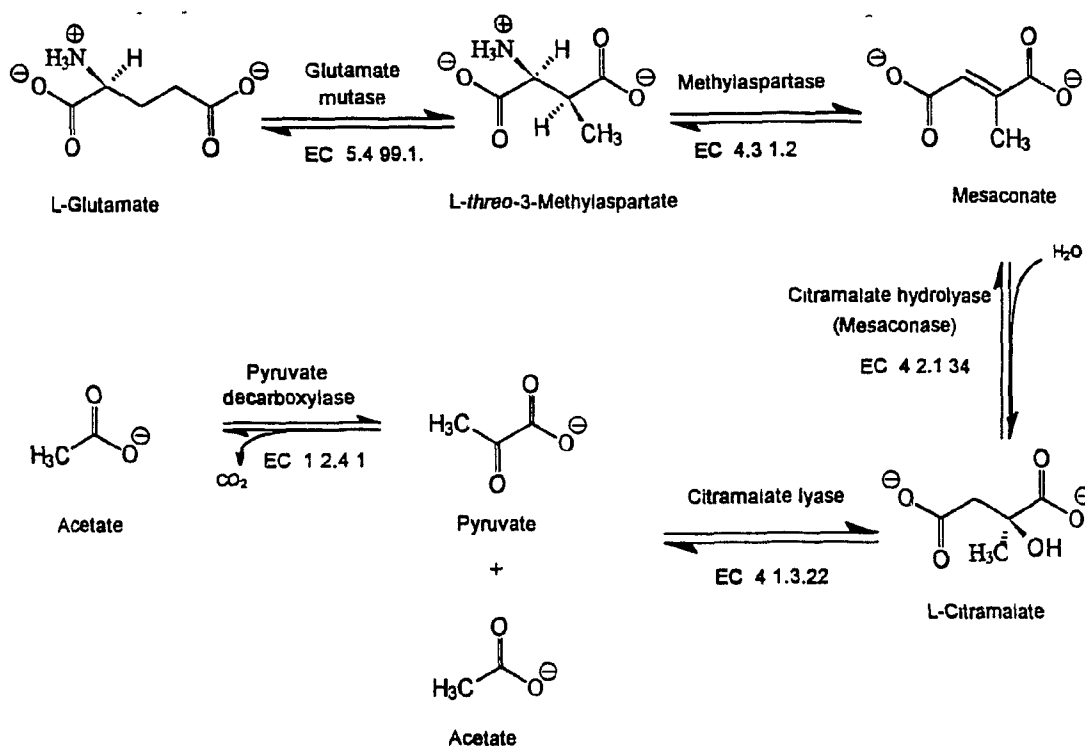


**Figure 8.** Glutamate catabolism via the methylaspartate pathway.

from L-[1-<sup>14</sup>C]glutamate and L-[2-<sup>14</sup>C]glutamate was located in C-1 and C-2 of acetate, respectively. These results indicated that C-1 and C-2 of glutamate are preferentially converted to acetate. However, more than 1 mole of acetate is produced when 1 mole of glutamate is fermented, suggesting that C-3 and C-4 of glutamate are also converted to acetate. Since it was known that glutamate is an intermediate in histidine degradation and that L-[2-<sup>14</sup>C]histidine is converted to L-[4-<sup>14</sup>C]glutamate, L-[2-<sup>14</sup>C]histidine was administered to resting cells of *C. tetanomorphum*. The butyrate obtained had approximately twice the specific radioactivity of the initial L-[2-<sup>14</sup>C]histidine, indicating that butyrate was synthesized from two C<sub>2</sub> units derived from C-4 of glutamate. The label was located equally and exclusively at C-1 and C-3 of butyrate. Furthermore, the specific radioactivity of butyrate formed either during the fermentation of L-[1-<sup>14</sup>C]glutamate and L-[2-<sup>14</sup>C]glutamate or during the fermentation of unlabelled glutamate in the presence of L-[1-<sup>14</sup>C]acetate was the same order of magnitude, indicating that the incorporation of C-1 and C-2 of glutamate into butyrate may occur *via* acetate (50).

Evidence for intermediates in this pathway were obtained using a cell-free extract of *C. tetanomorphum* which converted glutamate to ammonia, CO<sub>2</sub>, H<sub>2</sub>, and acetate, but not butyrate. It was found that degradation of L-glutamate produced an unsaturated dicarboxylic acid which was characterized as mesaconic acid (51). Formation of mesaconate from glutamate would mean rearrangement of the straight chain of glutamate by migration of either a single carbon atom or a pair of adjacent carbon atoms. To investigate the origin of the methyl carbon atom of

mesaconate, L-[4-<sup>14</sup>C]glutamate was incubated with the cell-free extract of *C. tetanomorphum* and mesaconate was isolated. Chemical degradation of the labelled mesaconate indicated that C-4 of glutamate was delivered to the carbon adjacent to the methyl group of mesaconate. This result demonstrated that the bond cleavage in glutamate must occur between C-2 and C-3 of glutamate (52).

The extract of *C. tetanomorphum* degraded the mesaconate to CO<sub>2</sub>, H<sub>2</sub>, pyruvate, and acetate, and another product, which appeared to be a dicarboxylic acid containing one or more hydroxy groups. Based on the structure of mesaconate, α- or β-methylmalic acid (also known as citramalic acid) formed by hydration of the double bond in mesaconate was considered as the accumulated product. However, the β-isomer of methylmalate was the more likely intermediate because an aldol type cleavage would convert it to pyruvate and acetate, known products of mesaconate degradation in this system. DL-Citramalate was degraded to pyruvate and acetate by a cell-free extract of *C. tetanomorphum*, indicating that mesaconate and citramalate are the intermediate in glutamate degradation (42). Later, citramalate hydrolyase (mesaconase) (EC 4.2.1.34) which catalyzes the reversible dehydration of mesaconate to L-citramalate was purified and characterized (53). The activity of the enzyme is dependent upon the presence of ferrous ion and cysteine and is inhibited by α',α'-dipyridyl and o-phenanthroline (42). The enzyme is inactivated by oxygen, but activity is restored by anaerobic incubation with sulfhydryl compounds (54). L-Citramalate, L-malate, mesaconate and fumarate are known substrates for this enzyme (55).

The conversion of L-citramalate to pyruvate and acetate is catalyzed by citramalate lyase (citramalate pyruvate lyase) (EC 4.1.3.22). This enzyme is unstable; incubation of the extract of *C. tetanomorphum* at 37°C for 1 hour leads to loss of the ability to degrade L-citramalate. Since most of the other enzymes involved in glutamate catabolism are more stable, this has been used to obtain L-citramalate by the degradation of other substrates (42). The only substrate known to be cleaved by this enzyme is L-citramalate, and a divalent cation such as  $Mg^{2+}$ ,  $Co^{2+}$ , or  $Mn^{2+}$  is needed for activity (56). The enzyme was also purified to homogeneity from extracts of *C. tetanomorphum*. It has a hexameric structure and contains an acetylated thioester residue in its active site which plays a central role in the catalytic mechanism. Catalytic activity can be restored by incubating the inactivated enzyme with dithiothreitol and acetic anhydride (57).

When a cell-free extract of *C. tetanomorphum* was treated with charcoal in the presence of o-phenanthroline, the conversion of glutamate to mesaconate was largely suppressed and a second amino acid accumulated in substantial amounts. That an amino acid other than glutamate formed in the charcoal-treated extract was supported by the observation that this amino acid did not decarboxylate when incubated with L-glutamate decarboxylase of *E. coli*. (42). The amino acid was isolated in large quantities and identified as L-threo- $\beta$ -methylaspartate (58), and the enzyme  $\beta$ -methylaspartase (EC 4.3.1.2) involved in the reversible conversion of this amino acid to mesaconate and ammonia was detected in partially purified extracts from *C. tetanomorphum*. L-threo- $\beta$ -Methylaspartate, L-erythro- $\beta$ -

methylaspartate and aspartate are substrates for the enzyme (59). Recently, mechanistic studies of the methylaspartase from *C. tetanomorphum* (60-62) and the cloning of the gene encoding the enzyme (663) have been reported. The enzyme has also been crystallized from *C. tetanomorphum* (64) and *E. coli* (65). As previously mentioned, C-4 of mesaconate is delivered to the carbon adjacent to the methyl group of mesaconate and, since mesaconate and  $\beta$ -methylaspartate have identical carbon skeletons, the same conclusion applies to  $\beta$ -methylaspartate (42).

The inability of cell-free extracts of *C. tetanomorphum* treated with charcoal to degrade glutamate was due to the removal of an essential cofactor, which was isolated from *C. tetanomorphum* and shown to be a yellow-orange compound readily inactivated by exposure to visible light. The cofactor is a derivative of vitamin B<sub>12</sub> containing an additional molecule of adenine (66). Glutamate mutase (E.C. 5.4.99.1) was the first example of a coenzyme B<sub>12</sub>-dependent enzyme. It has been partially purified and characterized and consists of two separable protein subunits called component E and component S. Both components are essential for activity (67). Pure preparations of each component were obtained from *C. cochlearium* (68). The genes from *C. tetanomorphum* encoding components E and S (69, 70, 71) and from *C. cochlearium* encoding component S (72) have been cloned and sequenced.

### 1.3.3 The Hydroxyglutarate Pathway

The degradation of glutamate by *M. aerogenes* yields butyrate, acetate, CO<sub>2</sub>, NH<sub>3</sub> in quantities similar to those formed by *C. tetanomorphum* via the methylaspartate pathway, but mesaconate and β-methylaspartate are not metabolized by *M. aerogenes* (73). Initial evidence for a different pathway of glutamate catabolism (Figure 9) was obtained by Horler *et al.* (74). When L-[1-<sup>14</sup>C]glutamate was supplied to *M. aerogenes*, most of the radioactivity in butyrate was located in C-1 with a smaller amount in C-3. Similar results were obtained with L-[2-<sup>14</sup>C]glutamate, *i.e.*, the radioactivity at C-2 was higher than that at C-4 of butyrate. The unequal distribution of radioactivity in the butyrate samples obtained in these experiments was not consistent with the methylaspartate pathway, and suggested that butyrate was formed from an intact four-carbon unit of glutamate. An experiment using DL-[3,4-<sup>14</sup>C]glutamate generated labelled butyrate with most of the radioactivity located at C-3 and C-4; all four carbons should have been equally radioactive if butyrate had been formed by the methylaspartate pathway. Similar results were reported for the catabolism of glutamate in two strains of *F. nucleatum* (75). The incorporation of C-1 of glutamate into C-1 of butyrate, C-4 into C-2,3,4 of butyrate, and the nonincorporation of C-5 of glutamate were consistent with the hydroxyglutarate pathway. In another study (2), no radioactivity was recovered in CO<sub>2</sub> when [1-<sup>14</sup>C]glutamate was used as the substrate, whereas 95% of the total radioactivity was released as CO<sub>2</sub> from [5-<sup>14</sup>C]glutamate by cells of *F. nucleatum*. These results

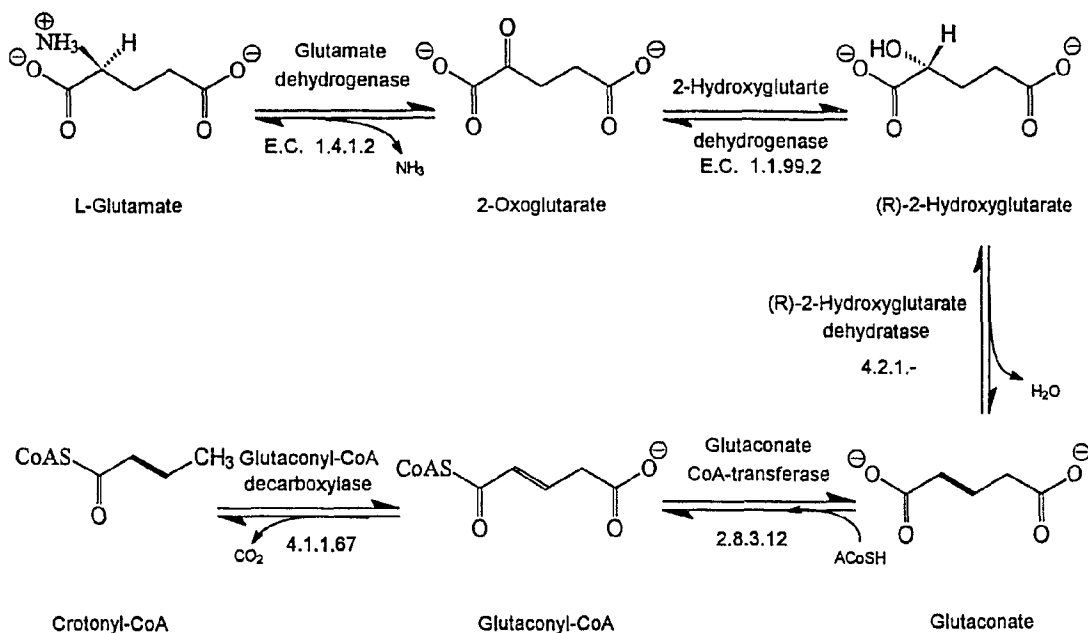


**Figure 9.** Glutamate catabolism via the hydroxyglutarate pathway.

are consistent with the hydroxyglutarate pathway. The first investigation of glutamate catabolism in *F. varium* was done when Foglesong *et al.* (76) investigated the pleomorphism of *F. varium* isolated from the cockroach hindgut. Administration of  $[1-^{14}\text{C}]$ glutamate to culture of *F. varium* resulted in butyrate labelled 26 times higher at C-1 than C-2,3,4 indicating the presence of the hydroxyglutarate pathway.

The results of these isotopic experiments suggested that butyrate was formed principally from the first four carbons of glutamate without cleavage of the

chain. In the early hours of the incubation, the  $^{14}\text{C}$  content of cultures supplemented with L-[5- $^{14}\text{C}$ ]glutamate was similar to cultures administered either L-[1- $^{14}\text{C}$ ]glutamate or L-[2- $^{14}\text{C}$ ]glutamate. At a longer times, C-5 of glutamate was lost from the culture as  $\text{CO}_2$ , suggesting that non-volatile components of the medium are intermediates rather than end-products of the reaction. Crotonic acid was considered as a possible intermediate, but it could not be detected in the medium (74). This finding led to the isolation and identification of glutaconyl-CoA as an intermediate in the hydroxyglutarate pathway of the glutamate catabolism in *M. aerogenes*. Glutaconyl-CoA was previously known as an intermediate in the fermentation of glutaryl-CoA by *Pseudomonas fluorescens* (77).

In a separate investigation,  $^{14}\text{C}$ -labelled 2-hydroxyglutarate was isolated from a cell-free extract of *M. aerogenes* incubated with [1- $^{14}\text{C}$ ]- or [5- $^{14}\text{C}$ ]-glutamate and  $\text{NAD}^+$ . To account for these observations, Johnson and Westlake proposed that 2-oxoglutarate and 2-hydroxyglutarate are formed from glutamate (78). Preliminary evidence was presented for the presence of enzymes catalyzing these reactions in *M. aerogenes*, and subsequently high levels of both glutamate dehydrogenase and hydroxyglutarate dehydrogenase (EC 1.1.99.2) activities were detected in cell-free extracts of *M. aerogenes* (79, 80) and *F. nucleatum* (2, 75). Glutamate dehydrogenase reductively deaminates the glutamate to 2-oxoglutarate and hydroxyglutarate dehydrogenase catalyzes the reduction of 2-oxoglutarate to 2-hydroxyglutarate. Both glutamate dehydrogenase (81) and hydroxyglutarate dehydrogenase were isolated, partially purified, and characterized from *M.*

*aerogenes* (82). The 2-hydroxyglutarate dehydrogenase was also purified from *F. nucleatum* and, among the 2-oxoacids tested, only 2-oxoglutarate was a substrate (83). Glutamate dehydrogenase also has been purified and characterized from *C. symbiosum*, which uses the hydroxyglutarate pathway for glutamate catabolism (84). From this isotopic and enzymatic evidence, Buckel and Barker (75) proposed the hydroxyglutarate pathway for the degradation of glutamate (Figure 9).

To this stage the fate of 2-hydroxyglutarate remained unclear, although it was postulated to be converted to crotonyl-CoA *via* glutaconyl-CoA. In support of his hypothesis, Buckel (85) found that the 3-*pro-S* hydrogen of 2-hydroxyglutarate is removed stereospecifically to give (*E*)-glutaconate by whole cells of *C. symbiosum* and *Acidaminococcus fermentans*. Cell-free extracts of *A. fermentans* were also able to ferment L-glutamate, (*R*)-2-hydroxyglutarate and (*E*)-glutaconate, whereas the conversion of 2-hydroxyglutarate to glutaconate required a catalytic amount of acetyl-CoA or coenzyme A and acetylphosphate. With regard to the latter observation, it was concluded that the dehydration and the subsequent decarboxylation of glutaconate occurred on the CoA ester. No reaction occurred with (*Z*)-glutaconate, (*S*)-2-hydroxyglutarate or 3-hydroxyglutarate in cell-free extracts, and additional evidence for the dehydration of (*R*)-2-hydroxyglutarate to (*E*)-glutaconate was achieved by trapping labelled (*E*)-glutaconate with an excess of unlabelled compound (85).

Dehydration of 2-hydroxyglutarate to glutaconate involves abstraction of a hydrogen which is not acidic enough to be removed by aqueous acid-base

catalysis. Also in the reverse direction, *i.e.*, hydration of glutaconate to 2-hydroxyglutarate, an ionic mechanism would favour the formation of 3-hydroxyglutarate rather than 2-hydroxyglutarate. With these facts and the observation of an extra signal in the ESR spectrum of activated enzyme compared to the inactivated form, Schweiger and Buckel (86) proposed a radical mechanism which involves participation of a hydroxy radical produced by the enzyme (Figure 10). The enzyme catalyzing this reversible reaction is a soluble enzyme and needs CoA, acetyl phosphate, NADH, MgCl<sub>2</sub>, dithioerythritol and FeSO<sub>4</sub> for its activity. Schweiger and Buckel were able to partially purify the 2-hydroxyglutaryl-CoA dehydratase (EC 4.2.1.-) from a cell-free extract of *A. fermentans* (86). The enzyme was also purified from *F. nucleatum* (87) and shown to contain iron, stable sulfur, and reduced riboflavin; the failure to detect free radicals by ESR led to a new hypothesis for 2-hydroxyglutaryl-CoA dehydratase (Figure 11).

As mentioned earlier (85), the dehydration of (*R*)-2-hydroxyglutarate to (*E*)-glutaconate followed by the decarboxylation of the unsaturated dicarboxylic acid requires acetyl-CoA, indicating that the actual substrates are the CoA esters. Klees *et al.* (87) were able to purify and characterize the glutaconate CoA-transferase (EC 2.8.3.12) from *A. fermentans*. The enzyme converts glutaconate to glutaconyl-CoA prior to decarboxylation. It was shown that only the (*E*)-isomer of glutaconate is the substrate and that the product of the reaction is glutaconyl-CoA esterified at the carboxyl group closest to the double bond, *i.e.*, the thiol ester is conjugated to the double bond. A high enzyme activity was also detected in two *Clostridia*

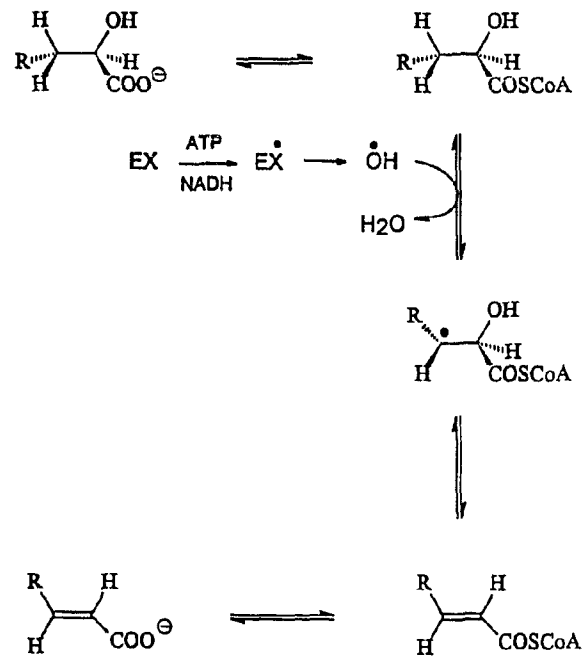


**Figure 10.** Proposed radical mechanism for the dehydratase from *A. fermentans*.

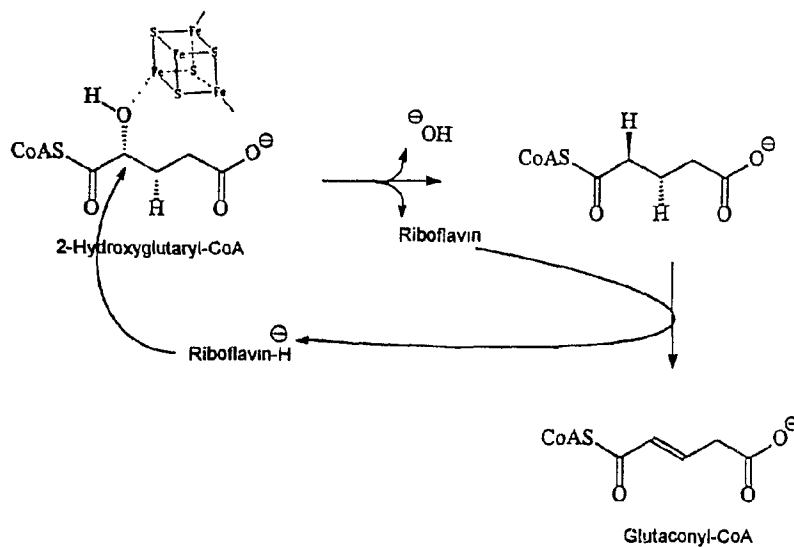


**Figure 11.** Hypothetical mechanism for the *syn*-dehydration of (*R*)-2-hydroxyglutaryl-CoA to (*E*)-glutaconyl-CoA by the dehydratase from *F. nucleatum*.

species (*C. symbiosum* and *C. sporophaeroides*) which ferment glutamate via the hydroxyglutarate pathway.

The next step in the formation of crotonyl-CoA from glutaconyl-CoA involves decarboxylation catalyzed by glutaconyl-CoA decarboxylase (EC 4.1.1.67). Stimulation of substrate fermentation by an excess of biotin and inhibition by avidin indicated that the decarboxylation of glutaconate is a biotin-dependent reaction (85). With purified enzyme from *A. fermentans*, it was demonstrated that glutaconyl-CoA decarboxylase is a biotin-dependent sodium pump (89) and that the decarboxylation reaction catalyzed by glutaconyl-CoA decarboxylase is stereospecific, proceeding with retention of configuration (90). The enzyme has also been purified from *F. nucleatum* (88) and the gene encoding the carboxytransferase subunit of the enzyme has been cloned into *E. coli* (92).

#### 1.3.4 The Aminobutyrate Pathway

The third pathway for glutamate catabolism (Figure 12) was proposed by Gharbia and Shah (2) to account for the relatively small amount of radioactive CO<sub>2</sub> released by cultures of *F. varium* supplemented with [1-<sup>14</sup>C]glutamate. This interpretation was supported by enzyme assay results which indicated that 4-hydroxybutyrate dehydrogenase (EC 1.1.1.61) and acetyl-CoA:4-hydroxybutyryl-CoA transferase were present in crude cell-free extracts. No other evidence for this pathway has been reported, but the degradation of 4-aminobutyrate by *C. aminobutyricum* has been documented (93, 94) as part of an investigation of the

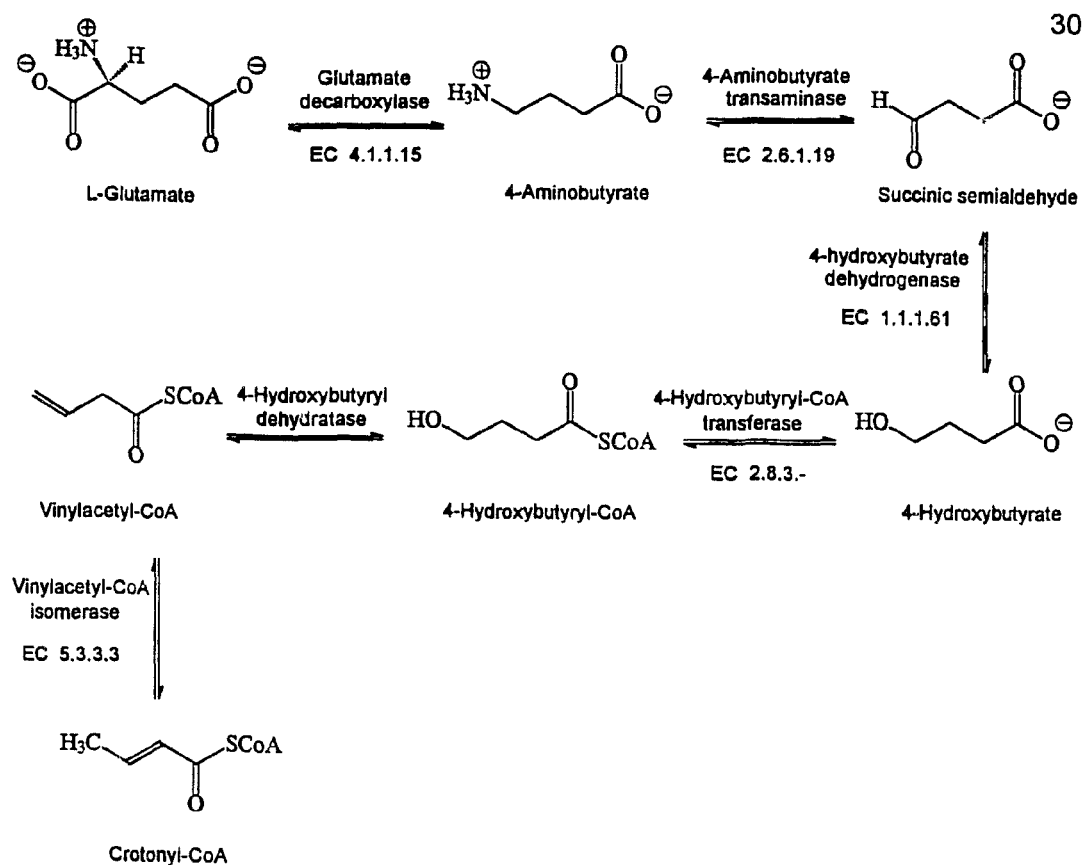


**Figure 12.** Glutamate catabolism *via* the aminobutyrate pathway.

energy-yielding portion of the reductive deamination of glycine. It was found that the initial step in the catabolism of 4-aminobutyrate, a homologue of glycine, is a balanced oxidation-reduction process catalyzed by a three-enzyme system: 4-aminobutyrate transaminase (EC 2.6.1.19), glutamate dehydrogenase, and 4-hydroxybutyrate dehydrogenase. The product from the first reaction (transamination) is succinic semialdehyde which undergoes reduction to give 4-hydroxybutyrate. Glutamate dehydrogenase generates 2-oxoglutarate required for

the transamination reaction as well as NADH which is needed for reduction of succinic semialdehyde. 2-Oxoglutarate is required for 4-aminobutyrate degradation and succinic semialdehyde accumulates in the absence of NADH. The presence of a glutamate dehydrogenase to provide the 2-oxoglutarate for the transamination reaction was supported by that fact that glutamate is converted to 2-oxoglutarate in the presence of  $\text{NAD}^+$  by the cell-free extract of *C. aminobutyricum*. (93).

The next step in the pathway is the reduction of succinate semialdehyde to 4-hydroxybutyrate. The enzyme catalyzing this reaction was detected and partially purified from a cell-free extract of *C. aminobutyricum* and 4-hydroxybutyrate was also isolated as a product of 4-aminobutyrate degradation (95). Furthermore, in the absence of glutamate, no metabolism of succinate semialdehyde was observed, indicating that  $\text{NAD}^+$  produced by oxidative deamination of glutamate was needed for reduction of succinate semialdehyde to 4-hydroxyglutarate by 4-hydroxyglutarate dehydrogenase (93).

The conversion of 4-hydroxybutyrate to acetate and butyrate was observed when a cell-free extract of *C. aminobutyricum* was incubated with either 4-hydroxybutyryl-CoA or 4-hydroxybutyrate plus acetyl-CoA. 4-Hydroxybutyrate was not metabolized under these conditions, indicating that the actual substrate is the CoA ester (94). Recently 4-hydroxybutyrate CoA-transferase (EC 2.8.3.-) was purified and characterized from *C. aminobutyricum*. The enzyme has a broad substrate specificity, but 4-hydroxybutyrate was the best substrate (96).

Formation of crotonyl-CoA from either 4-hydroxybutyryl-CoA or vinylacetyl-

CoA was also detected spectrophotometrically, but attempts to isolate vinylacetyl-CoA formed from 4-hydroxybutyryl-CoA failed (94). However, Bartsch and Barker (97) were able to obtain a partially purified vinylacetyl-CoA isomerase (E.C. 5.3.3.3) from *C. kluyveri* which converted vinylacetyl-CoA to crotonyl-CoA, but the reverse reaction, *i.e.*, crotonyl-CoA to vinylacetyl-CoA was not catalyzed.

4-Hydroxybutyryl-CoA dehydratase activity was detected in an extract of *C. aminobutyricum* by direct assay using 4-hydroxy[3-<sup>3</sup>H]butyric acid. About 50% of the tritium was recovered in water indicating that removal of hydrogen is stereospecific and, more importantly, excluding a mechanism involving an intramolecular coenzyme B<sub>12</sub>-dependent rearrangement to form 3-hydroxybutyryl-CoA (98).

### **1.3.5. Distribution of the Glutamate Pathways Among Anaerobic Bacteria**

Species of anaerobic bacteria have been classified based on either their ability to degrade amino acids or the end-products formed from amino acid catabolism. For example, 30 species of clostridia have been tested for amino acid catabolism and divided into four groups by Mead (99). Species in group one reduced proline, or arginine to  $\delta$ -aminovalerate by oxidizing phenylalanine and serine in a Stickland reaction. Group two utilized arginine and/or glycine. Group three used glutamate, histidine, and serine, whereas serine and threonine were utilized by group four.

*Clostridium* species in group three that utilized glutamate, as well as

histidine and serine, and species from other genus of anaerobic bacteria have been investigated for the different pathways by which glutamate is degraded. In these studies, both isotopically-labelled glutamate and enzyme assay have been employed. Buckel and Barker (75) found that eight out of nine species of clostridia used the methylaspartate pathway, whereas *A. fermentans*, *F. nucleatum* and *P. aerogenes* used the hydroxyglutarate pathway. This result indicated that the methylaspartate pathway only occurs in *Clostridium* species, and that the hydroxyglutarate route is present in different genera of anaerobic bacteria. A similar study (100) using doubly-labelled glutamate and enzyme assays demonstrated that the methylaspartate pathway was used by all species of clostridia tested except one, and that *A. fermentans* used the hydroxyglutarate pathway.

In a study on pathways of glutamate catabolism among fusobacteria, the occurrence of more than one pathway in some species was suggested (2). In addition, the presence of a third pathway for glutamate catabolism was proposed. The results indicated that, although the pathway used by fusobacteria bore no relationship to the site of isolation of the bacterium tested, it could be correlated to their chemotaxonomic properties, *i.e.*, fusobacteria with a peptidoglycan structure based on diaminopimelate used two or three pathways for glutamate catabolism, whereas species with lanthionine-based mucopeptide catabolized glutamate solely *via* the hydroxyglutarate pathway. However, it should be mentioned that isotopic experiments and enzyme assays performed in this

investigation did not conclusively support individual pathways.

#### 1.4 Outline of Thesis and Literature Discrepancies

In this thesis, the catabolism of amino acids, particularly glutamic acid is examined in two *Fusobacterium* species, *F. nucleatum* and *F. varium*.

*F. nucleatum* is a nonsporeforming, nonmotile and Gram negative bacterium in the family *Bacteroidaceae*. *F. nucleatum* can be found in the body cavities of humans and animals (102) and, of the microbial species that are statistically associated with periodontal disease, it is one of the most common species found in infections of other human body sites (7). The role of *F. nucleatum* in the development of periodontal diseases has lately attracted new interest. The bacterium increases in proportion as dental plaque forms (103). It has been isolated from infections associated with gingivitis (104). Positive correlations for periodontal, as well as endodontal diseases, have been observed between *F. nucleatum* and *C. rectus*, *Prevotella intermedia* and *Peptostreptococcus micros*, and most importantly, *P. intermedia*, another periodontal pathogen, can not be colonized without the presence of *F. nucleatum* (105).

Glutamate is a preferred substrate for *F. nucleatum* and inhibits the uptake of other fermentable amino acids, e.g., arginine, ornithine, histidine, and lysine (108, 15). Furthermore, glutamate constitutes a major fraction of the free amino acids in dental plaque (109), and may support the growth and the survival of this species *in vivo*. As a result, the catabolism of glutamate in *F. nucleatum* is of

important interest.

The end-products of glutamate catabolism are mainly acetate and butyrate. It has been shown that butyrate, propionate and ammonium ions inhibit proliferation of human gingival fibroblasts (106) and are present at high levels in plaque associated with periodontitis (107). As a result, these end-products may have an etiological role in periodontal diseases.

*F. varium* is an inhabitant of gastrointestinal tract. Although it is encountered less frequently than *F. nucleatum* in infectious diseases, it is relatively resistant to antibiotics and may cause serious infections in any part of body (104).

Amino acids are important substrates for fusobacteria and, as described in Section 1.1, several investigations on the uptake of amino acids by *F. nucleatum* have been undertaken (8-13). Generally, the stereochemistry of this process has not been considered; usually L- or DL-amino acids were employed, but frequently the stereochemistry of the substrate was not defined. In this thesis, an examination of the common amino acids revealed that several D- and L-amino acids are catabolized by fusobacteria. When the L-isomers were selectively catabolized, the anaerobic bacteria were employed to prepare gram-scale quantities of the corresponding D-amino acid from the racemate.

Based on feeding experiments using [ $^{14}\text{C}$ -labelled]glutamate and enzyme assays, it was documented in earlier sections that two pathways for glutamate catabolism have been established in anaerobic bacteria, and a third pathway was proposed for glutamate degradation in *F. varium*. The latter contradict the earlier

suggestion (76) that *F. varium* uses the hydroxyglutarate pathway for glutamate catabolism. Furthermore, for the first time, the operation of more than one pathway has been suggested in two species of *Fusobacterium*, i.e., *F. varium* and *F. mortiferum* (2). The substrates employed in these experiments were radioactively labelled, and the analysis of the isotopic patterns in end-products (acetate and butyrate) required chemical degradation. Often the exact position of isotope was not determined, and there is insufficient data to evaluate the importance of the third pathway and to determine whether two or three pathways operate simultaneously in a single species. In this investigation, substrates labelled with isotopes that can be located by nmr spectroscopy (e.g.,  $^{13}\text{C}$ ,  $^2\text{H}$ ) were used, and the present results support the hydroxyglutarate pathway in *F. nucleatum* and the methylaspartate pathway in *F. varium*.

Stereospecificity plays an important role in enzymatic reactions involved in the degradation of glutamate in anaerobic bacteria, and the stereospecificity of most of these enzyme-catalyzed reactions, occurring *via* either the 2-hydroxyglutarate or the methylaspartate pathway, has been established in the literature. However, despite an early report by Barker *et al.* (101), which indicated that both D- and L-glutamate were utilized and formed by a cell-free extract of *C. tetanomorphum*, no further experiments on the catabolism of D-glutamate have been reported. In fact, previous isotopic experiments have been carried out with both L- and DL-glutamates without considering possible differences in the catabolism of D- and L-glutamate. The catabolism of the individual stereoisomers of glutamate

was studied in this thesis. Both D- and L-glutamate were degraded by the methylaspartate pathway in *F. varium*, and a glutamate racemase, which catalyzes the interconversion of the stereoisomers, was partially purified from extracts of this organism.

## Chapter 2

### Results: Stereochemical Aspects of Amino Acid Uptake

#### 2.1 Uptake of D- and L-Amino Acids by *Fusobacterium* Species

The uptake of various amino acids by *F. nucleatum* and *F. varium* growing on peptone medium was investigated. Typically, the culture medium was supplemented with a racemic mixture of an amino acid (10 mM) and inoculated with cells of either *F. nucleatum* or *F. varium* cultured on sheep-blood agar. The amino acids in the culture were analyzed by hplc as fluorescent isoindole derivatives formed by reaction with *o*-phthalaldehyde and mercaptoethanol (110). The % uptake of each amino acid (Tables 2 and 3) was calculated by comparing the peak area measured after 36-40 h of incubation to that determined just after inoculation.

Of the 28 amino acids tested, some of the acidic, basic and polar amino acids (Table 2), but none of the aromatic and nonpolar  $\alpha$ -amino acids (Table 3) were metabolised; almost all the DL-glutamine, DL-histidine, and DL-lysine were utilized completely by *F. nucleatum*, while only DL-glutamic acid was completely assimilated by *F. varium*. The metabolism of both amino acid isomers indicated by these results was further investigated by incubating the individual D- and L-isomers of glutamine, histidine, and lysine with *F. nucleatum* and glutamate with *F. varium*. Both isomers of each amino acid were utilized (Table 2; Figures 13 and 14) suggesting that both D- and L-isomers were metabolized.

While the metabolism of L-glutamine, DL-histidine and DL-lysine by *F.*

Table 2. Uptake of amino acids with acidic, basic or polar side-chain substituents.

Amino Acid (10 mM)	Stereoisomer(s) Added Initially % Remaining at 40 h					
	<i>F. nucleatum</i>			<i>F. varium</i>		
	DL-	D-	L-	DL-	D-	L-
Arginine	101			38 <sup>a</sup>	99	48
Citrulline	83			91		
Ornithine	95		58	102		81
Lysine	15	5	3	66	4	3
Histidine	0	0	0	64	92	4
Aspartic Acid	96			95		
Asparagine	82			92		
Glutamic Acid (18 mM)	45 <sup>a</sup>	96	0	0	0	0
2-Aminoadipic Acid	97			96		
Diaminopimelic <sup>b</sup> Acid	70			110		
	54			109		
Glutamine	0	52	0	43	89	18
Serine	48 <sup>a</sup>	102	1	54 <sup>c</sup>	0	0
4-Oxonorvaline	102			82		
Homoserine	93			83		
Threonine	114			106		
Methionine	88			99		

<sup>a</sup> Metabolism of the L-isomer detected by chiral hplc.

<sup>b</sup> The *meso* and racemic forms were separated by hplc.

<sup>c</sup> Metabolism of both D- and L-isomers detected by chiral hplc.

Table 3. Uptake of amino acids with aromatic and hydrophobic side chains.

Amino Acid (10 mM)	Stereoisomer(s) Added Initially % Remaining at 40 h			
	<i>F. nucleatum</i>		<i>F. varium</i>	
	DL-	L-	DL-	L-
Phenylalanine	97		95	
<i>threo</i> - Phenylserine	102		93	
Tyrosine	101		107	
Tryptophan	127		114	
Alanine	124		99	
2-Aminobutyrate	99		87	
3-Aminobutyrate	104		61 <sup>a</sup>	
Valine	102		103	
Isoleucine	118		110	
Leucine	110		112	
Norleucine	132		134	
Norvaline		121		95

<sup>a</sup> Metabolism of both D- and L-isomers detected by chiral hplc

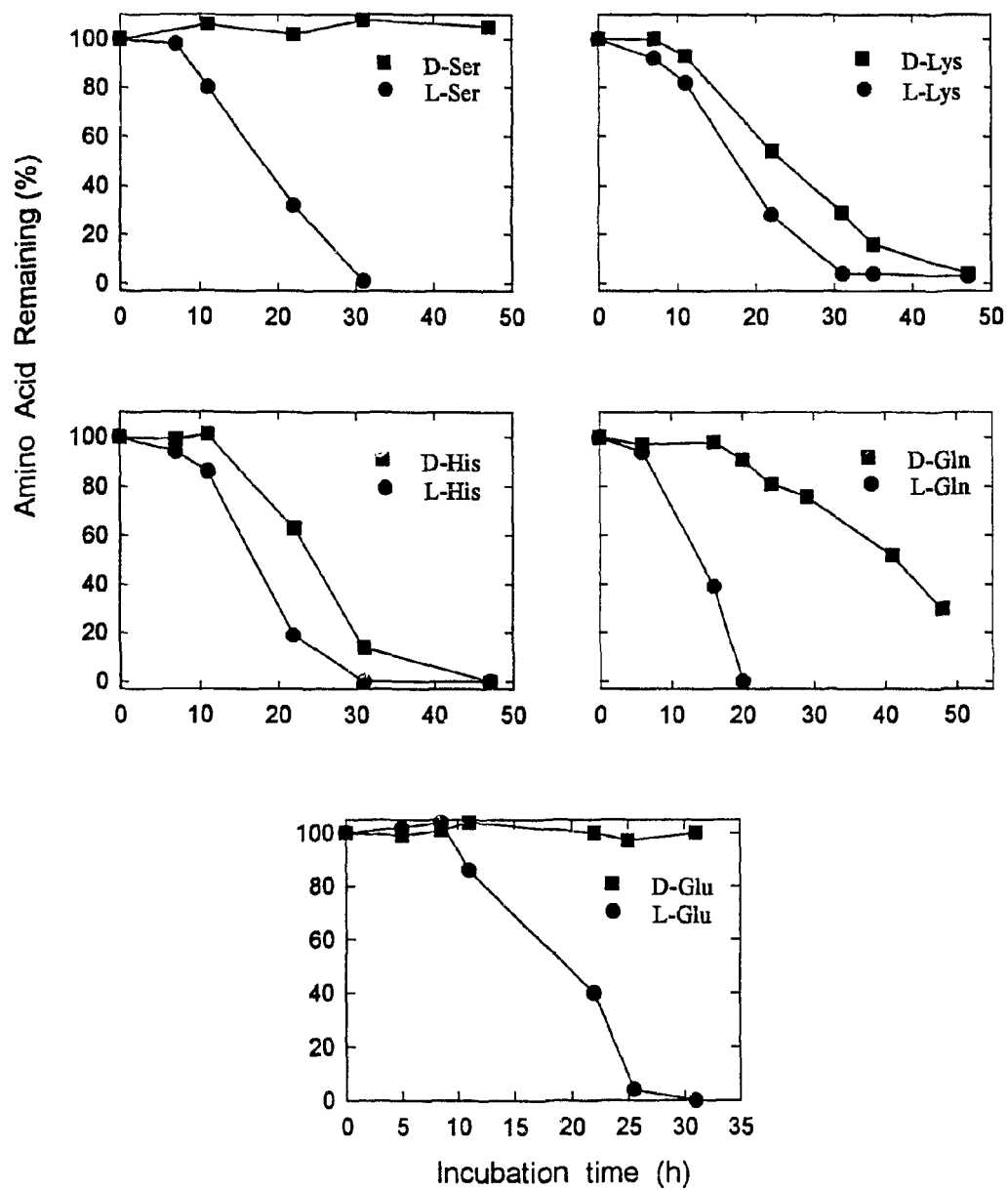


Figure 13. Uptake of D- and L-amino acids by *F. nucleatum*.

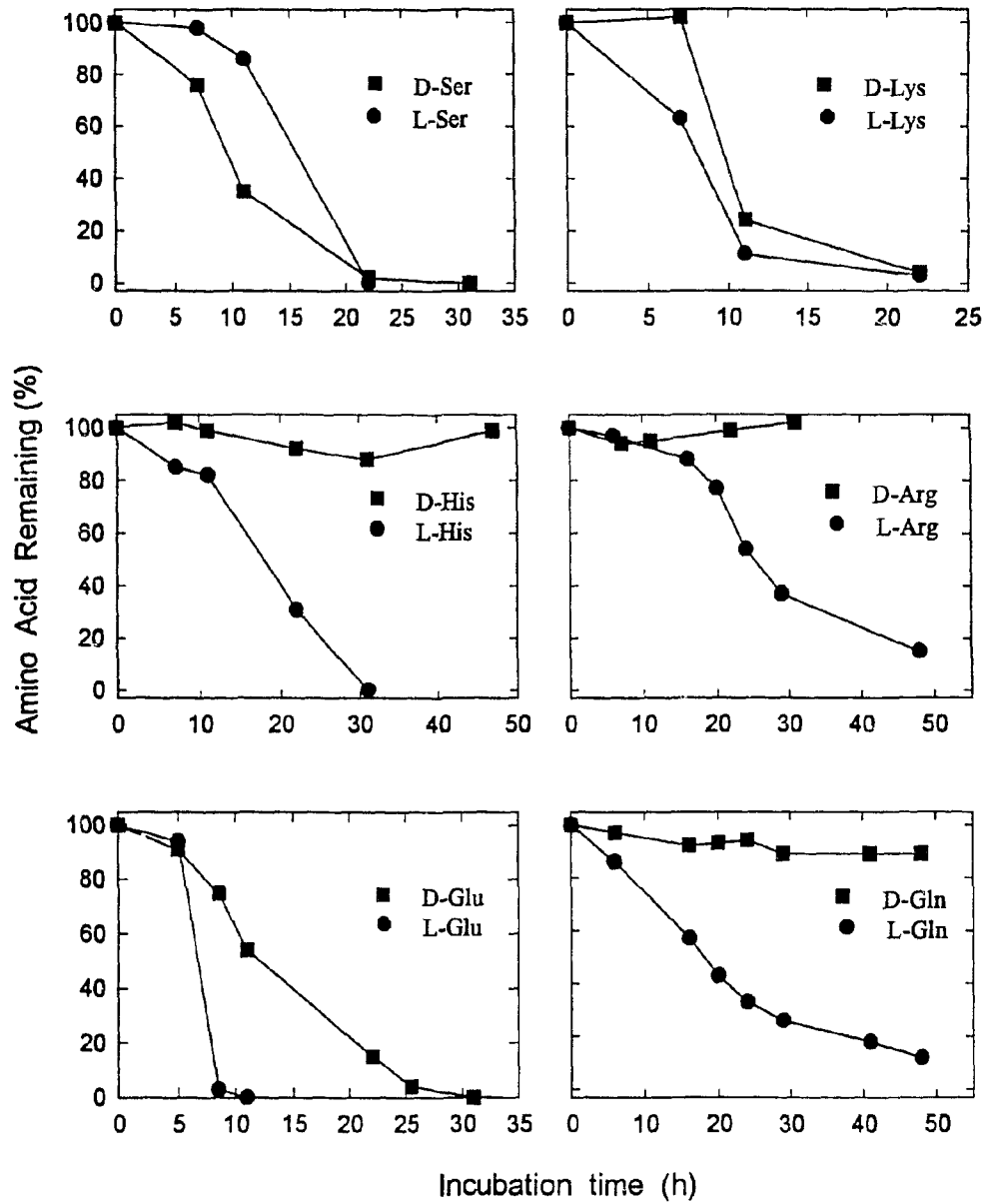


Figure 14. Uptake of D- and L-amino acids by *F. varium*.

*nucleatum* and DL-glutamic acid by *F. varium* did not lead to the accumulation of another amino acid in the culture fluid, a chromatographic peak corresponding to glutamic acid was present in the *F. nucleatum* culture supplemented with D-glutamine. The peak was initially due to the L-glutamic acid present in the peptone medium, but this was utilized by *F. nucleatum* during the first 20 h of the incubation. After 20 h, the glutamate peak increased in intensity, and the amount of glutamate in the culture corresponded to the amount of the glutamine degraded. The non-enzymatic hydrolysis of D-glutamine to D-glutamate is excluded because *F. varium* degraded significantly smaller amounts of D-glutamine under identical conditions (Table 2; Figures 13 and 14).

The D-stereochemistry of the glutamate present at 48 h of the incubation was confirmed by an hplc separation of fluorescent derivatives of amino acids formed by reaction with *o*-phthalaldehyde and *N*-acetylcysteine (111).

About half of the initial DL-glutamate and DL-serine were consumed by *F. nucleatum* (Table 2), whereas *F. varium* metabolized about half of DL-3-aminobutyric acid, DL-arginine, DL-glutamine, DL-histidine, DL-lysine, and DL-serine. Metabolism of about half of a racemic mixture of these amino acids by bacteria might be due to the preferential uptake of one enantiomer over the other, and this possibility was investigated in more detail.

Chiral hplc analysis demonstrated that both enantiomers of 3-aminobutyric acid and serine were assimilated, and the uptake of the individual serine isomers was substantiated in separate experiments (Figure 14). Incubation of the individual

isomers of lysine also demonstrated that the partial metabolism of the racemic mixture by *F. varium* was also due to the metabolism of both enantiomers and not to the selective uptake of one enantiomer (Figure 14).

For amino acids in which both isomers were catabolized, incubations of the single enantiomers demonstrated that the D-amino acids were assimilated at a slower rate (Figures 13 and 14). The only exception was the more rapid uptake of D-serine by *F. varium*.

Chiral hplc analysis indicated that the approximately 50% of DL-serine and DL-glutamic acid by *F. nucleatum* and DL-arginine by *F. varium* corresponds to selective uptake of the L-enantiomer of these amino acids by the respective bacteria. These observations and the partial uptake of DL-histidine were tested further by incubating single isomers of the amino acids and analyzing by hplc (Table 2 and Figures 13 and 14). The results of the single isomer incubations confirm that only the L-enantiomers of glutamic acid and serine are metabolized by *F. nucleatum*, and arginine and histidine by *F. varium*.

Partial metabolism of diaminopimelic acid by *F. nucleatum* was also observed (Table 2). The commercial sample was a mixture of *meso* and racemic forms and these were separated by hplc (retention times were 5.5 and 5.7 min). Although the hplc peaks were not assigned, the area of each decreased during the incubation, indicating that the *meso* isomer and either one or both of the enantiomeric forms of diaminopimelic acid were assimilated. Further analysis of the stereochemical aspects of diaminopimelic acid catabolism requires

stereochemically pure standards.

## 2.2 Preparation of D-Amino Acids from Racemic Mixtures

The enantioselective metabolism observed for the four amino acids suggested that incubation of racemic mixtures with anaerobic bacteria is a feasible approach for the preparation of D-amino acids. Growth conditions for the preparation of D-glutamic acid and D-serine by *F. nucleatum* and D-arginine by *F. varium* from their racemic mixtures were investigated either in peptone medium for D-glutamic acid preparation or in resuspension medium for D-arginine, D-glutamic acid, and D-serine preparation.

### 2.2.1 D-Amino Acid Preparation by *F. nucleatum* Cultures Growing on Peptone Medium

A preliminary experiment was carried out to prepare D-glutamic acid from its racemic mixture (30 mM) using *F. nucleatum* growing on peptone medium. The culture supernatant after 40 h of incubation was applied on to an Amberlite IR-120 column, and amino acids were eluted with ammonia (0.5 M). Fractions containing amino acid were combined and evaporated to dryness. The resulting solid was not pure enough to be recrystallized from water and EtOH, and required further chromatography on a Dowex 1-X8 column. The solid residue obtained by evaporating fractions containing glutamic acid was recrystallized from water and EtOH to give a 57% recovery. The enantiomeric excess of the D-glutamic acid was

97% by chiral hplc, but only 90% by optical rotation, indicating that impurities other than L-glutamic acid were present in the same sample.

Since two ion-exchange chromatography steps were needed to separate D-glutamic acid from the large amount of peptone in the culture medium, media containing 30 mM of DL-glutamic acid and smaller amounts of peptone and yeast extract (*i.e.*, peptone/2 and peptone/4 media) were incubated with *F. nucleatum*. The amino acid fraction from the Amberlite IR-120 column was recrystallized from water and EtOH to yield colored solids. The low recovery of D-glutamate (41%) from peptone/2 medium was increased to 64% by isolating D-glutamate from the mother liquor from the recrystallization step by chromatography on Dowex 1-X8. The enantiomeric excess of the initial D-glutamic acid was 99% by chiral hplc, but its optical rotation was larger than the standard. The recrystallized product from peptone/4 was isolated in 59% yield with an enantiomeric excess of 95% by chiral hplc and 91% by optical rotation.

In an initial attempt to improve the yield and purity of D-glutamic acid isolated from the peptone media, higher concentrations of DL-glutamic acid (*i.e.*, 36, 72, and 109 mM) were incubated with *F. nucleatum* growing on peptone medium. The enantiomeric excess of D-glutamate reached 90% or higher after 86 h of incubation for all three concentrations. However, longer times were required to reach these high levels at the higher concentrations of DL-glutamic acid (Figure 15).

Under the above conditions a practical limit of 100 mM DL-glutamate was reached, and another experiment was designed to investigate whether the initial

addition of more bacterial cells (*i.e.*, bigger inoculum size) could increase the rate of L-glutamate catabolism. Four portions of peptone medium containing DL-glutamic acid (121 mM) were inoculated with either 0.1, 0.3, 0.5, or 1 mL of *F. nucleatum* cell suspension, and the uptake and the enantiomeric excess of the remaining glutamic acid after 41 h of incubation were analyzed by normal and chiral hplc, respectively. As the size of inoculum was increased, the observed rate of L-glutamate catabolism increased, yielding D-glutamate of higher enantiomeric excess (Figure 16).

### 2.2.2 D-Amino Acid Preparation by Bacterial Resuspensions

As demonstrated by experiments in peptone medium, the rate and the extent of L-glutamic acid degradation depended on the number of bacterial cells, and the purity of the D-glutamate isolated depended on the ability to separate the D-amino acid from the components of the peptone medium. Both of these obstacles could be overcome by resuspending bacterial cells in a buffer containing a racemic mixture of the amino acid. Typically, bacterial cells grown in peptone medium (2.5 g damp cells/500 mL) were collected by centrifugation and resuspended in phosphate buffer (50 mL) where they remained viable for up to 3 days. For the optimization of the incubation parameters, samples were removed at time intervals, centrifuged, and the supernatants were analyzed using either normal or chiral hplc. The conditions for the preparation of D-glutamic acid and D-serine by *F. nucleatum* and D-arginine by *F. varium* were examined in

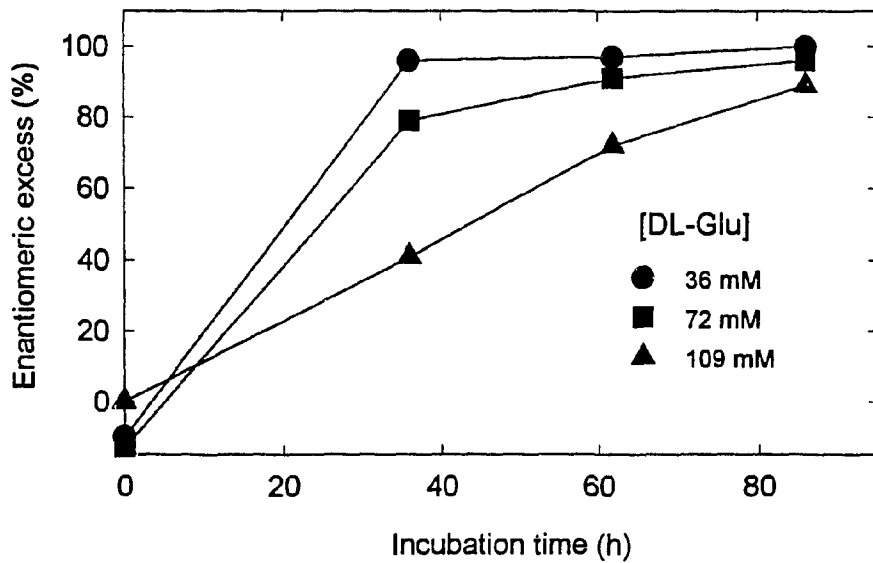


**Figure 15.** Effect of increasing the concentration of DL-glutamate on L-glutamate uptake by *F. nucleatum* in peptone medium.

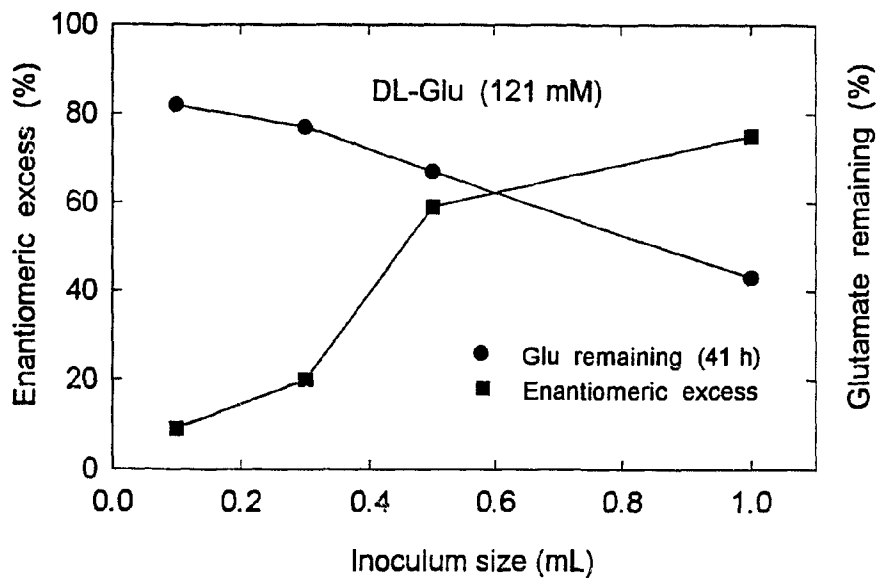


**Figure 16.** Effect of inoculum size on the rate of L-glutamate degradation by *F. nucleatum* in peptone medium.

resuspension buffer.

Preliminary experiments were carried out at three different concentrations of DL-glutamic acid (106, 176, and 242 mM) with no stirring. The enantiomeric excesses for D-glutamate in the 63-h supernatants were 83, 77, and 61%, respectively. Since cells of *F. nucleatum* and *F. varium* have the tendency to settle, this would probably affect the rate of L-amino acid degradation. The effect of stirring on the rate of L-glutamic acid and L-serine degradation by *F. nucleatum* was tested in resuspension buffer containing either 272 mM DL-glutamic acid or 343 mM DL-serine. The enantiomeric excess of D-glutamate in the supernatant collected after 16 h of incubation in the stirred medium (51%) was much higher than that in the static medium (24%) (Figure 17A) and corresponded to a 38 mM increase in L-glutamic acid uptake. For serine, after 16 h of incubation, stirring increased the enantiomeric excess from 59% in the static medium to 99% in the stirred medium (Figure 17B), an increase in L-serine uptake of 44 mM. Since stirring had a great effect on the rate of degradation of L-glutamic acid and L-serine, all subsequent resuspension experiments were stirred.

For the stirred resuspensions (Figure 17), the consumption of the L-amino acids occurred during the first 24 h of the incubation. All of the L-serine was degraded within 16 h, but only a 60% enantiomeric excess of D-glutamate was attained, indicating a partial degradation of the initial L-glutamate supplied in the racemate.

DL-Glutamic acid at 150, 200, and 250 mM was incubated with *F. nucleatum*

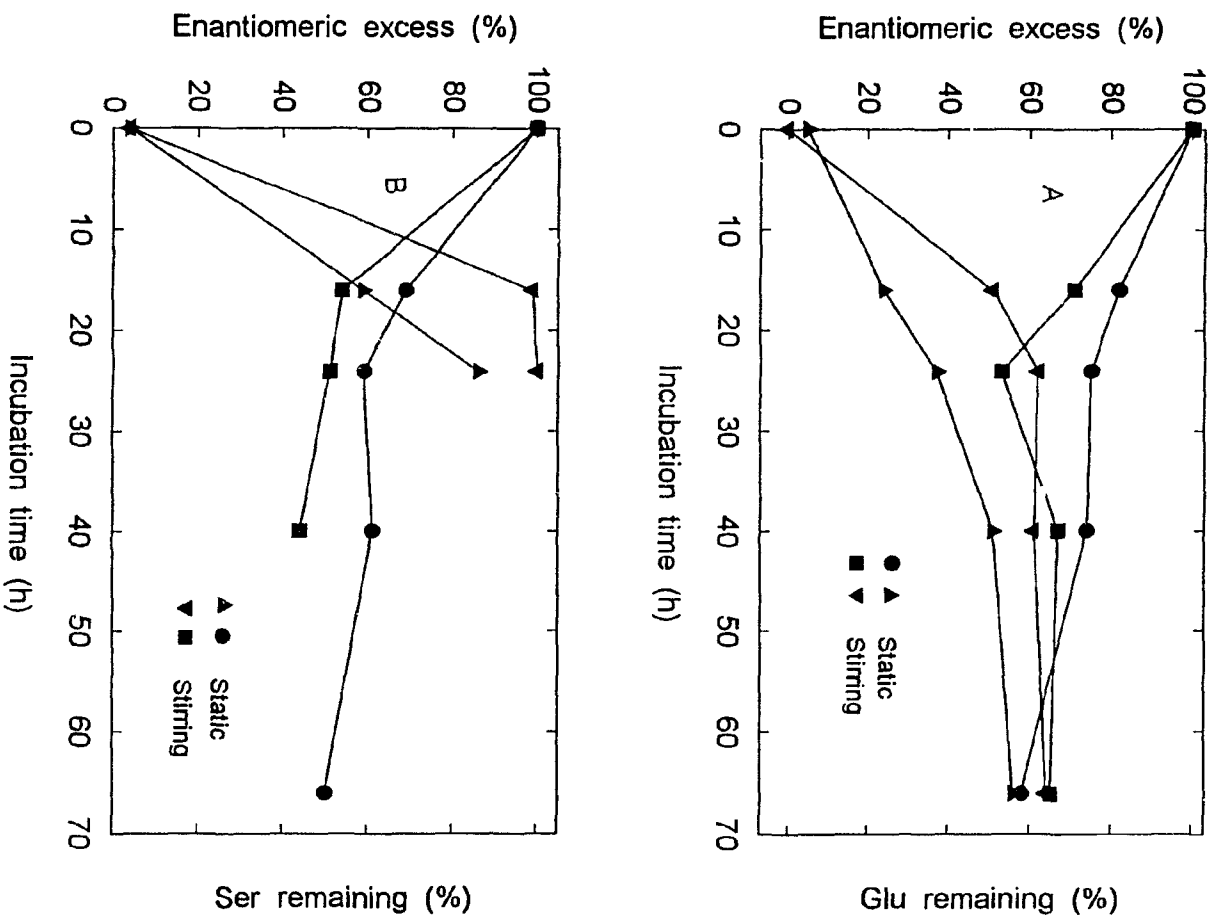


**Figure 17.** Effect of stirring on the rate of L-amino acid degradation in resuspension buffer containing either 270 mM DL-glutamate (A) or 340 mM DL-serine (B).

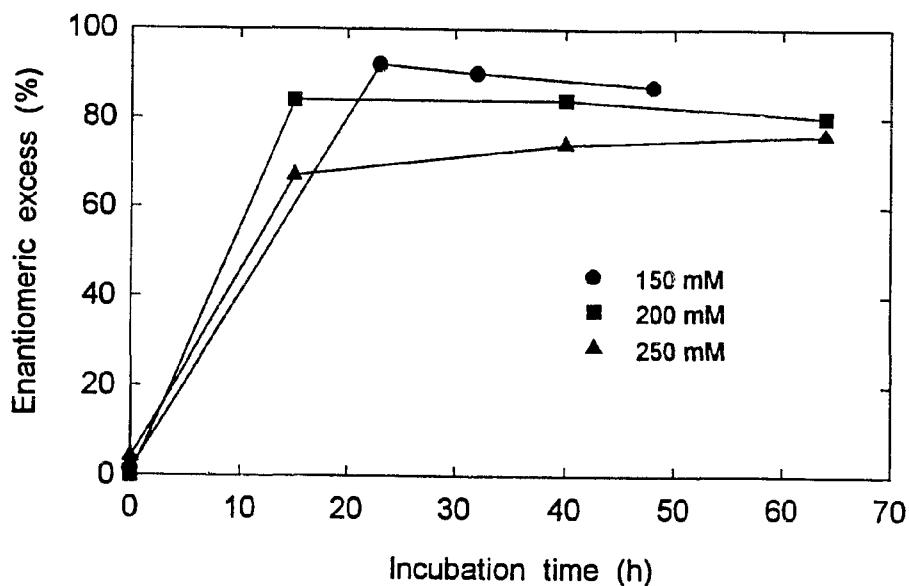


**Figure 18.** Effect of increasing the concentration of DL-glutamate on L-glutamate degradation by *F. nucleatum* in resuspension buffer.

to determine the maximum concentration at which complete catabolism of the L-isomer is attained. D-Glutamate with a 90% enantiomeric excess was obtained only at 150 mM DL-glutamate (Figure 18). Again rapid L-glutamic acid degradation was observed in the first 24 h. Although L-glutamic acid catabolism stopped at approximately 24 h, the *F. nucleatum* cells were still viable after 48 h of incubation, and the pH had only decreased from 7.4 to about 7.0. Neither of these factors is likely to have been responsible for stopping the catabolism of L-glutamic acid.

*F. nucleatum* rapidly assimilated L-serine from a racemic mixture. For example in the 900 mM DL-serine experiment, the enantiomeric excess of D-serine rose from 3 to 41% (corresponding to 231 mM L-serine uptake) within the first

hours of incubation. Within 15 h, nearly all the L-serine in racemates up to 900 mM was consumed (Figure 19).

DL-Serine at 900 mM (94.5 g/L) crystallized when the autoclaved buffer cooled to room temperature, and higher concentrations were not investigated. In contrast to the glutamate experiments, the consumption of L-serine did not stop before all the L-serine was depleted.

Resuspension buffer supplemented with DL-arginine (100, 200, and 300 mM) was used to examine the capacity of *F. varium* to degrade L-arginine. Since stirring had a positive effect on the rate and the extent of L-glutamic acid and L-serine catabolism, the *F. varium* resuspensions (2.5 g damp cells/L) were stirred. As the concentration of arginine decreased with time, the enantiomeric excess of unmetabolized D-arginine increased and reached more than 99% after 72 h of incubation (Figure 20). However, at higher concentrations of DL-arginine, a longer time is needed to obtain this high enantiomeric excess. After 44 h of incubation, the enantiomeric excess were 100, 90, and 80% for 100, 200, and 300 mM DL-arginine, respectively. The catabolism of L-arginine by *F. varium* was slower and continued over a much longer time than the degradation of L-glutamate and L-serine by *F. nucleatum*.

Unlike the serine and glutamate incubations, the appearance of a substance that formed a fluorescent derivative with o-phthalaldehyde and mercaptoethanol was observed by hplc (Figure 21). This substance coeluted with a standard sample of ornithine, presumably formed by hydrolysis of the guanidine group of L-arginine.

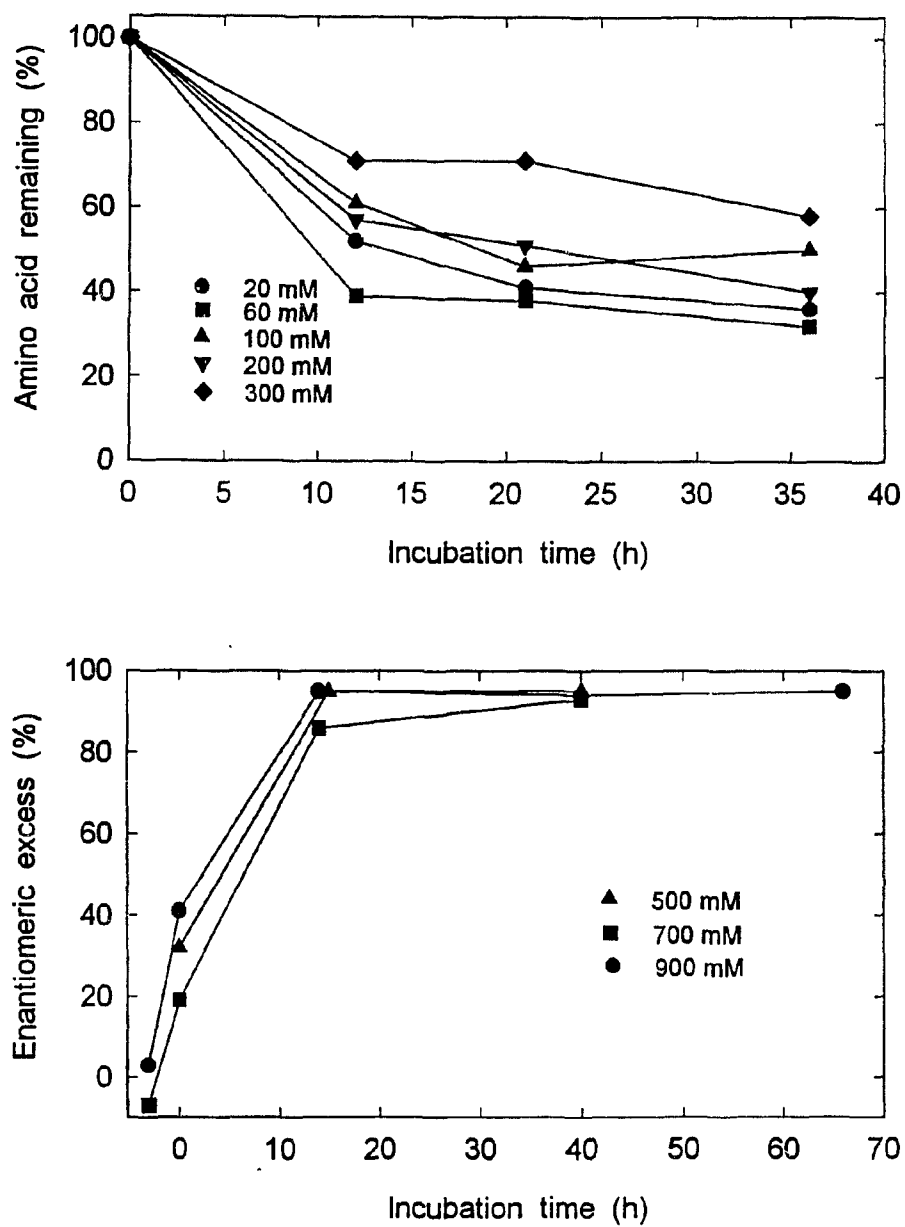


**Figure 19.** Effect of increasing the concentration of DL-serine on L-serine degradation by *F. nucleatum* in resuspension buffer at low concentrations of DL-serine analyzed by normal hplc (top), and at high concentrations of DL-serine analyzed by chiral hplc (bottom).

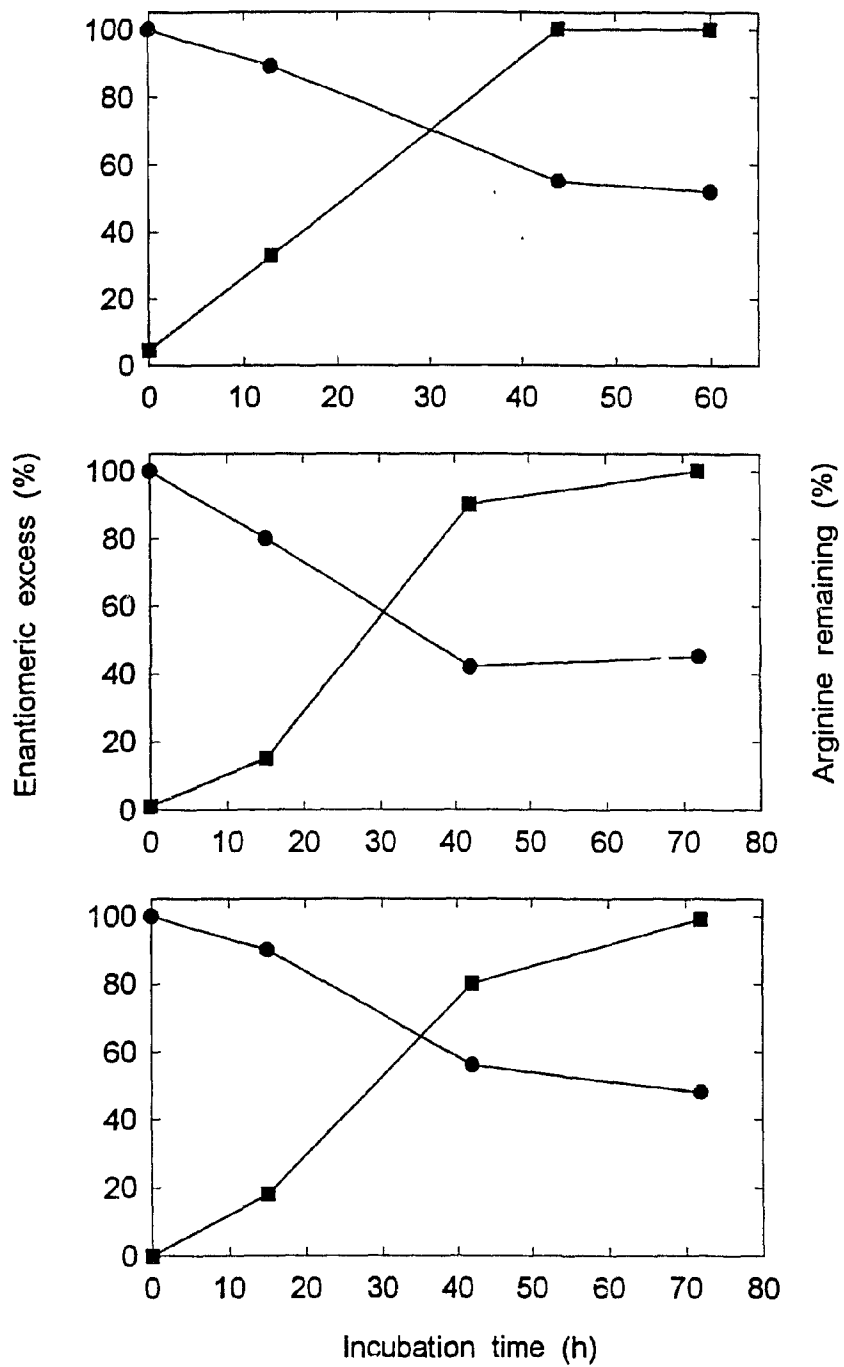


**Figure 20.** L-Arginine degradation by *F. varium* in resuspension buffer. The initial concentrations of DL-arginine were 100 (top), 200 (middle), and 300 (bottom) mM.

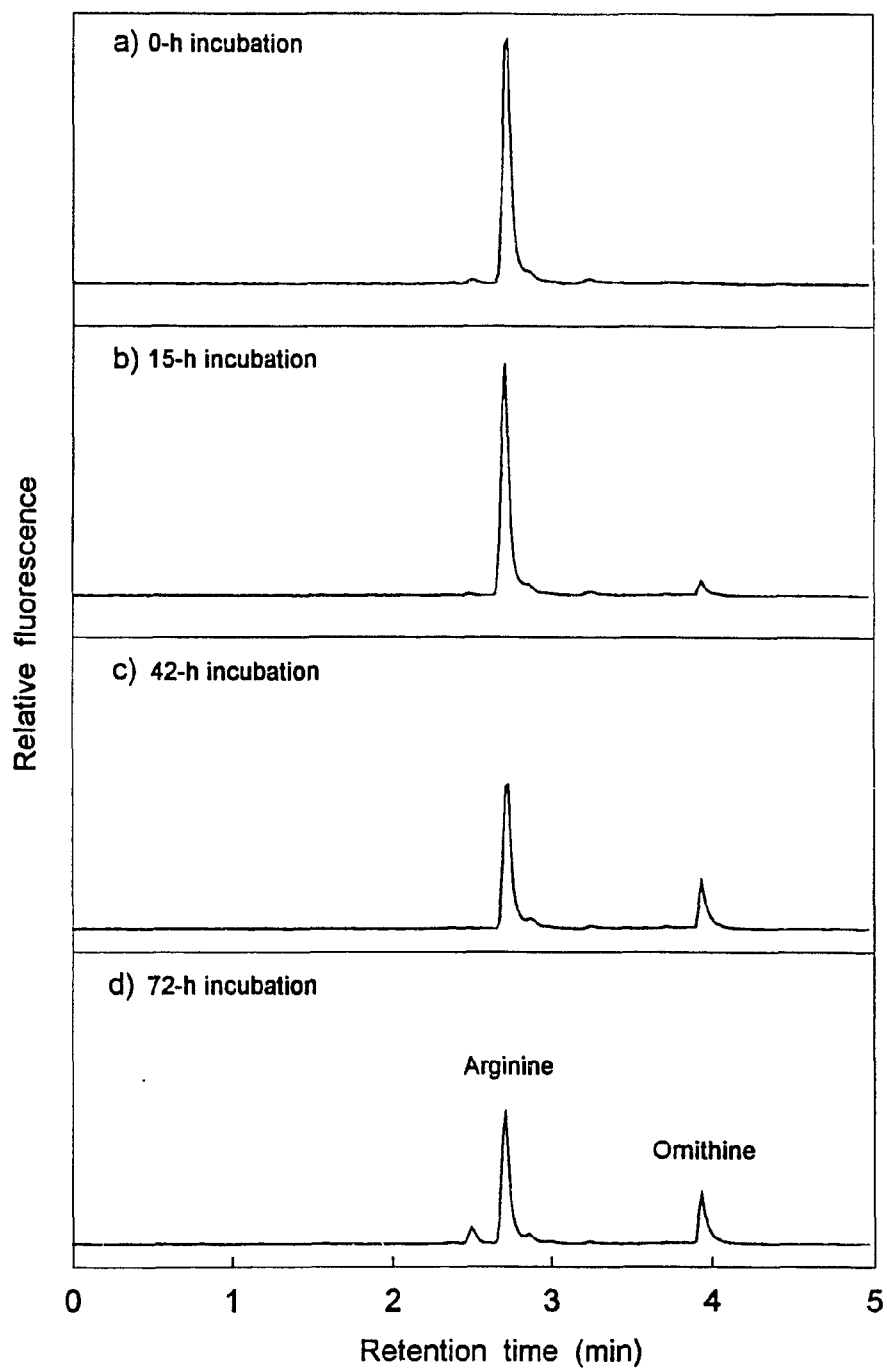


**Figure 21.** Hplc chromatograms of DL-arginine (300 mM) incubated with *F. varium* in resuspension buffer.

Resuspension buffer containing DL-histidine (50, 100, and 200 mM) was used to test the capacity of *F. varium* to catabolize L-histidine. At 200 mM of initial DL-histidine, only 17% of the initial DL-histidine was assimilated. At lower concentrations, *i.e.*, 50 and 100 mM, the initial DL-histidine was catabolized to 46 and 49%, respectively, indicating an efficient uptake of L-histidine. Since the chiral hplc method used for enantiomeric analysis of other amino acids in this investigation was not suitable for histidine analysis, the enantiomeric excess of histidine was not determined.

So far, all resuspension experiments were carried out using a cell density of 50 g damp cells/L. A preliminary experiment was done using a high initial concentration of DL-glutamic acid (485 mM). Under these conditions, a greater enantiomeric excess of D-glutamate was reached at higher cell densities (Figure 22). However, it did not exceed 50%, indicating an inherent limit to the amount of L-glutamate catabolized. At the highest cell density (200 g damp cells/L) examined, a very viscous solution which was difficult to manipulate was obtained. This concentration was not used in subsequent experiments.

To examine the conditions needed to obtain a high enantiomeric excess, lower concentrations of DL-glutamic acid were incubated with cell densities of 25, 50 and 100 g damp cells/L. As shown in Figure 23A, maximum enantiomeric excesses of 60-70% were attained from an initial concentration of 250 mM DL-glutamate. When the experiment was repeated at a lower DL-glutamic acid concentration (175 mM), enantiomeric excesses of above 90% were reached after

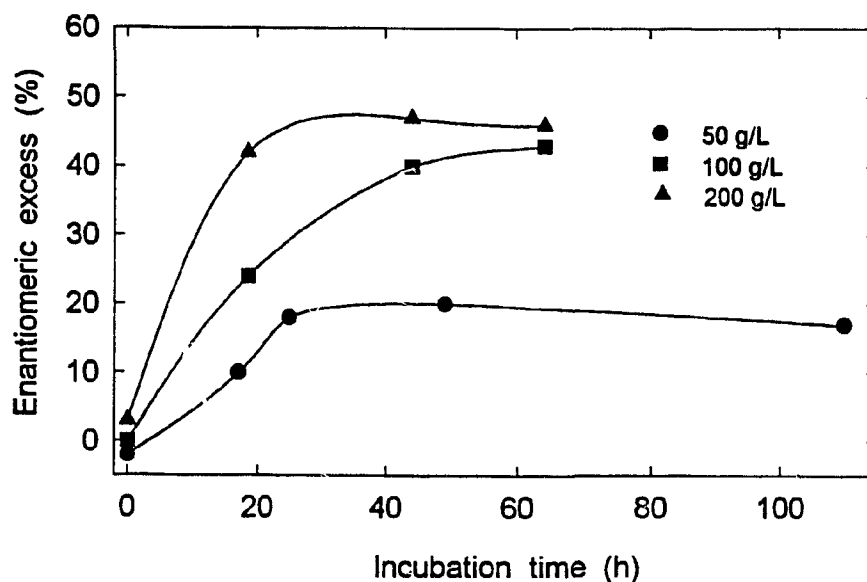


**Figure 22.** Effect of increasing the cell density on the rate of L-glutamate uptake by *F. nucleatum* in resuspension buffer at high concentrations of DL-glutamate (480 mM).

22 h of incubation for both the 50 and 100 g/L cell densities (Figure 23B). However, the rate of L-glutamate catabolism was faster at the higher cell densities, reaching an enantiomeric excess of 93% after 10 h of incubation.

Similar results were obtained for the catabolism of L-serine at various cell densities (Figure 24). At the two highest cell densities, a greater than 90% enantiomeric excess of D-serine was attained after approximately 30 h of incubation. Again, at the highest cell density, a shorter time is needed to reach a 90% enantiomeric excess.

The criteria for the optimum conditions for the preparation of a D-amino acid is a high yield of optically pure D-amino acid from the minimum amount of cells in

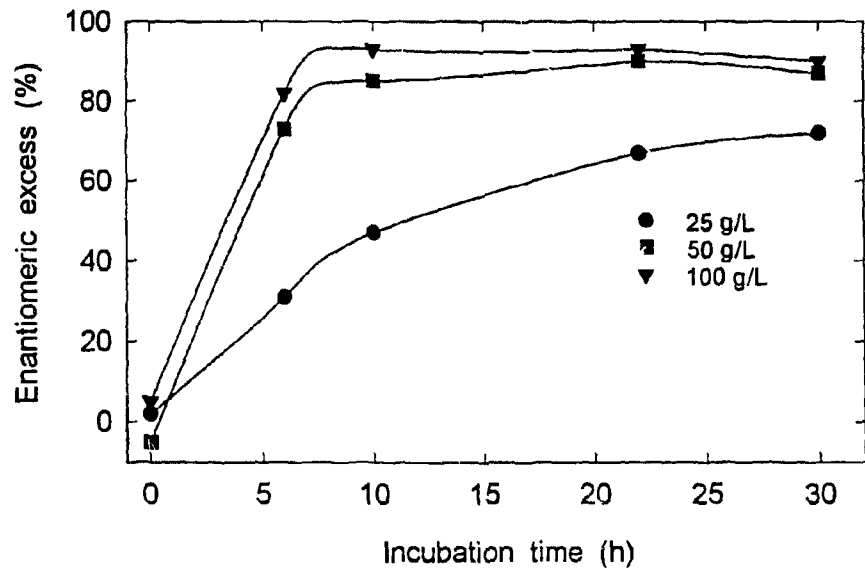
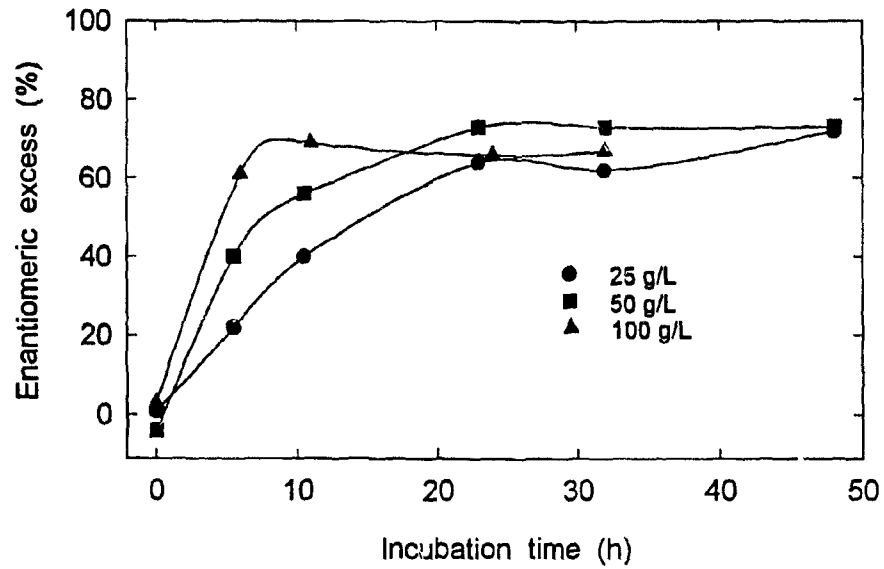


**Figure 23.** Effect of increasing the cell density on the rate of L-glutamate degradation by *F. nucleatum* in resuspension buffer at 250 mM (A) and 175 mM (B).

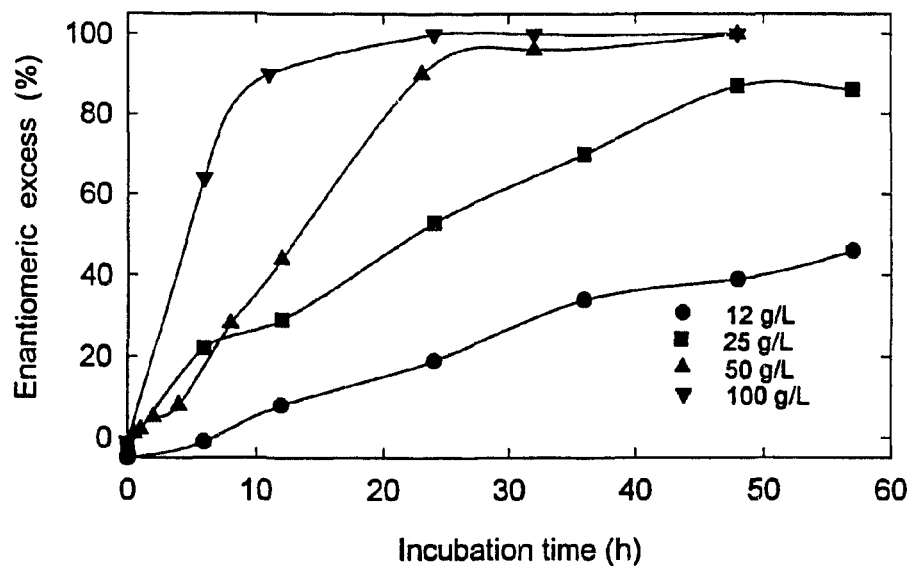


**Figure 24.** Effect of increasing the cell density on the rate of L-serine degradation by *F. nucleatum* in resuspension buffer containing 800 mM DL-serine.

the shortest period of time. For both glutamic acid and serine, a cell density of 50 g damp cells/L and an incubation time of 24-30 h are convenient. Since cells were viable for several days and the catabolism of L-serine was rapid, a double resuspension experiment was carried out. A suspension of *F. nucleatum* cells incubated in buffer with 800 mM DL-serine for 24 h was collected by centrifugation and resuspended in fresh buffer containing 800 mM DL-serine. An enantiomeric excess of only 67% was reached in the first 24 h incubation, but a value of 89% was attained after 51 h of the second incubation (Figure 25). The rate of L-serine uptake in the second incubation was slightly slower than in the first, but the results

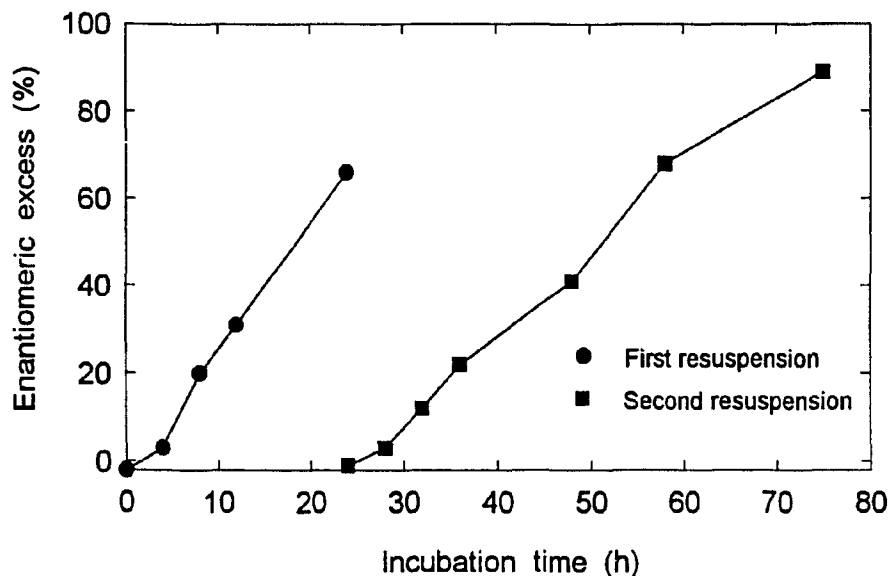


**Figure 25.** Effect of consecutive resuspensions on the ability of *F. nucleatum* to degrade L-serine in resuspension buffer containing 800 mM DL-serine.

demonstrated that the efficiency can be improved by using one batch of *F. nucleatum* cells to process two batches of DL-serine.

In preparation for isolating D-glutamate and D-serine from resuspension fluids, nmr spectroscopy was used to identify the nonvolatile metabolic end-products by comparison to standard samples. The  $^1\text{H}$ ,  $^{13}\text{C}$  and DEPT nmr spectra were obtained by dissolving freeze dried residues of resuspension fluid in  $\text{D}_2\text{O}$ .

When DL-glutamate was the substrate, both the  $^1\text{H}$ - and  $^{13}\text{C}$ -nmr spectra showed peaks corresponding to acetate, butyrate, and residual glutamate (Figure 26). Integration of the signals in the  $^1\text{H}$  nmr spectrum corresponding to the methyl groups of acetate and butyrate at 1.86 and 0.84 ppm, respectively, indicated that

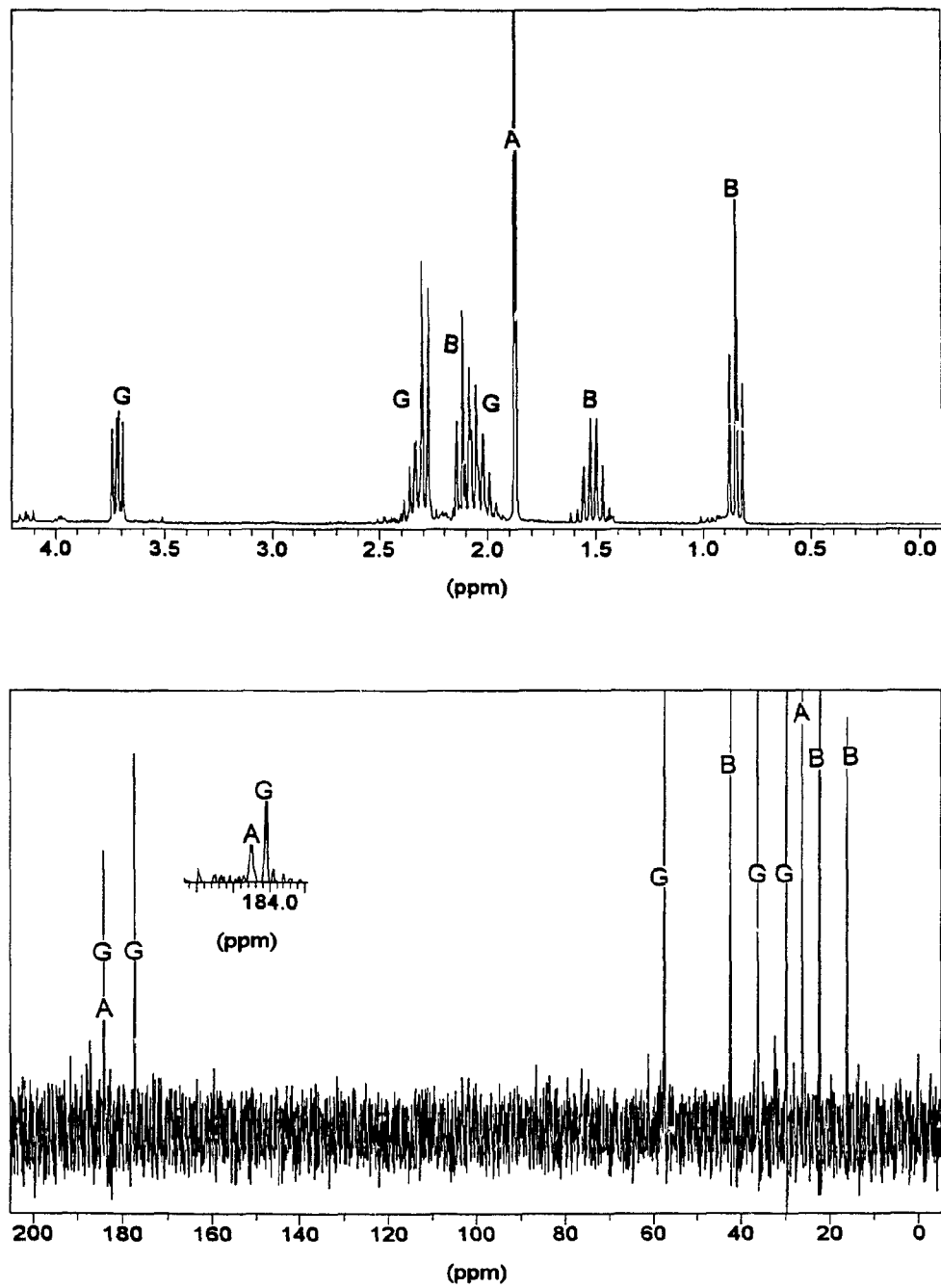


**Figure 26.**  $^1\text{H}$ - and  $^{13}\text{C}$ -nmr spectra of the residue from glutamic acid catabolism. The peaks in  $^{13}\text{C}$ -nmr spectrum are labelled as A, acetate; B, butyrate; and G, glutamate.

the ratio of acetate to butyrate was 2 to 1, in agreement with previous reports that fermentation of 2 moles L-glutamic acid produced 2 moles of acetate and 1 mol of butyrate (8, 73).

The end-products of L-serine degradation were identified as acetate, butyrate and lactate (Figure 27). A ratio of 20:1:22 for these three end-products was calculated from the integrals of signals at 1.84, 0.81 and 1.25 ppm corresponding to the methyl groups of acetate, butyrate and lactate, respectively (Figure 27). Thus the major end-products of L-serine degradation are acetate and lactate, and butyrate is only a minor end-products. No signals corresponding to pyruvate were detected.

Since a smaller relative amount of butyrate accumulated in the serine resuspension fluids, the inhibition of glutamate catabolism by butyrate was investigated. The maximum concentration of L-glutamic acid consumed in the previous experiments was about 90 mM, generating about 90 mM acetate and 45 mM butyrate. Therefore, four replicate flasks were prepared containing 175 mM DL-glutamic acid and 50 g damp cells/L. Either acetate (90 and 180 mM) or butyrate (90 mM) was added to each of three flasks and the fourth was used as a control. Chiral hplc analysis indicated that the presence of sodium acetate and butyrate at 90 mM has a small effect on the rate and amount of L-glutamic acid degraded compared to the control culture (Figure 28). The higher concentration of sodium acetate (180 mM) has a more significant effect on the rate and amount of L-glutamic acid degradation. The possible accumulative effect of both sodium

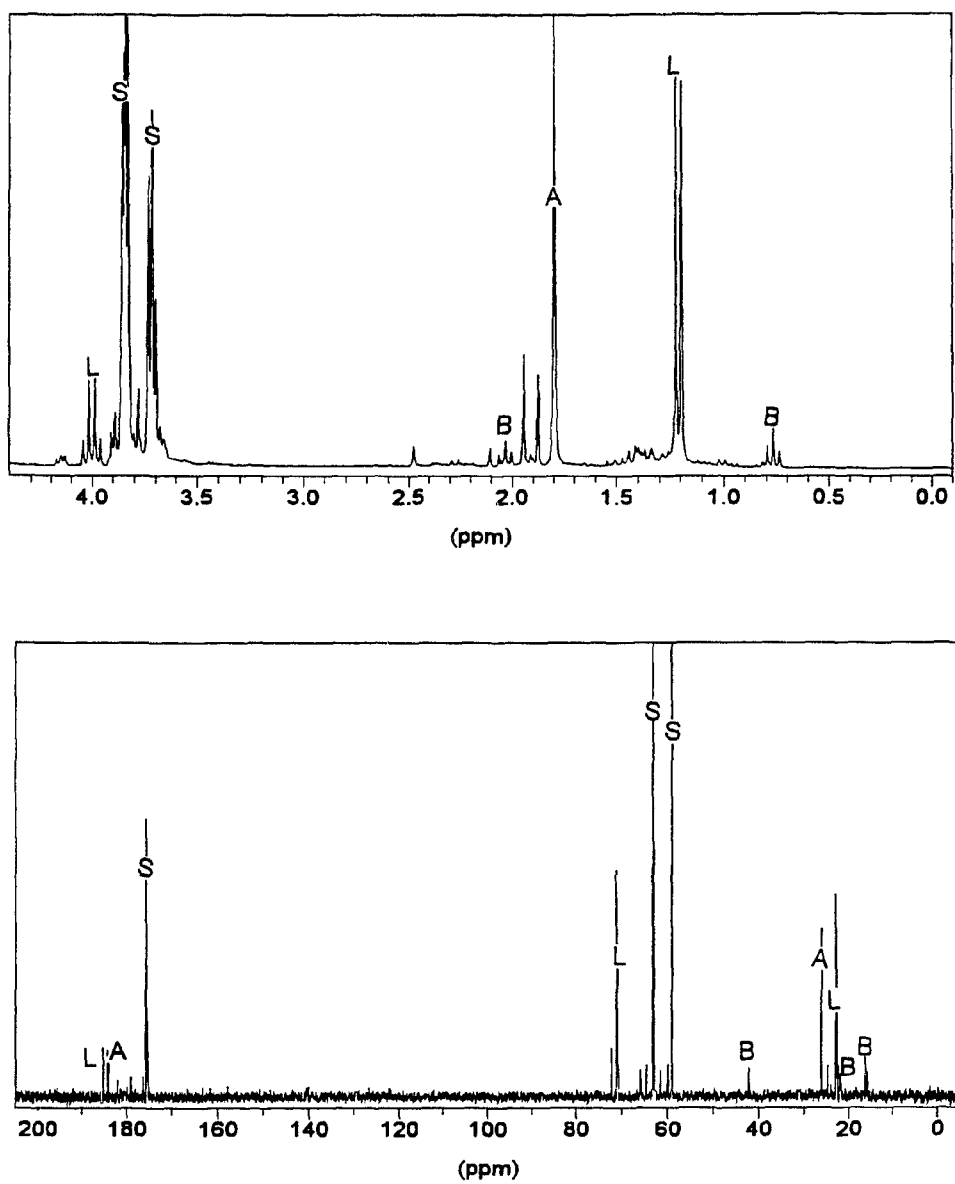


**Figure 27.**  $^1\text{H}$ - and  $^{13}\text{C}$ -nmr spectra of the residue from serine catabolism. The peaks in  $^{13}\text{C}$ -nmr spectrum are labelled as A, acetate; B, butyrate; and L, lactate; and S, serine.

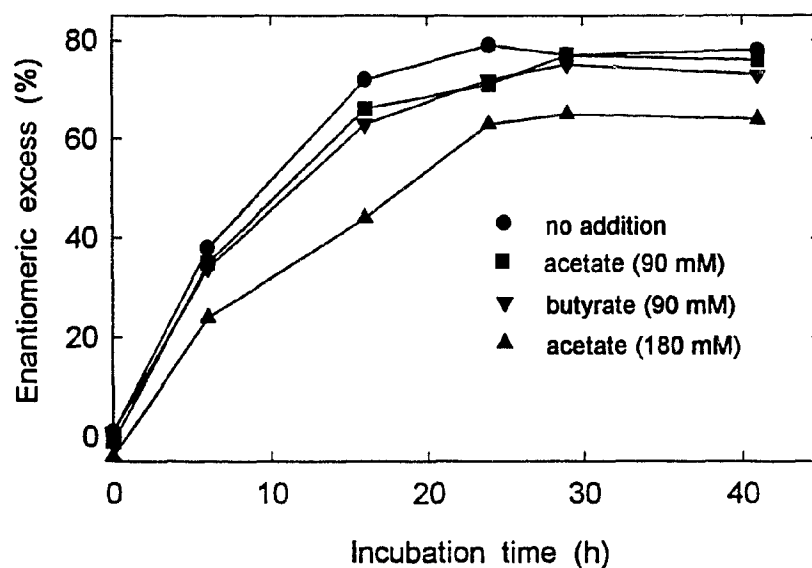


**Figure 28.** Effect of sodium acetate and butyrate on the rate of L-glutamate degradation by *F. nucleatum* resuspended in buffer containing 175 mM DL-glutamate.

acetate and butyrate on the rate of L-glutamic acid was not investigated, but the combination of end-products could exert a large effect.

The viability of this approach for the preparation of D-amino acids was demonstrated for *F. nucleatum* and two amino acid racemates under the optimized conditions defined by the above experiments.

Resuspension buffer (300 mL) containing 150 mM of DL-glutamic acid was incubated with *F. nucleatum* (7.5 g damp cell mass) at 37°C for 24 h. The incubation mixture was centrifuged, and the supernatant was applied to an Amberlite IR-120 column. The amino acid containing fractions eluted with ammonia

were evaporated to dryness, dissolved in hot water, and decolorized with charcoal. The white residue was recrystallized from water and EtOH to give 2.43 g white solid corresponding to a 73% recovery of D-glutamate. The enantiomeric excess was greater than 99% by both hplc and optical rotation.

When 800 mM DL-serine was incubated with *F. nucleatum* (5 g damp cells) in resuspension buffer (100 mM) and D-serine was isolated as described above, an 83% recovery was obtained. The sample had an enantiomeric excess greater than 99%, calculated from both hplc data and the optical rotation.

## Chapter 3

### **Results: Examination of the Pathways of Glutamic Acid Catabolism in *Fusobacterium* Species Using Isotopically-labelled Substrates**

#### **3.1 General Approach**

The carbon atoms of glutamic acid are delivered to different locations in acetate and butyrate (Figure 29) by the three distinct pathways proposed for the degradation of glutamic acid to ammonia, carbon dioxide, acetic and butyric acid. As a result, the catabolism of isotopically labelled glutamic acid by each pathway will generate different isotopic enrichment patterns in acetate and butyrate. However, some of the carbon atoms of glutamic acid are delivered to the same position in acetate and butyrate by more than one pathway, and the possible conversion of acetate to butyrate demonstrated in some anaerobic bacteria such as *C. kluyveri* (44), can complicate the distribution patterns (Figure 29). Consequently, a set of isotopic feeding experiments is necessary to substantiate which pathway or pathways operate in a given bacterium. The possibility of more than one pathway functioning in a single organism (2) has not been rigorously tested by isotopic experiments.

Previous studies on glutamic acid catabolism have used radiolabelled glutamic acid in which assessment of the enrichment patterns in acetate and butyrate required extensive degradation of acetic acid and butyric acid. In this study, substrates labelled with stable isotopes ( $^1\text{H}$ , and  $^{13}\text{C}$ ) were employed, and acetate and butyrate end-products were isolated for isotopic analysis as their *p*-

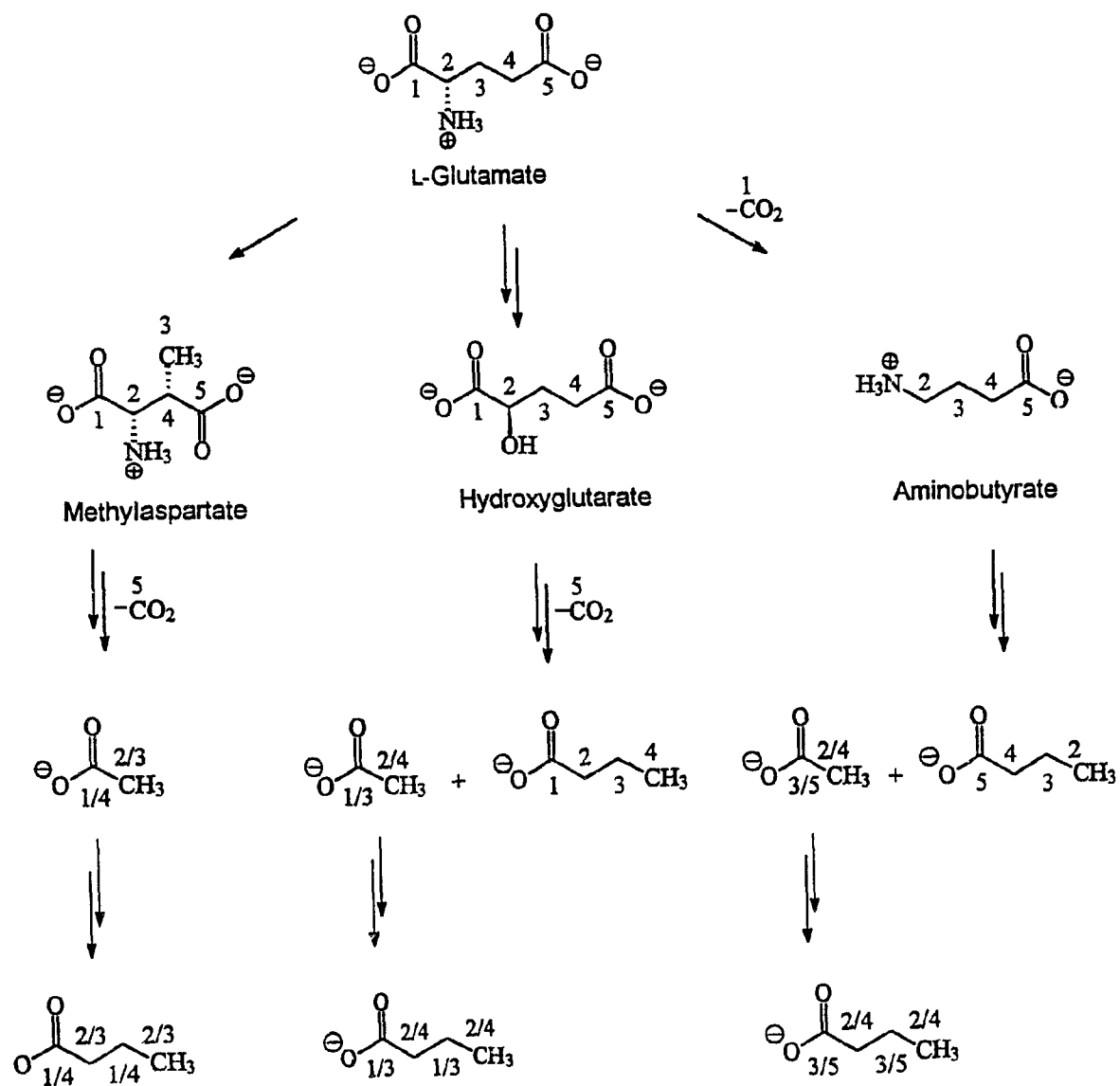


**Figure 29.** Incorporation patterns of the carbon atoms of glutamate into acetate and butyrate by three different pathways. The numbers correspond to the carbon atoms of glutamate.

bromophenacyl esters (Figure 30). The esters were prepared by suspending lyophilized culture supernatant in acetonitrile containing *p*-bromophenacyl bromide and a crown-ether catalyst (112). The acetate and butyrate esters were separated by silica-gel chromatography, and isotopic distributions and enrichments were determined. Complementary information was readily apparent from the nmr and MS spectra. While the amount of enrichment in individual carbon atoms of the acetate and butyrate esters was obtained from NMR spectra, the MS spectral data indicated the number of isotopic atoms incorporated per molecule, a result that is not easily obtained using  $^{14}\text{C}$ -labelled glutamic acid. Absence of fragmentation within the acetate and butyrate portions of the *p*-bromophenacyl derivatives (113) precluded an assignment of isotopic positions from mass spectral data. The natural abundance carbon atoms provided by the *p*-bromophenacyl moiety served as an internal standard to calculate the  $^{13}\text{C}$  enrichments from nmr peak-height measurements when all carbon atoms in the metabolite potentially were enriched (111). As a result, complete isotopic distributions were obtained in each experiment.

### 3.2 Catabolism of $^{13}\text{C}$ -Labelled L-Glutamates by *F. nucleatum*

A series of seven feeding experiments using isotopically labelled samples of glutamate and acetate were carried out to investigate glutamate catabolism in *F. nucleatum*. The details of these experiments are summarized in Table 4.

Experimental conditions were established using L-[1- $^{13}\text{C}$ ]glutamic acid (Expt.

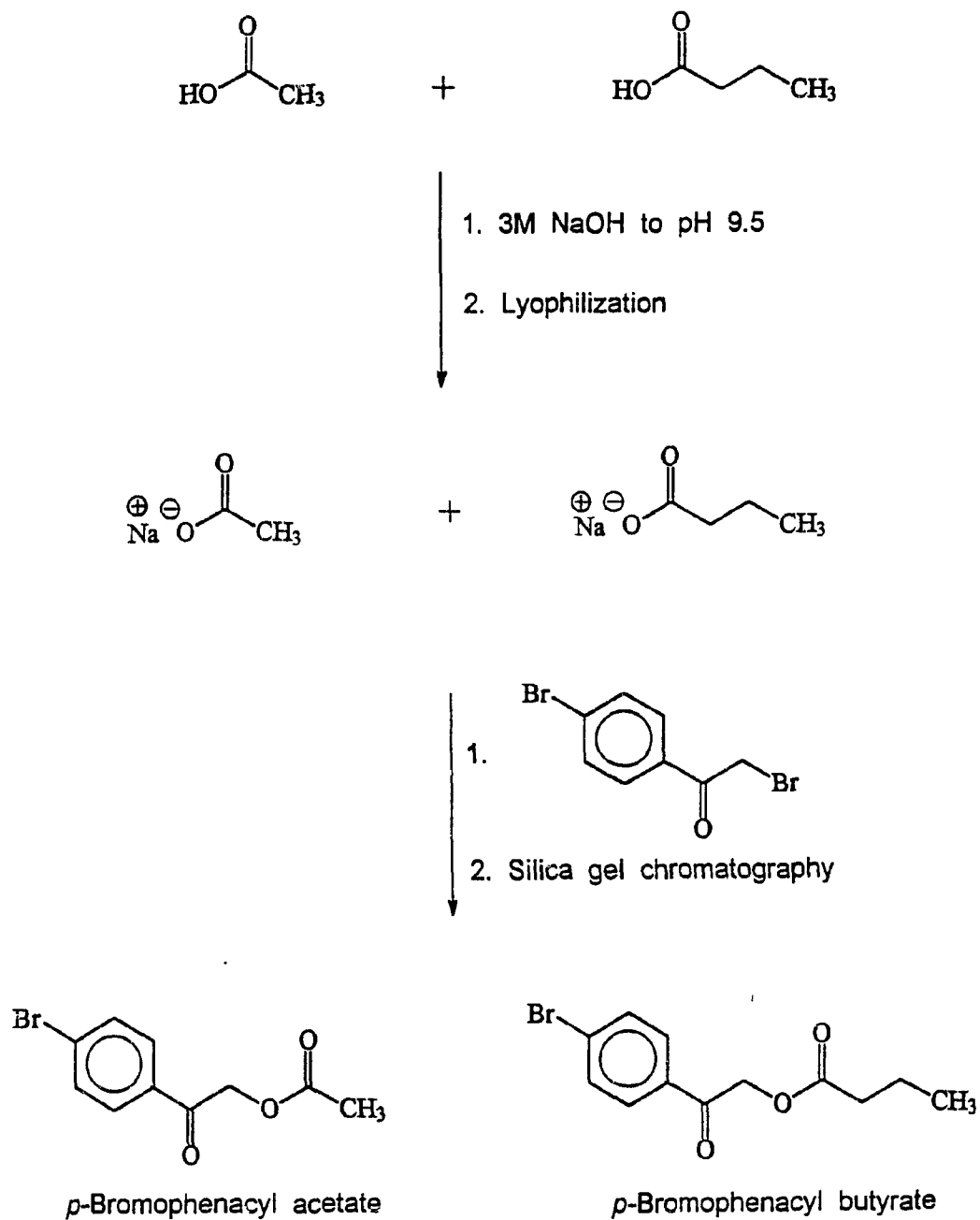


**Figure 30.** Isolation of the metabolic end-products (acetic and butyric acids) as *p*-bromophenacyl esters.

Table 4. Isotopic feeding experiments in *F. nucleatum*.

Expt. No.	Substrate	Atom (%)	Culture Volume (mL)	Amount Added (mg)		Amount of Phenacyl Ester Isolated (mmol)	
				Labelled Substrate	Unlabelled Glutamate	Acetate	Butyrate
1 <sup>a</sup>	L-[1- <sup>13</sup> C]Glutamate	99	100	75	175	0.07	0.07
2 <sup>b</sup>	L-[4- <sup>13</sup> C]Glutamate	95	50	50	75	0.33	0.12
3 <sup>b</sup>	L-[5- <sup>13</sup> C]Glutamate	99	50	50	75	0.31	0.44
4 <sup>a,c</sup>	Sodium [1,2- <sup>13</sup> C <sub>2</sub> ]acetate	99.3	50	42	125	- <sup>d</sup>	0.11
5 <sup>b</sup>	Sodium [1,2- <sup>13</sup> C <sub>2</sub> ]acetate	99.3	50	50	125	0.20	0.14
6 <sup>a</sup>	Sodium [ <sup>2</sup> H <sub>3</sub> ]acetate	99.5	50	42	125	- <sup>d</sup>	0.28
7 <sup>b</sup>	Sodium [ <sup>2</sup> H <sub>3</sub> ]acetate	99.5	50	50	125	0.20	0.04

<sup>a</sup> Unenriched peptone medium

<sup>b</sup> Peptone medium

<sup>c</sup> Culture was contaminated with an aerobic bacteria.

<sup>d</sup> Not isolated

1) as incorporation of label was predicted by both the methylaspartate and hydroxyglutarate pathways (Figure 29). MS indicated that the acetate and butyrate derivatives isolated from the *F. nucleatum* culture were enriched with one atom of  $^{13}\text{C}$ . The  $^{13}\text{C}$  label was located at C-1 of acetate and C-1 and C-3 of butyrate by nmr spectroscopy. The  $^{13}\text{C}$  enrichment at C-1 of butyrate (10.7%) was about 6.7 times that at C-3 (1.6%), and the sum of these enrichments (12.3%) corresponds to the overall enrichment determined by MS (13.1%) (Table 5). The high specific incorporation of label from L-[1- $^{13}\text{C}$ ]glutamate into butyrate (approx. 40%) verifies the major role of glutamate metabolism in *F. nucleatum*. In a second experiment (Expt. 3), label from L-[5- $^{13}\text{C}$ ]glutamate was not incorporated into either acetate or butyrate (Table 5), indicating that the aminobutyrate pathway is absent.

The high enrichment at C-1 of butyrate derived from L-[1- $^{13}\text{C}$ ]glutamate is most consistent with the hydroxyglutarate pathway, as the methylaspartate pathway would produce butyrate equally enriched at C-1 and C-3 of butyrate (Figure 29). However, if both pathways operate simultaneously, unsymmetrical enrichment at C-1 and C-3 of butyrate would be observed. The possible simultaneous operation of the hydroxyglutarate and methylaspartate pathways was tested by feeding L-[4- $^{13}\text{C}$ ]glutamic acid (Expt. 2), as C-4 of glutamate is delivered into different carbon atoms of acetate and butyrate by the two pathways.

Acetate derived from L-[4- $^{13}\text{C}$ ]glutamate was enriched at C-2 (~ 4%, Table 5 and Figure 31), and the butyrate was enriched to different extent at C-2 and C-4 (Table 5, Figure 32); the enrichment at C-4 (13.8%) was about 5.1 times that at

Table 5. Incorporation of L-[<sup>13</sup>C]glutamic acids into acetic and butyric acids by *F. nucleatum*.

Expt. No.	<sup>13</sup> C Labelled Glutamate		<sup>13</sup> C Enrichment (%)											
			MS Analysis <sup>b</sup>						NMR Analysis <sup>c</sup>					
			Acetate		Butyrate		Acetate		Butyrate					
			I <sub>0</sub>	I <sub>1</sub>	I <sub>0</sub>	I <sub>1</sub>	C-1	C-2	C-1	C-2	C-3	C-4		
1 <sup>d</sup>	1	30	96.2 (1.0)	4.5 (1.0)	87.0 (0.3)	13.1 (0.3)	3.4	0.1 (0.2)	10.7	-0.3	1.6	-0.3 (0.2)		
2 <sup>e</sup>	4	38	95.6 (0.2)	4.3 (0.2)	83.9 (0.4)	16.4 (0.2)	0.0	3.5 (0.1)	-0.1	2.7	-0.1	13.8 (0.1)		
3 <sup>e</sup>	5	40	99.4 (0.7)	1.0 (0.3)	99.8 (1.1)	1.0 (0.4)	-0.2	-0.1 (0.1)	0.0	0.0	0.05	0.01 (0.01)		

<sup>a</sup> Isotopic enrichment of glutamate added to the culture.

<sup>b</sup> The standard deviation calculated from replicate scans, typically 6, is given in parentheses.

<sup>c</sup> The standard deviation calculated from the peak heights of natural abundance signals contributed by the derivatization reagent is given in parenthesis.

<sup>d</sup> Unenriched peptone medium.

<sup>e</sup> Peptone medium.

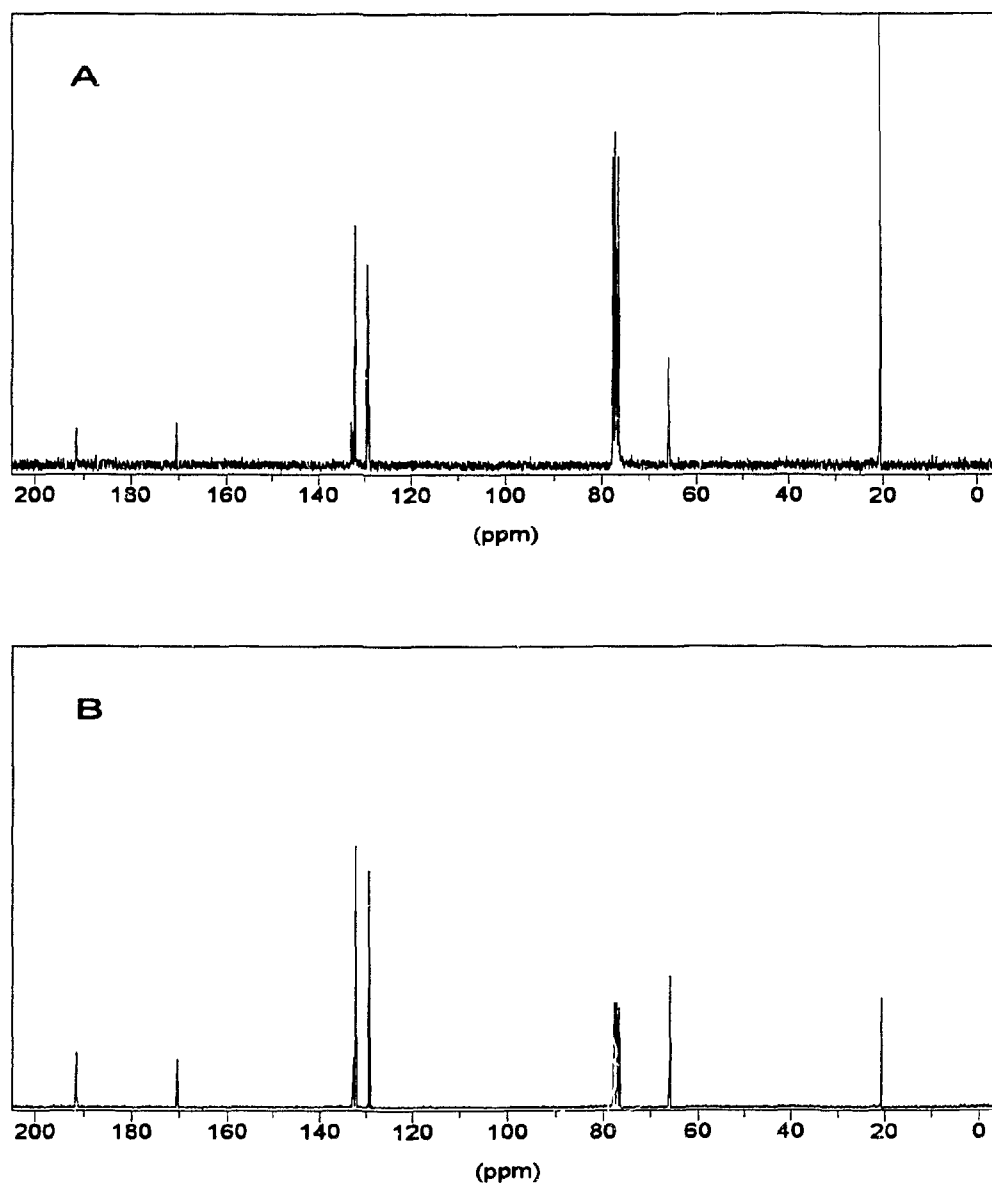


**Figure 31.**  $^{13}\text{C}$ -Nmr spectra of *p*-bromophenacyl acetate: (A) isolated from a culture of *F. nucleatum* supplemented with L-[4- $^{13}\text{C}$ ]glutamate and (B) a natural abundance sample.

C-2 (2.7%). The lack of  $^{13}\text{C}$  enrichment at C-1 of acetate and C-1 and C-3 of butyrate ruled out glutamate degradation by the methylaspartate pathway in *F. nucleatum*, and the large  $^{13}\text{C}$  enrichment at C-4 of butyrate supported the hydroxyglutarate pathway. In both Expts. 1 and 2, the  $^{13}\text{C}$  label was more efficiently incorporated into butyrate than acetate, indicating a more direct formation of butyrate from glutamate that is consistent with the hydroxyglutarate pathway.

### 3.2.1 Metabolism of $^2\text{H}$ - and $^{13}\text{C}$ -Labelled Acetate by *F. nucleatum*

Since the methylaspartate pathway does not contribute to glutamate catabolism in *F. nucleatum*, the smaller  $^{13}\text{C}$  enrichments observed at C-3 and C-2 of butyrate derived from L-[1- $^{13}\text{C}$ ]glutamate (Expt. 1) and L-[4- $^{13}\text{C}$ ]glutamate (Expt. 2), respectively, must represent the synthesis of butyrate from enriched acetate (or acetyl-CoA) formed in each of these experiments. This was tested by adding [1,2- $^{13}\text{C}_2$ ]acetate and unlabelled glutamic acid (Table 4; Expts. 4 and 5) to *F. nucleatum* cultures. The proton-decoupled  $^{13}\text{C}$ -nmr spectrum (Figure 33A) of the *p*-bromophenacyl butyrate ester isolated in each experiment contained singlets for the carbons provided by the *p*-bromophenacyl bromide reagent and a group of three signals for each carbon atom of butyrate, corresponding to a doublet arising from  $^{13}\text{C}$ - $^{13}\text{C}$  coupling superimposed on a singlet due to uncoupled, natural-abundance  $^{13}\text{C}$ . The coupling between C-1,2 (57.5 Hz) and C-3,4 (34.8 Hz) and the approximately equal enrichment at all four carbon atoms of butyrate (Table 6)

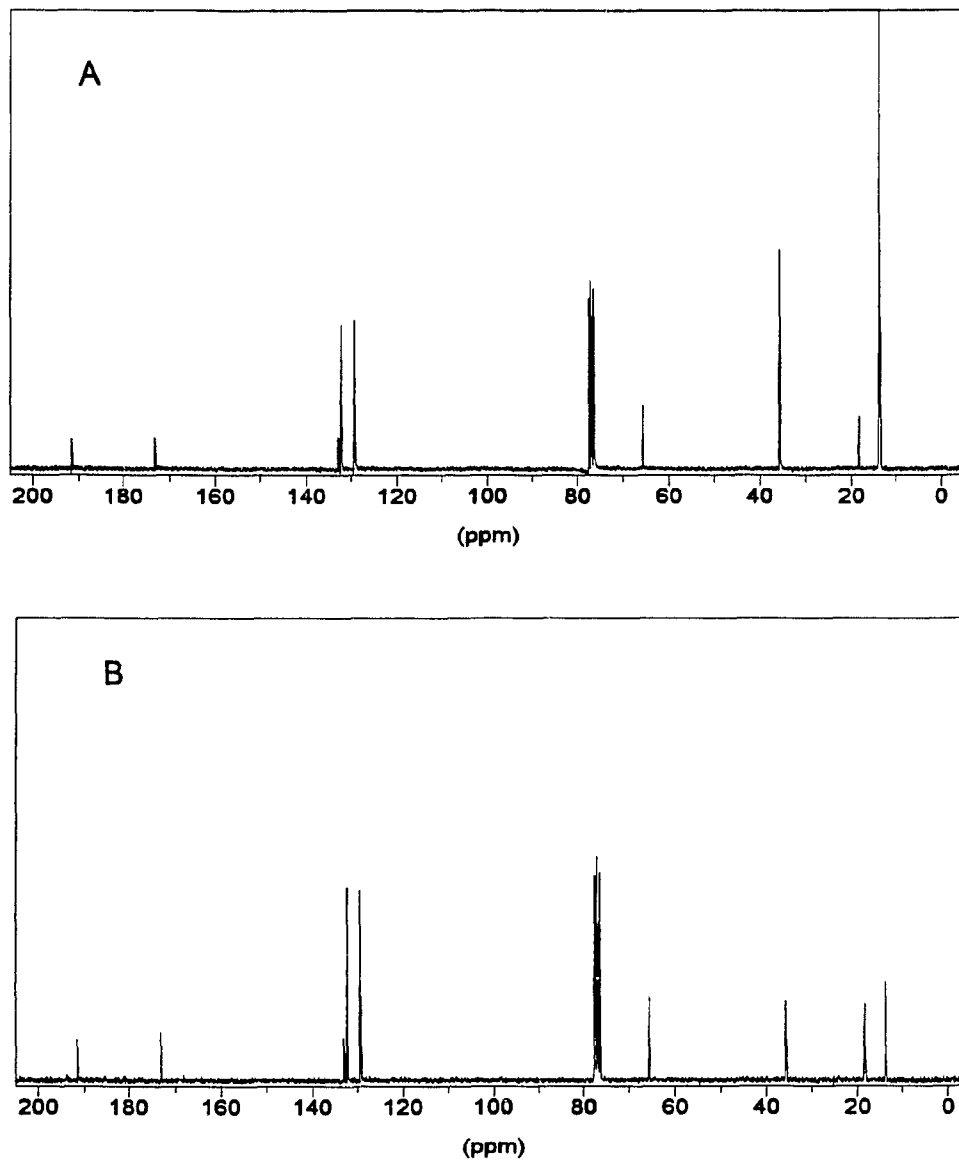


**Figure 32.**  $^{13}\text{C}$ -Nmr spectra of *p*-bromophenacyl butyrate: (A) isolated from a culture of *F. nucleatum* supplemented with L-[4- $^{13}\text{C}$ ]glutamate and (B) a natural abundance sample.

Table 6. Incorporation of labelled acetic acids into butyric acid by *F. nucleatum*.

Expt. No.	Labelled Acetate		Isotopic Enrichment (%) in <i>p</i> -Bromophenacyl Butyrate								
	Label	Atom % <sup>a</sup>	MS Analysis <sup>b</sup>					NMR Analysis <sup>c</sup>			
			I <sub>0</sub>	I <sub>1</sub>	I <sub>2</sub>	I <sub>3</sub>	I <sub>4</sub>	C-1	C-2	C-3	C-4
4 <sup>d</sup>	1,2- <sup>13</sup> C <sub>2</sub>	99.3	74.5 (0.6)	0.7 (0.2)	19.4 (0.4)	-0.8 (0.2)	6.1 (0.3)	11.1	9.5	10.5	12.3 (0.5)
5 <sup>e</sup>	1,2- <sup>13</sup> C <sub>2</sub>	99.3	92.0 (0.5)	0.6 (0.2)	7.0 (0.5)	-1.1 (0.5)	1.2 (0.4)	4.3	4.0	4.0	4.2 (0.1)
6 <sup>d</sup>	2- <sup>2</sup> H <sub>3</sub>	99.5	62.0 (0.1)	9.1 (0.02)	3.9 (0.1)	14.9 (0.3)	10.9 (0.1)	-	-	-	-
7 <sup>e</sup>	2- <sup>2</sup> H <sub>3</sub>	99.5	94.3 (1.5)	4.0 (0.9)	-0.5 (1.0)	1.0 (0.3)	1.6 (0.8)	-	0.7	-	3.3 -

<sup>a</sup> Isotopic enrichments of glutamates added to cultures.

<sup>b</sup> The standard deviation calculated from replicate scans, typically 3, is given in parentheses.

<sup>c</sup> The standard deviation calculated from the peak heights of natural abundance signals contributed by the derivatization reagent is given in parenthesis.

<sup>d</sup> Unenriched peptone medium.

<sup>e</sup> Peptone medium.

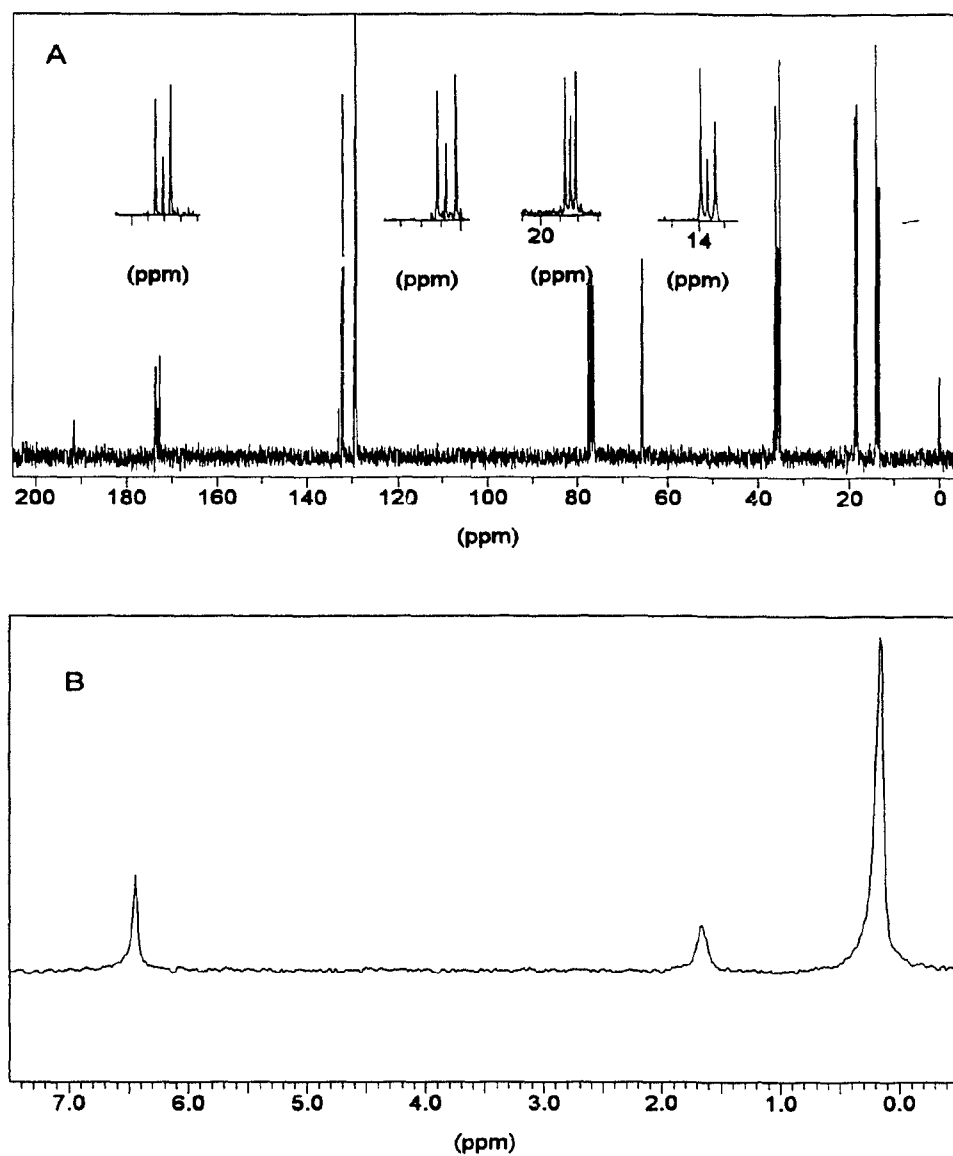


**Figure 33.**  $^{13}\text{C}$ -Nmr (A) and  $^2\text{H}$ -nmr (B) spectra of *p*-bromophenacyl butyrate isolated from cultures of *F. nucleatum* supplemented with  $[1,2-^{13}\text{C}_2]$  acetate and  $[^2\text{H}_3]$ acetate, respectively.

demonstrate that two intact acetate units combine to form butyrate. The lack of enrichment of the singlet signals indicates that only  $^{13}\text{C}_2$  units were incorporated. MS confirmed that the major isotopically labelled species of butyrate contained two atoms of  $^{13}\text{C}$  (Table 6). Thus, acetate is converted into butyrate, accounting for the smaller enrichments observed at a second position of butyrate in the L-[1- $^{13}\text{C}$ ]- and L-[4- $^{13}\text{C}$ ]glutamate experiments.

Confirmation of the conversion of acetate into butyrate was obtained using [ $^2\text{H}_3$ ]acetate, and the incorporation of  $^2\text{H}$  was detected by MS and  $^2\text{H}$ -nmr spectroscopy (Table 6; Expts. 6 and 7). That only two positions of butyrate were labelled was readily seen in the  $^2\text{H}$ -nmr spectrum of *p*-bromophenacyl butyrate (Figure 33B), which showed signals at 0.99 (C-4) and 2.48 (C-2) ppm corresponding to a 2.2% overall enrichment (averaged over five atoms). A similar enrichment (2.5%) was calculated from the mass spectrum of *p*-bromophenacyl butyrate, which showed isotopically labelled species containing one, three or four atoms of  $^2\text{H}$ . The ratio of  $^2\text{H}$  atoms at C-4 and C-2 was 7:3 by  $^2\text{H}$ -nmr spectroscopy.

In both Expts. 4 and 5, the  $^{13}\text{C}$ -nmr spectrum of the isolated butyrate (Figure 33A) contained a low-intensity doublet-of-doublets peak pattern for C-2 and C-3, demonstrating that these carbons were coupled to each other ( $J = 34$  Hz) as well as to C-1 and C-4, respectively. This confirms the incorporation of two labelled acetate units into a single butyrate molecule indicated by the presence of  $^{13}\text{C}_4$  and  $^2\text{H}_4$  species in the mass spectra. In Expt. 4, the heights of the individual signals

in the doublet of doublets pattern were slightly higher than the corresponding natural-abundance singlet in the same nmr spectrum indicating that approximately 5% of the butyrate molecules were derived from two labelled acetate units. A similar  $^{13}\text{C}_4$  enrichment of 6% was measured by MS.

- The overall incorporation of label from acetate into butyrate (Table 6) was significantly higher when fewer nutrients were available in the medium (20 versus 8%  $^{13}\text{C}$  in Expts. 4 and 5, and 21 versus 2.5%  $^2\text{H}$  in expts. 6 and 7), and a larger proportion of the butyrate was formed from two labelled acetate units (Expts. 4 and 6 versus Expts. 5 and 7, respectively). Both observations were consistent with the formation of larger quantities of unlabelled acetate in peptone medium. Also, the incorporation of  $\text{C}^2\text{H}_3$  units was much lower on peptone medium (Expt. 7); the acetate recovered from the culture supernatant in this experiment contained less than 5%  $^2\text{H}$ , and only  $2.6 \pm 0.6\%$  contained three  $^2\text{H}$  atoms.

### 3.3 Catabolism of $^{13}\text{C}$ -Labelled Glutamic Acids by *F. varium*

In this investigation, four  $^{13}\text{C}$ -labelled D- and L-glutamic acids and two labelled acetates were used to establish the pathway or the pathways involved in glutamate catabolism by *F. varium*. The experimental conditions are summarized in Table 7.

In the initial experiment, L-[1- $^{13}\text{C}$ ]glutamate (Expt. 8) was administered to a culture of *F. varium*; enrichment at C-1 of acetate (2.4%) and equal enrichment at C-1 and C-3 of butyrate (6.2 and 6.6%, Table 8) were observed by nmr

Table 7. Isotopic feeding experiments in *F. varium*.

Expt. No. <sup>a</sup>	Substrate	Atom (%)	Culture Volume (mL)	Amount Added (mg)		Amount of Phenacyl Ester isolated (mmol)	
				Labelled Substrate	Unlabelled Glutamate	Acetate	Butyrate
8	L-[1- <sup>13</sup> C]Glutamate	99	50	50	75	0.19	0.36
9	L-[4- <sup>13</sup> C]Glutamate	95	50	50	75	0.11	0.14
10	L-[5- <sup>13</sup> C]Glutamate	99	50	50	75	0.12	0.18
11	D-[3- <sup>13</sup> C]Glutamate	99	50	50	75	0.20	0.51
12	Sodium [1,2- <sup>13</sup> C <sub>2</sub> ]acetate	99.3	100	50	250	<sup>b</sup>	0.25
13	Sodium [ <sup>2</sup> H <sub>2</sub> ]acetate	99.5	100	50	250	0.10	0.15

<sup>a</sup> Peptone medium was used for all experiments.

<sup>b</sup> Not isolated.

Table 8. Incorporation of [<sup>13</sup>C]glutamic acids into acetic and butyric acids by *F. vanum*.

Expt. No	13C Labelled Glutamate		13C Enrichment (%)											
	Position of Label	Atom % <sup>a</sup>	MS Analysis <sup>b</sup>				NMR Analysis <sup>c</sup>							
			Acetate		Butyrate		Acetate		Butyrate					
			I <sub>0</sub>	I <sub>1</sub>	I <sub>0</sub>	I <sub>1</sub>	C-1	C-2	C-1	C-2	C-3	C-4		
8	1	40	96.3 (0.6)	3.7 (0.3)	87.7 (0.9)	13.0 (0.4)	2.4	0.0	(0.1)	6.2	-0.1	6.8	-0.1	(0.02)
9	4	38	97.8 (0.3)	2.3 (0.1)	87.5 (0.5)	12.2 (0.1)	1.9	-0.02	(0.1)	6.0	-0.1	6.3	0.0	(0.02)
10	5	40	99.9 (0.8)	0.3 (0.3)	99.4 (0.9)	0.5 (0.6)	-0.2	-0.1	(0.06)	-0.3	-0.3	-0.3	-0.4	(0.5)
11 <sup>d</sup>	3	40	97.4 (1.1)	2.3 (0.3)	90.1 (0.5)	10.5 (0.2)	0.07	1.54	(0.02)	-0.0	5.3	0.2	5.4	(0.04)

<sup>a</sup> Isotopic enrichment of glutamate added to the culture.

<sup>b</sup> The standard deviation calculated from replicate scans, typically 6, is given in parentheses.

<sup>c</sup> The standard deviation calculated from the natural abundance signals contributed by the derivatization reagent is given in parentheses.

<sup>d</sup> D-Glutamate

spectroscopy. The sum of the butyrate enrichments (12.8%) corresponds to the overall enrichment measured by MS (13%), and the major species of butyrate was singly labelled (Table 8). The equal enrichment in butyrate (Figure 29), supports the methylaspartate pathway, but the location of the  $^{13}\text{C}$  enrichment in acetate and butyrate would not be different if the hydroxyglutarate pathway was simultaneously operative. No incorporation of label into acetate and butyrate was observed when L-[5- $^{13}\text{C}$ ]glutamate was degraded by *F. varium* (Table 8, Expt. 10), excluding the aminobutyrate pathway.

The simultaneous operation of the methylaspartate and the hydroxyglutarate pathways was tested by feeding L-[4- $^{13}\text{C}$ ]glutamate (Expt. 9) to *F. varium*; the acetate and butyrate produced by each pathway would have different enrichment patterns (Figure 29). Nmr spectroscopy demonstrated that acetate derived from L-[4- $^{13}\text{C}$ ]glutamate was enriched at C-1 (1.9%), and C-1 and C-3 of butyrate were enriched equally (6.0 and 6.3%, Table 8). MS analysis indicated that only singly labelled butyrate was present, and the total enrichment (12.2%) was equivalent to the sum of the enrichments at C-1 and C-3 (12.3% ,Table 8) determined by nmr spectroscopy. These results demonstrate that the methylaspartate pathway is responsible for L-glutamate catabolism in *F. varium*.

Since the literature results suggesting the simultaneous operation of three pathways in *F. varium* (2) were obtained in cultures supplemented with DL-[ $^{14}\text{C}$ ]glutamate (114) and both D- and L-glutamate are taken up by *F. varium* (Section 2.1), the possible existence of different pathways for the catabolism of D-

and L-glutamate was investigated. To test whether D-glutamate accumulated inside the cells or was metabolized, *F. varium* cells grown in liquid culture containing D-glutamate were sampled at time intervals and extracted with aqueous ethanol (80%). The ethanolic solutions were analyzed by hplc, and glutamate was not detected

Prior to an isotopic feeding experiment with labelled D-glutamate, the yield of *p*-bromophenacyl esters of acetate and butyrate from the cultures supplemented with different concentrations of D-glutamate (7 and 17 mM) was examined (Table 9). The yields of *p*-bromophenacyl esters were not significantly different than those obtained from cultures of *F. varium* supplemented with L-glutamic acid (Table 7)

Table 9. Yield of acetate and butyrate isolated from a culture supplemented with D-glutamate

D-Glutamate Initial (mM)	<i>p</i> -Bromophenacyl Esters Isolated (mmol)	
	Acetate	Butyrate
7	0.60	0.17
17	0.60	0.55

Degradation of D-[3-<sup>13</sup>C]glutamate (Expt. 11), by *F. varium* generated acetate labelled at C-2 (1.54%) and butyrate labelled at C-2 and C-4 (5.3% and 5.4%, respectively) (Table 8) These isotopic enrichment patterns were equivalent to those expected from the catabolism of L-[3-<sup>13</sup>C]glutamate by the methylaspartate

pathway (Figure 29). Therefore, both D- and L-glutamate are degraded by the methiaspartate pathway in *F. varium*.

### 3.3.1 Metabolism of $^2\text{H}$ - and $^{13}\text{C}$ -Labelled Acetate by *F. varium*

*p*-Bromophenacyl butyrate isolated from a culture of *F. varium* supplemented with  $[1,2-^{13}\text{C}_2]$ acetate (Expt. 12) and L-glutamate had three signals for each carbon atom of butyrate and singlets for the carbon atoms derived from the *p*-bromophenacyl moiety in its proton-decoupled  $^{13}\text{C}$ -nmr spectrum. In the three peak pattern, the middle peaks arises from the superposition of a doublet due to  $^{13}\text{C}$ - $^{13}\text{C}$  coupling on a natural abundance singlet. The coupling constants between C-1,2 and C-3,4 were 35 and 57 Hz, respectively, indicating the incorporation of two  $\text{C}_2$  units. All carbon atoms were enriched nearly to the same extent ( $\sim 4.5\%$ ) and the major species of labelled butyrate contained two atoms of  $^{13}\text{C}$  by MS spectrometry (Table 10).

Further support for the formation of butyrate from acetate was obtained using  $[^2\text{H}_3]$ acetate (Expt. 13). The mass spectrum of *p*-bromophenacyl butyrate isolated in this experiment showed peaks corresponding to butyrate molecules containing up to three atoms of  $^2\text{H}$ . The  $^2\text{H}$ -nmr spectrum contained two broad signals at 0.99 ppm ( $^2\text{H}$ -4) and 2.47 ppm ( $^2\text{H}$ -2) in a ratio of 6.8 (Table 10). Therefore, the intact incorporation of acetate into butyrate in *F. varium* is very similar to that in *F. nucleatum*.

Table 10. Incorporation of labelled acetic acids into butyric acid by *F. varium*

Expt. No.	Labelled Acetate		Isotopic Enrichment (%) in <i>p</i> -Bromophenacyl Butyrate									
	Label	Atom % <sup>a</sup>	MS Analysis <sup>b</sup>					NMR Analysis <sup>c</sup>				
			<i>I</i> <sub>0</sub>	<i>I</i> <sub>1</sub>	<i>I</i> <sub>2</sub>	<i>I</i> <sub>3</sub>	<i>I</i> <sub>4</sub>	C-1	C-2	C-3	C-4	
12	1,2- <sup>13</sup> C <sub>2</sub>	99.3	91.1 (0.4)	0.8 (0.2)	8.3 (0.4)	-0.1 (0.3)	1.2 (0.3)	4.7	4.4	4.7	4.8	(0.1)
13	2- <sup>2</sup> H <sub>3</sub>	99.5	91.9 (0.3)	4.4 (0.3)	1.1 (0.3)	1.8 (0.3)	0.2 (0.3)	-	0.9	-	4.2	

<sup>a</sup> Isotopic enrichment of acetate added to the culture.

<sup>b</sup> The standard deviation calculated from replicate scans, typically 3, is given in parentheses.

<sup>c</sup> The standard deviation calculated from the natural abundance signals contributed by the derivatization reagent is given in parentheses.

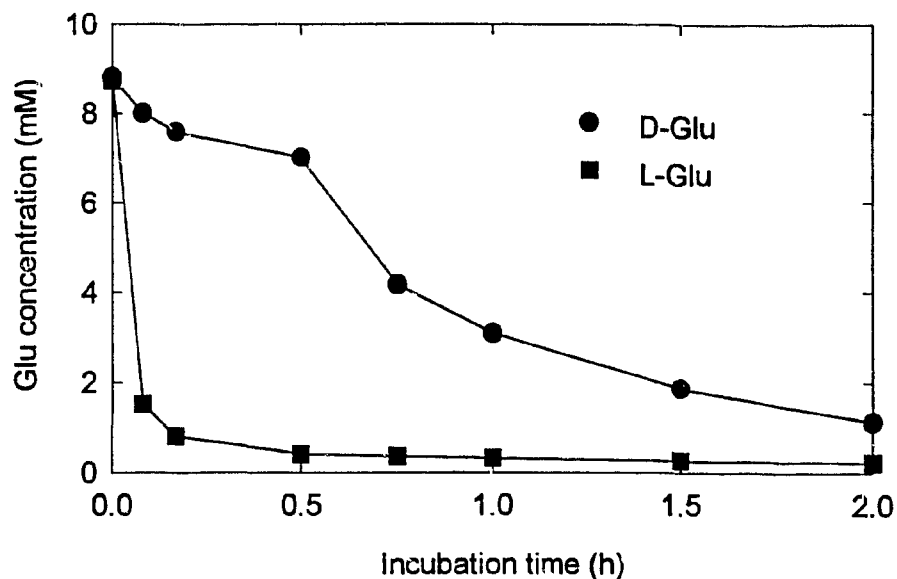


**Figure 34.** Catabolism of D- and L-glutamate by a crude cell-free extract of *F. varium*.

### 3.4 Detection and Partial Purification of Enzymes in the Methylaspartate Pathway

The enzymatic reactions comprising the initial steps of the methylaspartate pathway were investigated in cell-free extracts of *F. varium* by nmr and hplc. Crude cell-free extracts corresponded to the supernatant of a sonicated cell suspension, and the partially purified extract was prepared from the crude extract by protamine sulfate and ammonium sulfate fractionation.

The catabolism of D- and L-glutamate (9 mM) by crude cell-free extracts of *F. varium* was examined by hplc. The two enantiomers were degraded at different rates: 9 mM L-glutamate disappeared from the reaction mixture after 10 min, whereas the D-glutamate was reduced to approximately 1 mM after 2 h (Figure

34). The formation of other amino acids was not observed, indicating that both D- and L-glutamate were degraded to substances that did not contain a primary amino group. The different rates of D- and L-glutamate degradation are consistent with the presence of an additional, slower step for the degradation of the D-isomer.

The degradation of L-[4-<sup>13</sup>C]glutamate in crude cell-free extract supplemented with *o*-phenanthroline, an inhibitor of citramalate hydrolyase (EC 4.2.1.34) (58), was monitored by <sup>13</sup>C nmr. In addition to the residual L-glutamate signal (36.2 ppm, C-4) two other signals corresponding to mesaconate (141.5 ppm, C-2) and  $\beta$ -methylaspartate (42.7 ppm, C-3) were detected after 200 min of incubation (Figure 35B). The formation of these intermediates of the methylaspartate pathway is consistent with the presence of glutamate mutase (EC 5.4.99.1) and methylaspartase (E.C. 4.3.1.2) in the *F. varium* extract.

The formation of  $\beta$ -methylaspartate and glutamate was detected by hplc when partially purified cell-free extract was incubated with mesaconate and *o*-phenanthroline (Figure 36A). The peaks corresponding to  $\beta$ -methylaspartate (0.36 mM) and glutamate (0.67 mM) formed in the incubation mixture after 5 min. The level of  $\beta$ -methylaspartate reached a maximum after 15 min and remained constant for 30 min, whereas the glutamate level increased constantly (Figure 37A).

Reduced glutamate mutase activity has been observed in extracts of *C. tetanomorphum* treated with charcoal to remove coenzyme B<sub>12</sub> (115). A charcoal treated, partially purified extract of *F. varium* was incubated with mesaconate

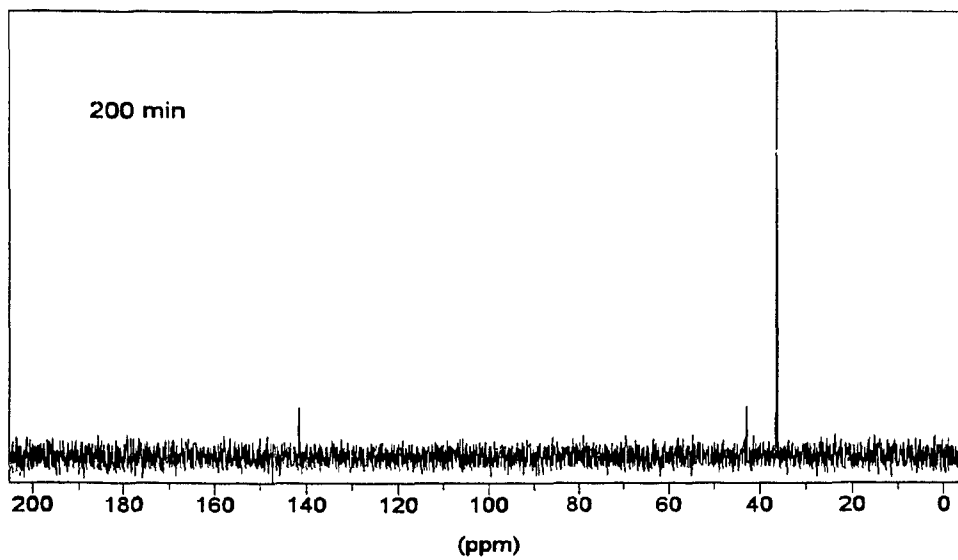
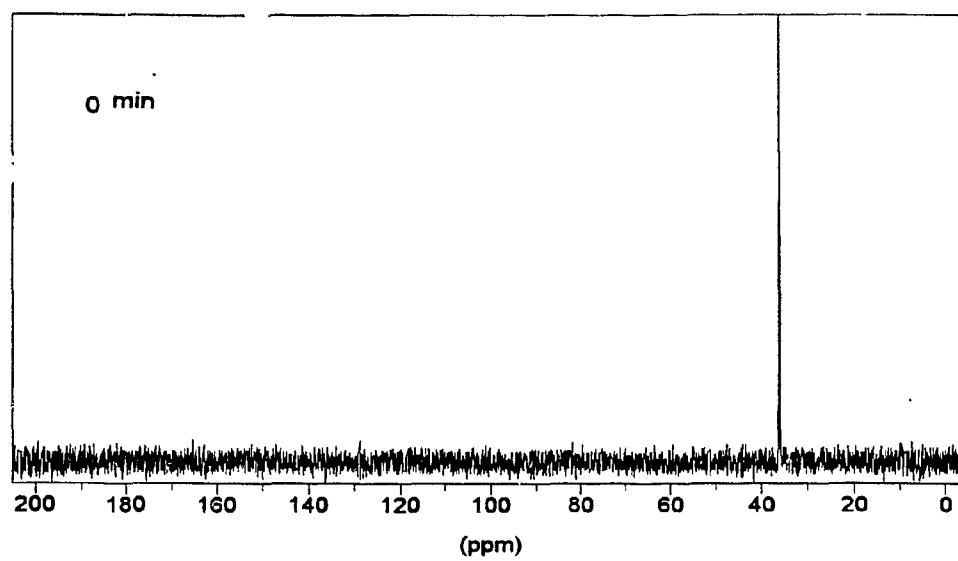


**Figure 35.**  $^{13}\text{C}$ -Nmr spectra of a cell-free extract of *F. varium* incubated with L-[4- $^{13}\text{C}$ ]glutamate.

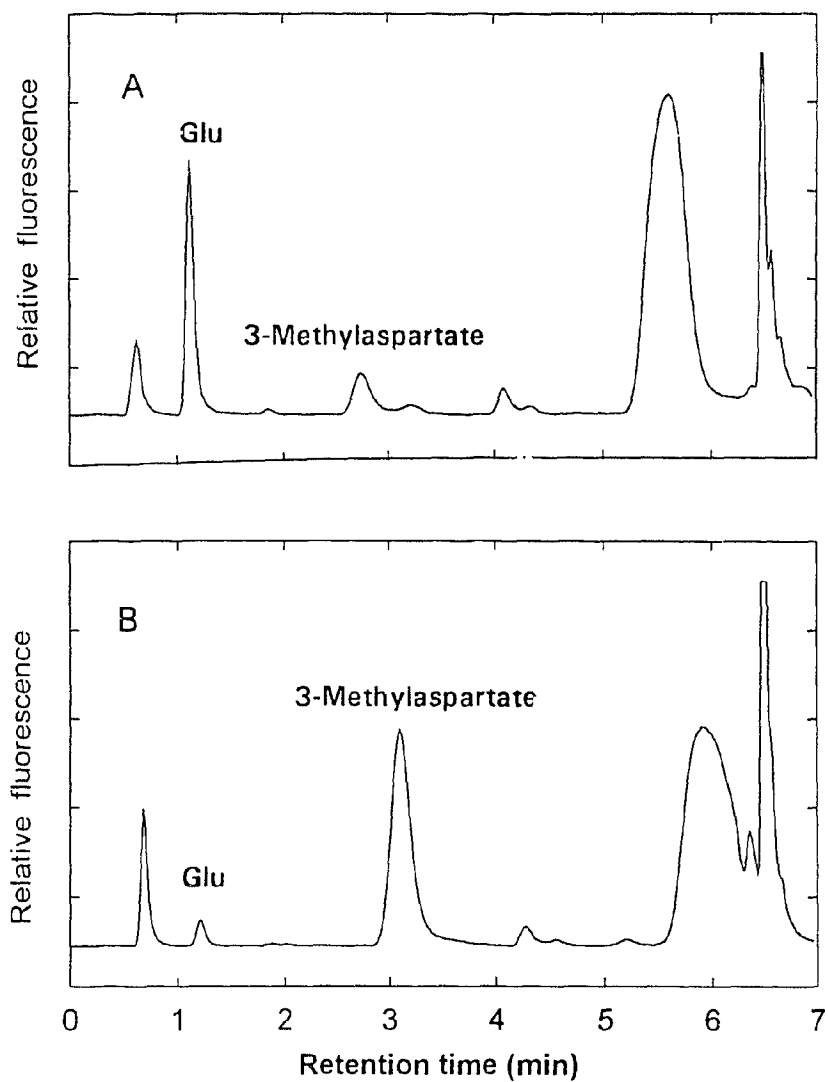


**Figure 36.** Hplc chromatograms of crude cell-free extract (A) and charcoal treated cell-free extract (B) of *F. varium* incubated with mesaconate for 5 min.

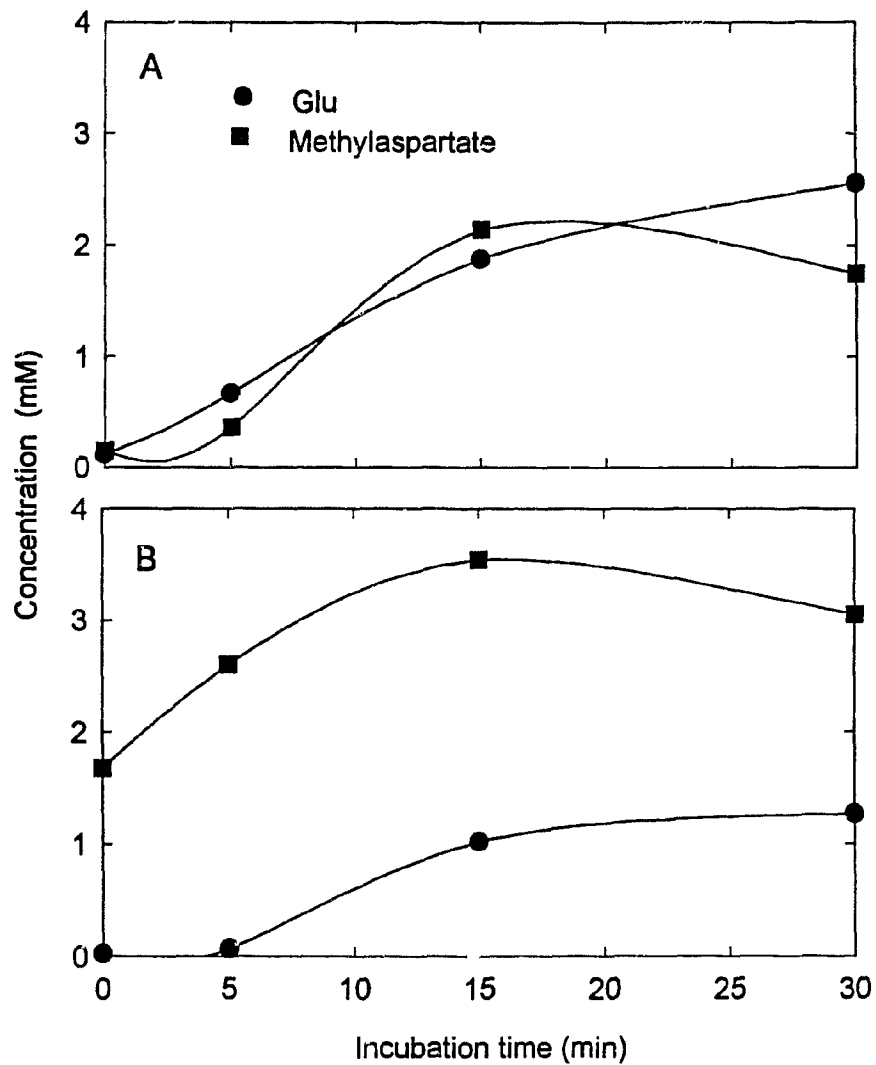


**Figure 37.** Formation of  $\beta$ -methylaspartate and glutamate from mesaconate by crude cell-free extract (A) and charcoal treated cell-free extract (B) of *F. varium* detected by hplc.

under identical conditions, and the formation of  $\beta$ -methylaspartate and glutamate was monitored by hplc. After 5 min of incubation, less glutamate (0.07 mM) and more  $\beta$ -methylaspartate (2.6 mM) were formed (Figure 36B). Maximum concentrations of glutamate (1.3 mM) and  $\beta$ -methylaspartate (3.5 mM) were reached after 30 and 15 min, respectively (Figure 37B). The relatively larger accumulation of  $\beta$ -methylaspartate in the charcoal treated extract supports the presence of a coenzyme B<sub>12</sub>-dependent glutamate mutase.

Partially purified extract was applied to a column of Sephadex G-150; methylaspartase activity was located in the fractions by incubating the fractions with DL-*threo*- $\beta$ -methylaspartate and monitoring the increase in absorbance at 240 nm due to the formation of mesaconate. The relationship between elution volume and molecular mass was calibrated using four standard proteins (Figure 38): alcohol dehydrogenase (150 kDa), bovine serum albumin (66 kDa), carbonic anhydrase (29 kDa) and cytochrome C (12.4 kDa). A molecular mass of 105 kDa was calculated for methylaspartase.

The methylaspartase purified on a Sephadex G-150 column was incubated with mesaconate at 37°C for 3 h and the sample was analyzed by chiral hplc. The chromatogram showed the formation of two products which eluted at 4.5 and 17.1 min, respectively (Figure 39A). Comparison to the chromatogram of standard sample containing DL-*erythro*- $\beta$ -methylaspartate, DL-glutamate and DL-*threo*- $\beta$ -methylaspartate (Figure 39B), indicated that the peaks in the incubation sample correspond to one enantiomer of either *erythro*- or *threo*- $\beta$ -methylaspartate. This

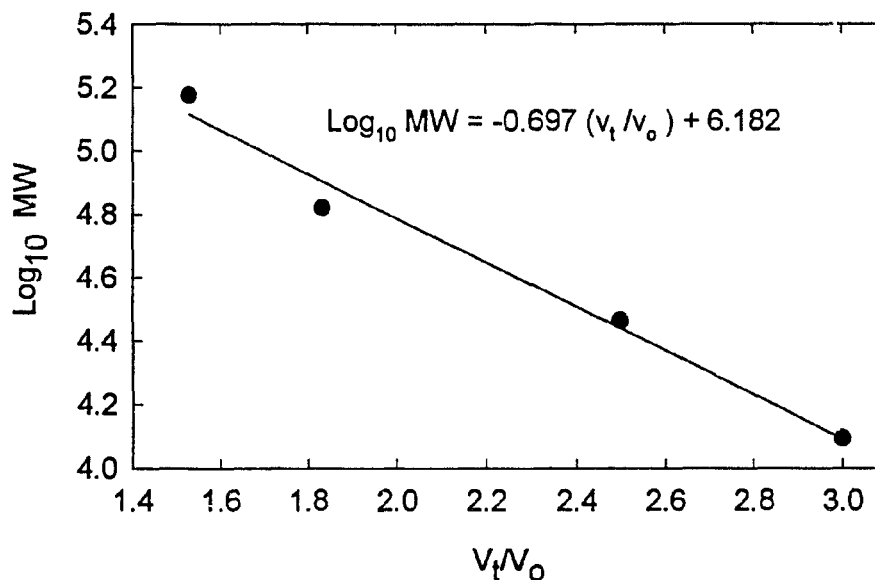


**Figure 38.** Standard curve relating molecular mass to the elution volume from a Sephadex G-150 column.

finding was confirmed by coinjecting of a mixture of standard and incubation samples. No extra peaks were observed and the peak area of one *erythro*- and one *threo*-3-methylaspartate peak increased (Figure 39C).

### 3.5 Detection and Partial Purification of Glutamate Racemase

Since both D- and L-glutamate are degraded by the methylaspartate pathway, the existence of an enzymatic system that can interconvert the isomers of glutamate was investigated. Two routes are possible: racemization catalyzed by a glutamate racemase (E.C. 5.1.1.3) and deamination catalyzed by a D-amino acid

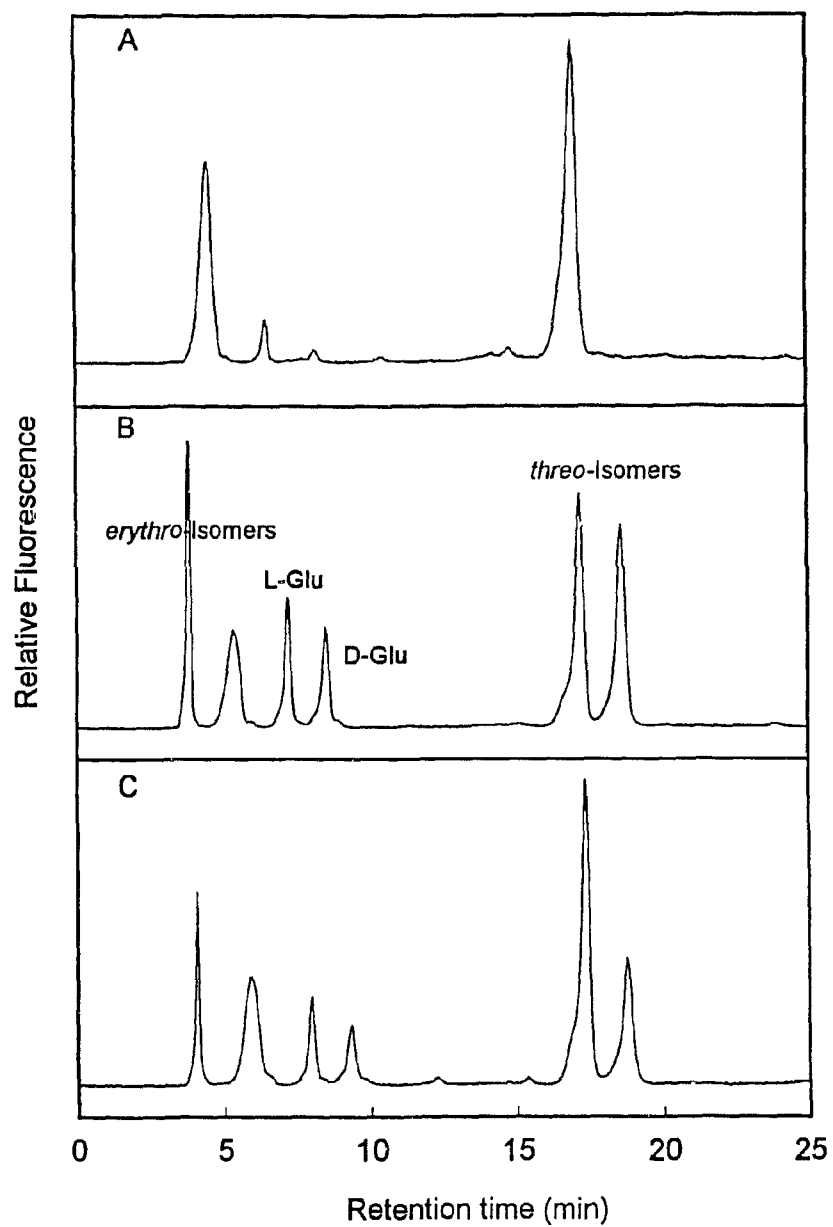


**Figure 39.** Chromatograms of the products from the incubation of mesaconate with methylaspartase eluted from Sephadex G-150 column (A), the 3-methylaspartate and DL-glutamate standard sample (B), and the mixture of standard and incubation samples analyzed (C) by chiral hplc.

transaminase (EC 2.6.1.21) or dehydrogenase followed by reamination of 2-oxoglutarate catalyzed by an L-amino acid transaminase or glutamate dehydrogenase. Both of these possibilities were tested in crude cell-free extract of *F. varium*.

The presence of D-amino acid transaminase was tested by incubating the crude cell-free extract containing 2-oxoglutarate with either DL-alanine, DL-aspartate and DL-phenylalanine. No increase in the level of glutamate over the control mixture lacking DL-amino acid was observed by hplc when DL-alanine and DL-phenylalanine were the substrate. However, the level of glutamate increased sharply compared to the control when DL-aspartate was the substrate.

Since the racemic mixture of aspartic acid was used, it was not known whether the formation of glutamate was due to a D- or L-amino acid transaminase. To test this, D- and L-aspartic acid were incubated separately with crude extract and 2-oxoglutarate. Only the reaction mixture containing L-aspartate produced glutamate at higher levels than the control incubation, excluding the presence of a D-amino acid transaminase.

Glutamate dehydrogenase activity was assayed in cell-free extracts of *F. varium* by following the change in uv absorbance at 340 nm. Although a low level of activity was detected for L-glutamate as the substrate ( $6.4 \mu\text{mol. min.}^{-1}$ ), but when L-glutamate was replaced with D-glutamate, under identical conditions, no activity was detected, ruling out the presence of a D-glutamate dehydrogenase.

The racemization of glutamate was investigated in charcoal-treated, partially

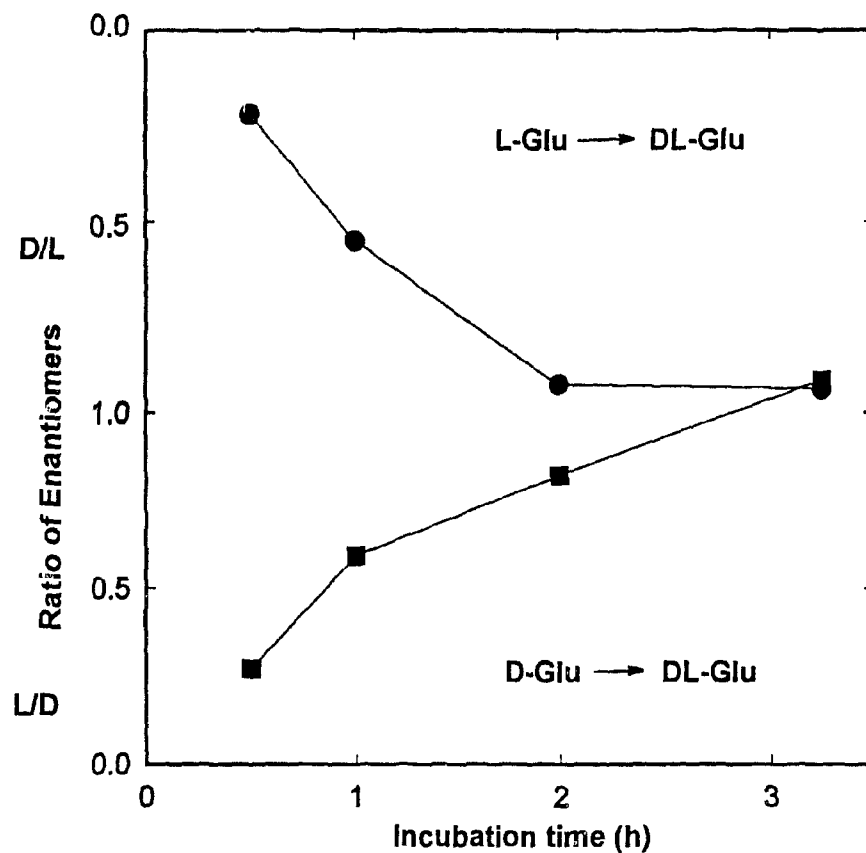


**Figure 40.** Racemization of either D- or L-glutamate by a charcoal treated, partially purified cell-free extract of *F. varium*.

purified cell-free extract. Both D- and L-glutamate (10 mM) were incubated with the extract, and the progress of the racemization was monitored by hplc and chiral hplc. With D- or L-glutamate as the substrate, a racemic mixture was obtained after 3 h of incubation (Figure 40). The total amount of glutamate in the extract remained constant during the incubation period, indicating that glutamate mutase

was inactivated by the charcoal treatment and that the racemization was catalyzed by a racemase.

To investigate whether the enzyme is inducible or constitutive, partially purified extracts were prepared from cells grown on peptone medium supplemented with either D- or L-glutamate (17 mM), and incubated separately with D- and L-glutamate under identical conditions. No significant difference in the rate and degree of racemization was observed by chiral hplc, indicating that the enzyme is constitutive (Figure 41).

The co-factor requirements of known racemases vary. While an anine racemase (EC 5.1.1.1) (116) requires pyridoxal phosphate, others such as proline racemase (EC 5.1.1.4) (117) and glutamate racemase (118) are cofactor independent. The effect of series of possible cofactors on the racemase activity was tested. Addition of  $\text{NAD}^+$ ,  $\text{NADP}^+$ , FMN and pyridoxal-5'-phosphate at 1 mM concentration to a partially purified extract containing D-glutamate (10 mM) had no effect on the rate of racemization compared to a control sample lacking any of the above cofactors (Figure 42). The molecular mass was determined using the same calibration curve constructed for methylaspartase, and racemase activity was monitored by incubating fractions eluted from Sephadex G-150 with D-glutamate (10 mM) and analyzing them by chiral hplc. A molecular mass of 17.6 KDa was obtained.

The incubation of D-glutamate (10 mM) with partially purified cell-free extract dissolved in  $\text{D}_2\text{O}$  resulted in the disappearance over time of the  $^1\text{H}$ -nmr signal at

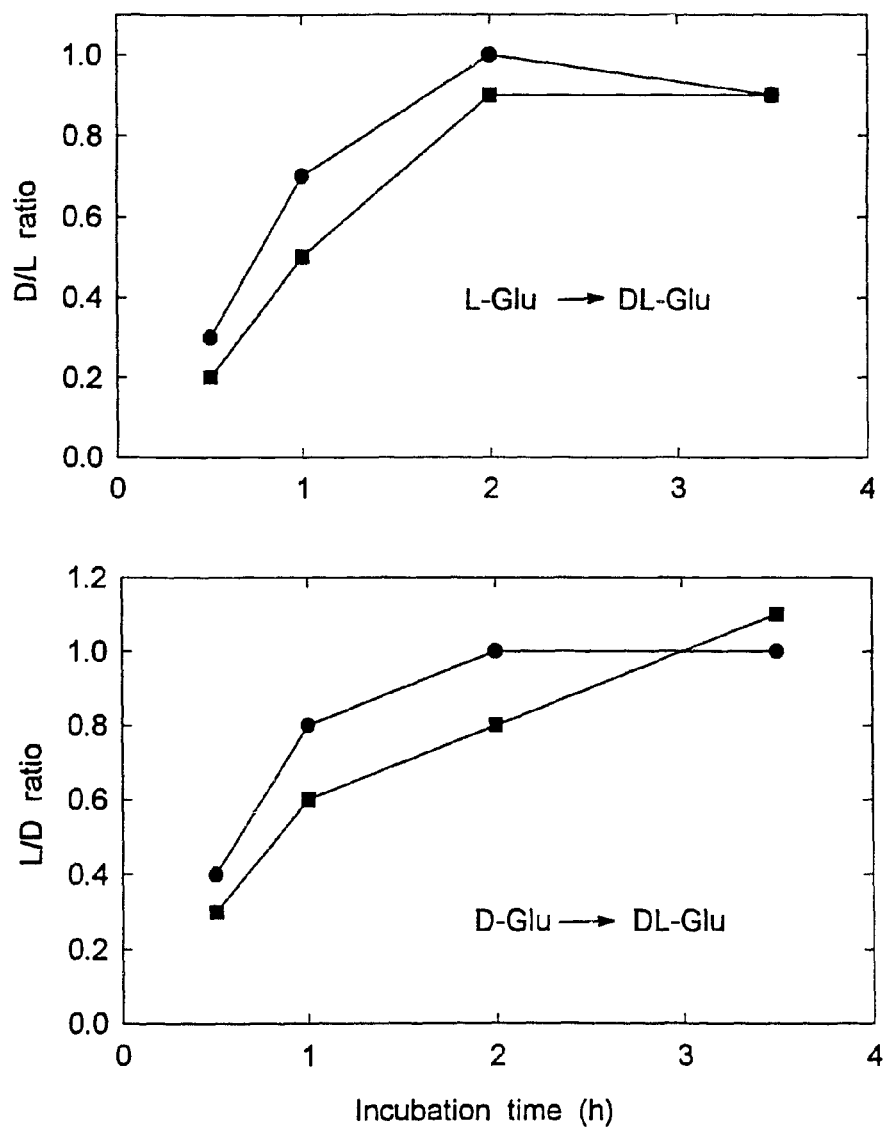


**Figure 41.** Racemization of D-glutamate (bottom) and L-glutamate (top) by a charcoal treated, partially purified cell-free extract of *F. varium* grown on either D-glutamate (■) or L-glutamate (●).

3.7 ppm corresponding to the  $\alpha$ - $^1\text{H}$  of glutamate (Figure 43). The reduced intensity of the signal was noticeable after 15 h and readily apparent after 48 h of incubation. At 48 h, the reaction mixture contained both L- and D-glutamate in a 7/10 ratio by chiral hplc. Therefore, the racemization process involves exchange of the  $\alpha$ -H of glutamate.

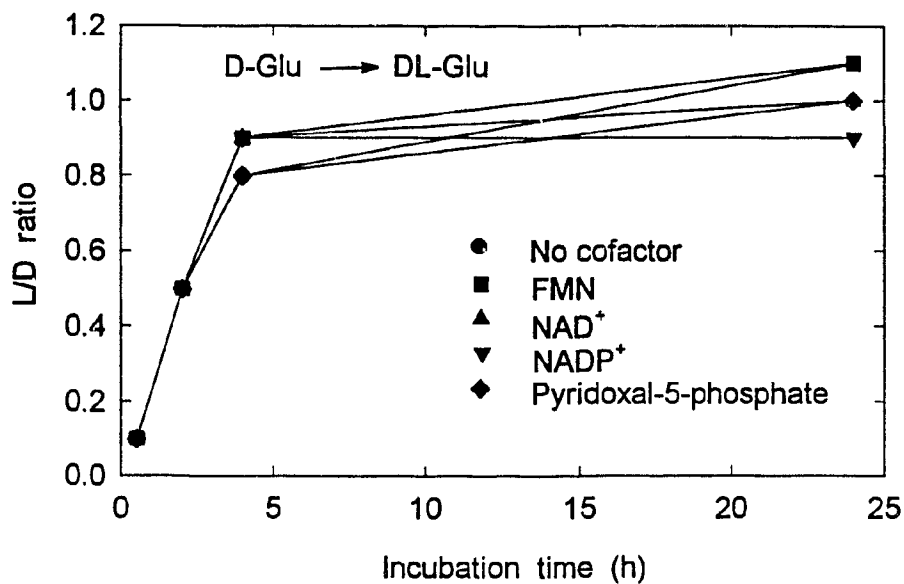


**Figure 42.** Effect of addition of cofactors on the rate and degree of racemization by a charcoal treated, partially purified cell-free extract of *F. varium*.

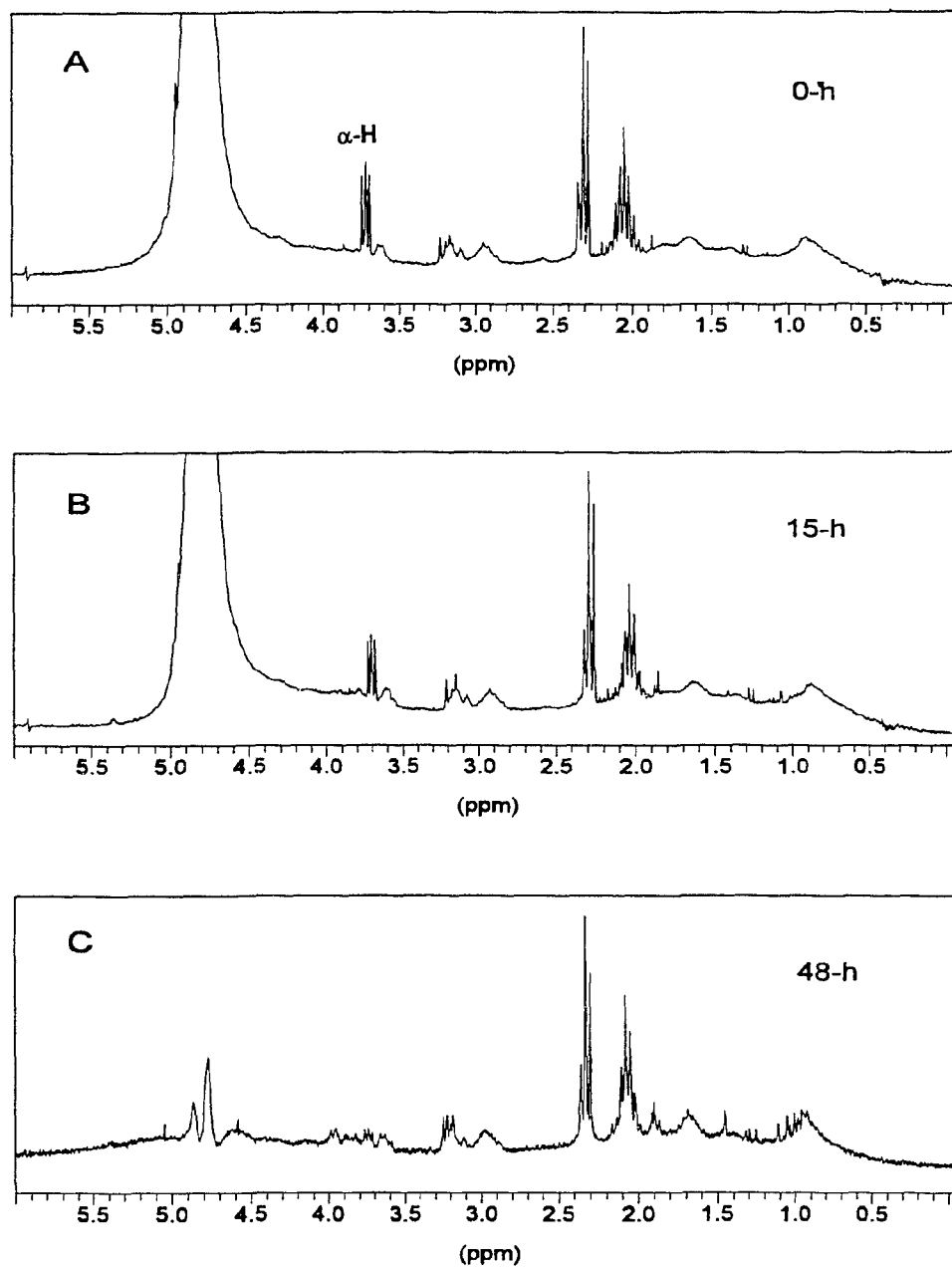


**Figure 43.**  $^1\text{H-NMR}$  spectra of the products from the racemization of D-glutamate in  $\text{D}_2\text{O}$ . Spectrum C was recorded while the residual water signal was saturated.

## Chapter 4

### Discussion

#### 4.1 Amino Acid Uptake by *Fusobacterium* Species

Amino acids are a major source of energy for many anaerobic bacteria (3), and several are readily assimilated by *Fusobacterium* species (10, 12, 13, 15). In this investigation, the stereoselective uptake of amino acids by *F. nucleatum* and *F. varium* was investigated. In the initial screening, the bacteria were incubated in a peptone medium containing a racemic mixture of an amino acid to save time and materials compared to an investigation of each isomer individually. Nonetheless, definitive results were obtained when neither enantiomer was assimilated and when both enantiomers were completely catabolized. Whether a partial uptake over the fixed time period was due to the selective assimilation of one enantiomer or to the partial catabolism of each stereoisomer was examined by chiral hplc and/or separate incubations of each stereoisomer.

Only six and seven of the 28 amino acids tested (Tables 2 and 3) were assimilated by *F. nucleatum* and *F. varium*, respectively (Table 11). The lack of uptake for an amino acid could be due to either the lack of transport system or absence of the enzymes responsible for the catabolism of that amino acid. However, it is not very likely that a bacterium lacking a transport system for an amino acid contains the enzymes for the catabolism of that amino acid. The number of amino acids assimilated was smaller than those reported for the same strain of *F. nucleatum* (15) and several strains of *F. varium* (14). This difference

Table 11. Stereochemistry of the amino acids assimilated by fusobacteria. <sup>a</sup>

<i>F. nucleatum</i>		<i>F. varium</i>	
L-	D- and L-	L-	D- and L-
Glutamic Acid	Glutamine	Arginine	3-Aminobutyric Acid
	Histidine	Glutamine	Glutamic Acid
Serine	Lysine		Lysine
	Diaminopimelic Acid <sup>b</sup>	Histidine	Serine

<sup>a</sup> Summary of data presented in Tables 2 and 3 and Figures 13 and 14.

<sup>b</sup> *meso*-Diaminopimelic acid and either one or both isomers of the racemate.

in the amino acid uptake profile might be due to the different media used; the peptone medium in this study *versus* the defined medium containing amino acids as the only sources of carbon and nitrogen in the previous investigations.

Among 120 strains of *F. nucleatum* tested for their ability to assimilate amino acids, asparagine, cysteine, glutamic acid, glutamine, histidine, lysine and serine were utilized by all strains, whereas aspartic acid, methionine, tryptophan, and tyrosine were taken up by some strains. Other amino acids were not assimilated by any strain of *F. nucleatum* (12). Similarly, strains of *F. varium* showed different amino acid patterns, but arginine, asparagine, cysteine, glutamic acid, histidine, lysine, serine and threonine were metabolized in high quantities by all four strains tested (14).

Both the stimulation and suppression of amino acid uptake by other amino acids or peptide has been reported. The effect of adding glutamate on the amino acid uptake profile of *F. nucleatum* resulted in complete suppression of the dibasic amino acids, arginine, histidine and ornithine (15). Yeast extract, as a source of peptides, stimulated the uptake of several amino acids by *F. varium*, such as histidine and glutamate, whereas other such as asparagine, methionine and threonine were suppressed. The uptake of other amino acids such as arginine, aspartic acid, lysine and ornithine was unaffected by the presence of peptides (14).

Of the eight amino acids utilized by *F. nucleatum* and *F. varium*, a group of five (glutamic acid, glutamine, histidine, lysine, and serine) were assimilated by both organisms (Table 11). However, the stereochemical preferences of *F. nucleatum* and *F. varium* were only the same for lysine. For the other four amino acids, the L-isomers was used selectively by one species and the other species assimilated both D- and L-isomers. While glutamate, histidine, lysine and serine are considered to be sources of energy for several strains of *F. nucleatum* (13) and peptides containing these amino acids are utilized rapidly (119), very little is known about the stereochemical preferences of this organism. Other than the suggestion that two different pathways are used for the degradation of D- and L-lysine (48), the stereochemistry of the amino acids used in most uptake studies in fusobacteria was either not defined (8, 11, 13-15) or focused on the naturally occurring L-isomers (10, 12). Consequently, only the assimilation of the L-isomers of these amino acids by *F. nucleatum* has been reported (9, 10, 12, 13, 15), and the

catabolism of D-amino acids has been overlooked.

The uptake of D-histidine and D-lysine, but not D-glutamate and D-serine, by *F. nucleatum* along with the hydrolysis of D-glutamine was observed (Table 11). Although the uptake of the L-isomers of glutamate, histidine, lysine and serine is general among *F. nucleatum* strains, it does not necessarily apply to the D-isomer, indicating that it might be possible to employ the D-amino acid uptake pattern of *F. nucleatum* strains or other amino acid-fermenting bacteria, such as clostridia, for taxonomic studies.

As D-glutamine degraded in the *F. nucleatum* culture, D-glutamate accumulated in the medium, indicating that the bacterium has enzyme activity which catalyzes the hydrolysis of the amide side-chain of D-glutamine to glutamic acid. Peptidase activity towards small peptides has been reported in *F. nucleatum* (10, 119). Also, it is very likely that L-glutamine was converted to L-glutamate, which was efficiently catabolized to acetate and butyrate. Smaller amounts of D-glutamine are catabolized by *F. varium* (Table 2), and this could be due to non-enzymatic hydrolysis during the incubation.

Only L-glutamate was assimilated by *F. nucleatum*, whereas both isomers of glutamate were catabolized by *F. varium*. The details of these pathways have been investigated in this thesis and are discussed in sections 4.4 and 4.5.

It has been reported that glutamate is an intermediate in histidine catabolism to acetate, butyrate and formate by *Clostridium tetanomorphum* and *Aerobacter aerogenes* (3). The pathway proceeds by elimination of ammonia,

catalyzed by histidine-ammonia lyase (EC 4.3.1.3), followed by opening of the imidazole ring to generate the C-1,2,N fragment of glutamate. Since only L-glutamate is degraded by *F. nucleatum* (Table 11) and no D-glutamate accumulated when D-histidine was catabolized, D-glutamate is not an intermediate of D-histidine catabolism. The histidine pathway could involve either enzyme-catalyzed elimination of ammonia from D-histidine or enzymatic racemization (e.g., histidine racemase).

Lysine was the only amino acid that both isomers were catabolized by *F. nucleatum* and *F. varium* (Table 11), indicating that lysine catabolism might play an important role as a source of energy in fusobacteria. It has been reported that two different pathways are involved in D- and L-lysine degradation in clostridia (120). Another study by Barker *et al.* (48) in *F. nucleatum* used isotopically labelled lysine and indicated that the carbon skeleton of lysine was cleaved at two different locations. Each cleavage was attributed to a separate pathway, *i.e.*, one for each isomer, and enzymes for L-lysine degradation were detected in cell-free extracts of *F. nucleatum*. Since the isotopic experiments were carried out using racemic mixtures of lysine, it is not certain if D-lysine was degraded by a different pathway. No attempt was made to detect the enzymes in D-lysine degradation pathway. It is necessary to perform isotopic experiments using enantiomerically pure lysine in order to assess the catabolism of D- and L-lysine in fusobacteria.

*F. varium* partially assimilated the racemate of 3-aminobutyrate (Table 3), and chiral hplc indicated that both isomers were consumed. 3-Aminobutyrate has

been proposed as an intermediate of lysine degradation in *F. nucleatum* (48), but it is not known which isomer is the true intermediate, as 3-aminobutyrate deaminase was assayed using racemic 3-aminobutyrate. Surprisingly, *F. nucleatum* did not metabolize 3-aminobutyrate (Table 3). This might be due to the lack of transport system for 3-aminobutyrate. To investigate this possibility, it is necessary to incubate 3-aminobutyrate with a cell-free extract of *F. nucleatum*.

To the best of our knowledge, the catabolism of diaminopimelic acid in fusobacteria has not been reported. As stated previously, hplc results are consistent with the catabolism of at least two of three isomers (*i.e.*, DD-, LL-, and *meso*-). Due to the unavailability of pure isomers, it was not possible to investigate this uptake in more detail. It is likely that diaminopimelic acid undergoes decarboxylation to generate lysine. Whether the D- or L-stereocentre, or both, are decarboxylated requires further investigation.

Unlike *F. nucleatum*, *F. varium* utilized both isomers of serine (Table 11). The presence of two separate serine dehydratases for D- and L-serine has been reported in *Escherichia coli* (121) and *Clostridium acidurici* (122). The high levels of lactate produced from L-serine degradation in *F. nucleatum* is consistent with the formation of pyruvate by L-serine dehydratase (Figure 44). The catabolism of both D- and L-serine by *F. varium* is consistent with the presence of two dehydratases (Figure 44), but the possibility of a serine racemase should also be considered.

Generally the rate of catabolism of the D-isomers of the amino acids was slower than that of the corresponding L-isomers (Figures 13 and 14). However, the

rate of D-serine uptake was faster than that of L-serine (Figure 14), indicating higher enzymatic activity towards D-serine. This result is more consistent with the presence of D-serine dehydratase (Figure 44) than a racemase catalyzed conversion to L-serine.

#### 4.2 Preparation of D-Amino Acids

The stereoselective uptake of L-glutamate and L-serine by *F. nucleatum* and L-arginine and L-histidine by *F. varium* prompted us to employ them for the preparation of the respective D-amino acids.

A first attempt prepared D-glutamic acid from *F. nucleatum* growing on a peptone medium containing DL-glutamate. A cation-exchange fractionation of the supernatant was not sufficient to generate a sample that could be recrystallized, and an anion-exchange column available for glutamate purification (110) was required. The crystallized D-glutamate had a high enantiomeric purity by hplc, but the optical rotation was low, indicating that the sample contained optically inactive impurities. The recovery was relatively low (57%). Since the anion-exchange column is not suitable for the purification of amino acids other than those containing acidic side-chains, changes to the culture medium were made in an attempt to simplify the purification and avoid using a second column. However, peptone media containing less yeast extract and peptone did not generate D-glutamate samples with improved enantiomeric purities and higher recoveries.

In a second approach to improving the recovery of D-glutamate, the initial

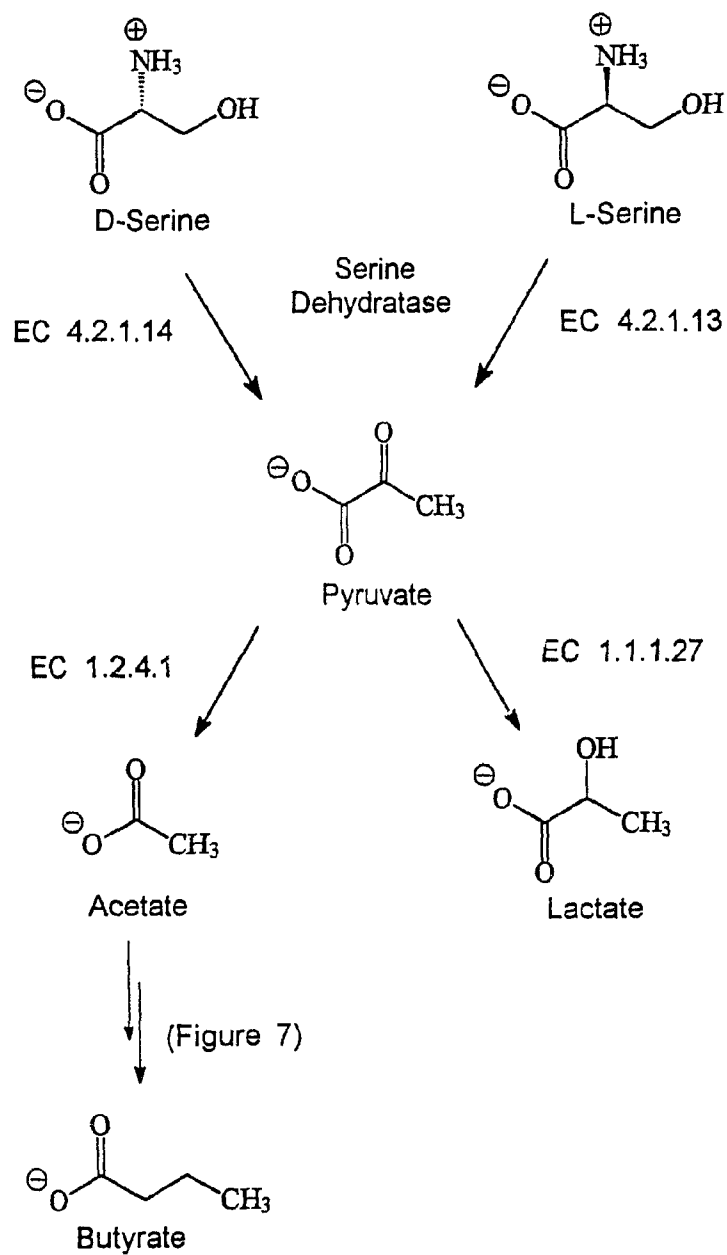


Figure 44. Proposed route for serine catabolism in *F. nucleatum*.

concentration of DL-glutamate was increased, but longer incubation times were required to obtain a high enantiomeric excess (Figure 15). Although the incubation time could be shortened by using a larger inoculum size (Figure 16), the maximum initial concentration of DL-glutamate was limited to about 100 mM.

The increased rate of L-glutamate uptake observed with the larger inoculum size indicated that a suspension of bacterial cells in buffer containing DL-amino acid might provide a more efficient way to prepare D-amino acids. The purification procedure would be simpler, and a higher initial concentration of DL-amino acids might be used. This approach has been used for the preparation of D-alanine (28), D-glutamate (30, 31), and D-mandelic acid (123).

In the first trial, a high enantiomeric excess was not attained by *F. nucleatum* cells grown on peptone medium and resuspended in buffer containing DL-glutamate, and it was noted that the *F. nucleatum* cells had a tendency to settle. A literature report (15) indicated that *F. nucleatum* cells grown in medium containing glutamate were morphologically distended and had a tendency to clump. To prevent the cells from clumping, the resuspensions were stirred and the stirring had a positive effect on the rate of L-glutamate and L-serine uptake from their racemic mixtures (Figure 17).

An increase in the cell density of the resuspension mixture resulted in a faster rate of L-glutamate and L-serine uptake. However, in the case of glutamate, the higher cell densities did not yield high enantiomeric excess of D-glutamate at high concentrations of DL-glutamate.

After 24 h of incubation, the enantiomeric excess of D-glutamate usually reached a constant level (Figures 22 and 23). The degradation of the L-alanine in a racemic mixture by *Candida maltosa* stopped as the pH of the resuspension buffer increased due to the liberation of ammonia, and adjustment of the pH during the incubation overcame the problem (28). However, the pH of the resuspension buffer during the degradation of L-glutamate decreased slightly (*i.e.*, from 7.4 to 7.0), and it is unlikely that the pH change is the limiting factor in L-glutamate degradation. Also, the *F. nucleatum* cells were viable after 48 h of incubation, whereas the uptake of L-glutamate stopped before 24 h in all incubations (Figures 18, 22 and 23).

Another possible factor affecting L-glutamate uptake might be end-product inhibition (*i.e.*, acetate and butyrate). Although acetate and butyrate at low concentrations (90 mM) had a minor effect, the effect was more noticeable at a higher concentration of acetate (Figure 28). Since, acetate is also one of the major end-products of L-serine degradation by *F. nucleatum* and serine degradation proceeded at very high concentrations of DL-serine, acetate can not be the major factor inhibiting L-glutamate uptake. The possible accumulative inhibition effect of acetate and butyrate was not investigated.

Unlike L-glutamate, L-serine was degraded at a much higher rate and no inhibition was observed; the solubility of DL-serine in resuspension buffer was the limiting factor (*i.e.*, concentrations more than 800 mM). For 800 mM DL-serine incubated with 50 g damp cells/L, most of the L-serine was degraded in less than

24 h, and the cells were still viable. This suggested the possibility of using the same batch of cells twice, which would increase the efficiency of the process to 1600 mM of DL-serine. Although cells incubated for 24 h in resuspension buffer containing 800 mM DL-serine did not result in a high enantiomeric excess (Figure 25), a high enantiomeric excess was reached in the second incubation, and it was evident that the cells continued to degrade the L-serine up to 70 h or more. This indicated that the first resuspension could be allowed to proceed for a longer time to reach a high enantiomeric excess and that a second batch of stereochemically pure D-serine could be obtained by resuspending the *F. nucleatum* cells in fresh medium.

The end-products of L-glutamate and L-serine degradation in resuspension medium were identified by nmr spectroscopy. The 2:1 ratio of acetate and butyrate formed from L-glutamate was consistent with that reported in literature (9). Lactate which was not detected by nmr in this experiment, was previously found to be an additional end-product in *F. nucleatum* DB6 (8).

L-Serine produced mainly acetate and lactate, and a minor amount of butyrate in a ratio of 20:22:1. No extra peaks corresponding to pyruvate were detected. Literature reports indicate that different strains of *F. nucleatum* produce end-products from serine in different ratios. While *F. nucleatum* 7CF produced mainly acetate and a small amount of lactate, *F. nucleatum* 53F produced all three end-products in equal quantities (9). On the other hand, *F. nucleatum* DB6 was reported to produce equal amounts of acetate and butyrate with less lactate, in

addition to ethyl alcohol (8).

The preparation of gram quantities of D-glutamate and D-serine from bacterial resuspensions was carried out. The initial concentration of DL-glutamate and DL-serine were 150 and 800 mM, respectively, and the products were purified by recrystallization after one ion-exchange column. Chemically pure D-glutamate and D-serine with high enantiomeric excesses were obtained by this approach.

Compared to the preparation of D-glutamate from peptone medium, a larger amount of DL-glutamate was processed and a simpler purification procedure yielded a cleaner product in high yield. This process compares favourably with a literature process for the purification of D-glutamate from L-glutamate (30) using a strain of *Lactobacillus brevis* that contains both glutamate racemase and glutamate decarboxylase. An advantage of using L-glutamate instead of the racemic mixture is that L-glutamate is produced in large quantities by fermentation and is cheaper. However, the process needed more manipulation as the pH of the buffer must be adjusted from 8.5 to 4.0 after 24 h of incubation in order to activate the glutamate decarboxylase, and the yield of D-glutamate from L-glutamate is also limited to 50%. Furthermore, the yield of cells for resuspension is very low, but this problem was addressed by cloning the glutamate racemase gene into *E. coli* and using another strain of *E. coli* as a source of L-glutamate decarboxylase. It is claimed that this method is the most efficient among the methods of D-glutamate production so far reported (31).

It was demonstrated that only the L-isomers of arginine and histidine were

degraded by *F. varium*. Consequently, the possible use of *F. varium* for the preparation of D-arginine and D-histidine was investigated. A longer time was needed for high concentrations of DL-arginine to reach a high enantiomeric excess (Figure 20), and another compound was formed in all incubation mixtures as the L-arginine degraded. The compound was identified by hplc as ornithine and, since only L-arginine was degraded, it is most likely L-ornithine. L-Ornithine is produced on commercial scales from L-arginine by enzymatic hydrolysis using arginase (EC 3.5.3.1) (14). Therefore, it would be possible to obtain both D-arginine and L-ornithine from DL-arginine using *F. varium*. The same approach has been used for the commercial production of D-aspartate and L-alanine from DL-aspartate using immobilized cells of *Pseudomonas dacunhae* that decarboxylate L-aspartate to L-alanine (27).

At 200 mM only a small portion of the initial DL-histidine was assimilated by the *F. varium* suspension. At lower concentrations, the uptake proceeded to 50%, indicating a complete catabolism of the L-isomer. Since the chiral hplc method was not suitable for histidine analysis, the enantiomeric excess of the residual D-histidine was not determined. These preliminary results suggest that histidine catabolism is limited by factors similar to those observed for glutamate catabolism. This is likely, since glutamate is formed from histidine (3).

#### **4.3 Conversion of Acetate to Butyrate**

Three distinct pathways have been proposed for the catabolism of

glutamate to acetate, butyrate, CO<sub>2</sub>, and NH<sub>3</sub> in anaerobic bacteria. While acetate and pyruvate are formed directly from glutamate in the methylaspartate pathway (Figure 8), crotonyl-CoA, a known intermediate in acetate and butyrate interconversion, is formed from glutamate in the hydroxyglutarate and aminobutyrate pathways (Figures 9 and 12, respectively). This indicates that the formation of butyrate by the methylaspartate pathway and formation of both acetate and butyrate from crotonyl-CoA by the hydroxyglutarate and aminobutyrate pathways involve the interconversion of acetate and butyrate. The establishment of this interconversion pathway is necessary prior to the investigation of glutamate catabolism in *F. nucleatum* and *F. varium*, because it would generate a more complicated isotopic enrichment pattern in butyrate (Figure 29).

The possibility of the presence of a pathway for acetate and butyrate interconversion was investigated in both *F. nucleatum* and *F. varium* using [1,2-<sup>13</sup>C<sub>2</sub>]acetate and [<sup>2</sup>H<sub>3</sub>]acetate. The major isotopically labelled species of butyrate contained two atoms of <sup>13</sup>C; <sup>13</sup>C-<sup>13</sup>C coupling was observed between C-1,2 and C-3,4, and the carbon atoms of butyrate were enriched to the same extent (Tables 6, and 12, Expts. 4, 5, and 12) These observations are fully consistent with the symmetrical incorporation of two intact acetate units into butyrate, according to the sequence of reactions (acetate → acetyl-CoA → acetoacetyl-CoA → 3-hydroxybutyryl-CoA → crotonyl-CoA → butyryl-CoA → butyrate in Figure 7) known for the conversion of acetate to butyrate in *Clostridium* species (44). Most of the enzymes associated with this sequence have been detected in crude extracts of

*F. nucleatum*, but an unsymmetrical incorporation of [1-<sup>14</sup>C]acetate into butyrate was observed in cultures supplemented with L-lysine (48). The latter was attributed to the formation of acetoacetyl-CoA from one acetate unit and two carbon atoms of 3-keto-5-aminohexanoate, an intermediate of L-lysine catabolism.

Confirmation of the conversion of acetate to butyrate was obtained using [<sup>2</sup>H<sub>3</sub>]acetate. Both the position and the number of <sup>2</sup>H atoms incorporated (Tables 6 and 10) are consistent with the conversion of acetate into butyrate *via* an intermediate in which one <sup>2</sup>H atom is retained at C-2 and three at C-4 (*i.e.*, crotonyl-CoA). However, instead of the expected 3:1 ratio of deuterium atoms at C-4 and C-2, ratios of 7.3:1 and 6.8:1 were found by <sup>2</sup>H nmr spectroscopy in *F. nucleatum* and *F. varium*, respectively. Partial exchange of deuterium from the methylene position (*i.e.*, C-2) of acetoacetyl-CoA can account for a ratio greater than 3, and more rapid exchange is expected at the methylene position of a 3-oxoacid (124). The large incorporation of two labelled acetates into a single molecule of butyrate suggests that the labelled acetate was converted to butyrate before sufficient unlabelled acetate was produced to dilute the labelled material. Thus the acetate to butyrate conversion probably occurs during the initial growth phase of the culture, and serves to regenerate the NAD<sup>+</sup> needed for the oxidative deamination of glutamate (44).

Comparison of the incorporation of C<sup>2</sup>H<sub>3</sub> units into butyrate in unenriched peptone medium and peptone medium (Table 6; Expts. 7 vs 6) by *F. nucleatum* indicated that <sup>2</sup>H exchange was reduced on the unenriched peptone medium. A

net flow of acetate to butyrate by reduction of acetoacetyl-CoA *versus* the establishment of an equilibrium between acetyl-CoA and acetoacetyl-CoA on peptone medium would account for these results. Under the equilibrium conditions deuterium would be lost by the successive deprotonations of acetyl-CoA during acetoacetate synthesis.

#### 4.4 Glutamate Catabolism in *F. nucleatum*

While the incorporation of label from L-[1-<sup>13</sup>C]glutamate into C-1 of both acetate and butyrate and the non-incorporation of label from L-[5-<sup>13</sup>C]glutamate (Table 5) are consistent with both the hydroxyglutarate and methylaspartate pathways, and complement the results of earlier CO<sub>2</sub> trapping experiments using [1-<sup>14</sup>C]- and [5-<sup>14</sup>C]glutamate (2), the unsymmetrical incorporation of label from L-[1-<sup>13</sup>C]glutamate (Table 5) into two positions of butyrate cannot be attributed directly to one pathway. Similar results have been obtained previously using radioactive isotopes: DL-[1-<sup>14</sup>C]glutamate was incorporated mostly into C-1 of butyrate (>90%) by two strains of *F. nucleatum* (4355 and 4357), *Peptococcus aerogenes*, and *Clostridium microsporium* (75), but only 70% of the label incorporated into butyrate by *Acidaminococcus fermentans* was found at C-1 (75). Also, label was located at both C-1 (77%) and C-3 (24%) of butyrate when L-[1-<sup>14</sup>C]glutamate was degraded by *Peptococcus aerogenes* (74). The larger incorporation at C-1 of butyrate is indicative of the hydroxyglutarate pathway, and the incorporation of <sup>14</sup>C into a second site was attributed to the synthesis of butyrate from labelled acetate

derived from [ $^{14}\text{C}$ ]glutamate (74, 75).

Although butyrate synthesis from acetate was demonstrated in *F. nucleatum*, labelled acetate can be produced by both the methylaspartate and hydroxyglutarate pathways. The possible operation of both the hydroxyglutarate and methylaspartate pathways was tested by feeding L-[4- $^{13}\text{C}$ ]glutamate to *F. nucleatum*; label in this position of glutamate is delivered to different carbon atoms in acetate and butyrate by the two pathways (Figure 29). The enrichment at C-2 of acetate and C-2 and C-4 of butyrate together with the lack of enrichment at the other carbons of acetate and butyrate (Table 5) supported the hydroxyglutarate pathway for L-glutamate catabolism by *F. nucleatum*, and excluded the methylaspartate pathway. Thus the small incorporations of  $^{13}\text{C}$  into C-3 and C-2 of butyrate by feeding L-[1- $^{13}\text{C}$ ]- and L-[4- $^{13}\text{C}$ ]glutamate, respectively, to *F. nucleatum* result from the synthesis of butyrate from acetate produced by the hydroxyglutarate pathway. In earlier cell-suspension experiments using DL-[4- $^{14}\text{C}$ ]glutamate (75), almost all the incorporated radioactivity was located in C-3 and C-4 (*C. microsporum* and *A. fermentans*) or C-2 to C-4 of butyrate (*P. aerogenes* and two strains of *F. nucleatum*). These results are consistent with the hydroxyglutarate pathway, but extensive chemical degradations were not carried out to determine the exact position or positions of the radioactive label.

In both Expts. 1 and 2 and previous experiments employing radioactive isotopes (74, 75), label was incorporated more efficiently into butyrate than acetate, indicating a more direct formation of butyrate from glutamate by the

hydroxyglutarate route. Further support for the hydroxyglutarate pathway in *F. nucleatum* is provided by the detection of glutamate dehydrogenase (EC 1.4.1.2) and hydroxyglutarate dehydrogenase (EC 1.1.99.2) activities in crude cell-free extracts (2). The enzymes hydroxyglutarate dehydrogenase (83), 2-hydroxyglutaryl-CoA dehydratase (EC 4.2.1.-) (87), and glutaconyl-CoA decarboxylase (EC 4.1.1.67) (91) have been purified from *F. nucleatum*. Moreover, the enzymes in the methylaspartate and aminobutyrate pathways are absent; the activities of methylaspartase (EC 4.1.3.2), 4-hydroxybutyrate dehydrogenase (EC 1.1.1.61) and acetyl-CoA: hydroxybutyrate-CoA transferase were less than  $0.001 \mu\text{mol min}^{-1} (\text{mg protein})^{-1}$  (2).

#### 4.5 Glutamate Catabolism in *F. varium*

The equal isotopic incorporation at C-1 and C-3 of butyrate derived from L-[1-<sup>13</sup>C]glutamate (Table 8) is consistent with the methylaspartate pathway in *F. varium*. A literature report indicated that most of the radioactivity incorporated from [1-<sup>14</sup>C]glutamate was located at C-1 of butyrate; only a small fraction of the total radioactivity was recovered in C-2,3,4 of butyrate, indicating that the hydroxyglutarate pathway was present (76). In a separate study (2), degradation of [1-<sup>14</sup>C]glutamate produced radioactive CO<sub>2</sub> containing 14% of the total initial radioactivity. Decarboxylation of glutamate at C-1 is consistent with this observation, and indicated the presence of the aminobutyrate pathway in addition to the hydroxyglutarate and methylaspartate pathways. This proposal was further

supported by feeding [5-<sup>14</sup>C]glutamate; only 86% of the total radioactivity was recovered in CO<sub>2</sub>, indicating that C-5 of glutamate was incorporated into products other than CO<sub>2</sub> (possibly acetate and butyrate).

The equal incorporation at C-1 and C-3 of butyrate derived from L-[1-<sup>13</sup>C]glutamate (Table 8) is consistent with the methylaspartate pathway. However, the simultaneous operation of the hydroxyglutarate and aminobutyrate pathways would deliver the <sup>13</sup>C label to the same positions (Figure 29). Again glutamate labelled at C-4 was used to assess the importance of other pathways. Administration of L-[4-<sup>13</sup>C]glutamate to a *F. varium* culture resulted in equal incorporation of <sup>13</sup>C label at C-1 and C-3 of butyrate (Table 8), and confirmed the presence of the methylaspartate pathway for L-glutamate degradation. The lack of <sup>13</sup>C enrichment at C-2 of acetate and C-2 and C-4 of butyrate ruled out both the aminobutyrate and hydroxyglutarate pathways. The non-incorporation of label from L-[5-<sup>13</sup>C]glutamate (Table 8) also excluded the aminobutyrate pathway for L-glutamate catabolism in *F. varium*.

That the methylaspartate pathway is exclusively responsible for L-glutamate catabolism in *F. varium* contradicts the previous hypotheses that suggested either the simultaneous operation of three pathways (2) or the operation of only the hydroxyglutarate pathway (76). An apparent difference between the isotopic experiments in this thesis with those reported in the literature is the use of labelled L-glutamate rather than a racemic mixture, and this might contribute to the discrepancies. The possible presence of distinct pathways for D- and L-glutamate

is preceded by the catabolism of D- and L-lysine in *Clostridium sticklandii* via two different routes (120). Catabolism of D- and L-glutamate would produce distinct isotopic enrichment patterns in the end-products. Furthermore, a brief report on an enzymic system from *Clostridium tetanomorphum* that degraded and formed both D- and L-glutamate was made by Barker *et al.* in 1957 (101). Later it was found that *C. tetanomorphum* employed the methylaspartate pathway for glutamate catabolism (75, 100).

The uptake of both D- and L-glutamate by *F. varium* demonstrated earlier in this thesis supported the possible presence of a different pathway for D-glutamate catabolism. However, the degradation of D-[3-<sup>13</sup>C]glutamate by *F. varium* produced acetate labelled at C-2, and butyrate equally enriched at C-2 and C-4 (Table 8), results consistent with degradation of D-glutamate by the methylaspartate pathway. Thus, differential metabolism of stereoisomers cannot account for the contradictory hypotheses.

In the report suggesting the hydroxyglutarate pathway for glutamate catabolism by *F. varium* (76), the radioactivity incorporated into carbon atoms of butyrate was reported as the total radioactivity (52000 cpm). After Schmidt degradation, only 26450 cpm were accounted for (*i.e.*, 13000 cpm in CO<sub>2</sub>, 13000 cpm in unreacted butyrate, and 450 cpm in propionate). Consequently, reaching a conclusion as to what extent <sup>14</sup>C label from glutamate was delivered into the individual carbon atoms of butyrate would not be appropriate unless the specific radioactivities were determined and more care had been used to establish the

purity of the isolated butyrate.

On the other hand, results leading to the proposal of the aminobutyrate pathway in *F. varium* (2) have other shortcomings. The incomplete recovery of radioactivity in CO<sub>2</sub> from [5-<sup>14</sup>C]glutamate does not necessarily imply that the rest of radioactivity was incorporated into acetate and butyrate. Furthermore, glutamate decarboxylase (EC 4.1.1.15), a key enzyme in the aminobutyrate pathway was not assayed. Very low activities for 4-hydroxybutyrate dehydrogenase (0.2 μmol. min<sup>-1</sup>. mg protein<sup>-1</sup>) and acetyl-CoA:butyryl-CoA transferase (0.06 μmol. min<sup>-1</sup>. mg protein<sup>-1</sup>) were detected. The latter enzyme was detected and purified from *Clostridium aminobutyricum* (96), a bacterium that degrades 4-aminobutyrate, but not glutamate, to acetate and butyrate.

The occurrence of the hydroxyglutarate pathway in *F. varium* was suggested on the basis of the release of CO<sub>2</sub> from C-5 of glutamate (2), which could also be due to the methylaspartate pathway. Further support for the hydroxyglutarate pathway was obtained by assaying the two first enzymes in the pathway (*i.e.*, glutamate dehydrogenase and hydroxyglutarate dehydrogenase). High activities for these two enzymes were detected, 20 and 18 μmol. min<sup>-1</sup> mg protein<sup>-1</sup>, respectively, but both activities were also detected in a cell-free extract of *Clostridium* species (100) that degraded glutamate solely *via* the methylaspartate pathway. The presence of these enzymes in *F. varium* might be unrelated to the catabolism of glutamate to acetate and butyrate.

Further support for the methylaspartate pathway in *F. varium* was obtained

by detecting the accumulated intermediates by nmr spectroscopy and hplc. The formation of 3-methylaspartate and mesaconate from L-[4-<sup>13</sup>C]glutamate (Figure 35) and the formation of glutamate and 3-methylaspartate from mesaconate (Figure 36) indicated that glutamate mutase and methylaspartase activities are present in extracts of *F. varium*. Also, the formation of glutamate from mesaconate was suppressed in a charcoal-treated, partially purified cell-free extract of *F. varium* (Figure 36B), indicating that the glutamate mutase in *F. varium* is a coenzyme B<sub>12</sub>-dependent mutase. This behaviour is consistent with the glutamate mutase purified from *C. tetanomorphum* (67) and *C. cochlearium* (68).

The formation of *erythro*- and *threo*-stereoisomers of 3-methylaspartate from mesaconate by partially purified (i.e., after Sephadex G-150) methylaspartase was demonstrated by chiral hplc (Figure 39). The assignment of the peaks to specific isomers of 3-methylaspartate was not possible due to unavailability of the separate stereoisomers of 3-methylaspartate. The formation of two stereoisomers of 3-methylaspartate (i.e., L-*erythro*- and L-*threo*-isomers) from mesaconate by methylaspartase from *C. tetanomorphum* has been reported. The L-*threo*-isomer was formed initially, and after extended incubation times, the L-*erythro*-isomer was also formed (125).

There are three possible explanations for how both D- and L-glutamate are degraded by the methylaspartate pathway: 1) D-glutamate is a substrate for glutamate mutase; 2) separate glutamate mutases exist for D- and L-glutamate, as has been reported for D- and L-lysine (120); and 3) the racemization of D- and L-

glutamate is enzyme-catalyzed.

It has been reported (115, 126) that a partially purified glutamate mutase from *C. tetanomorphum* degraded L-glutamate 100 times faster than the D-isomer, but the slower rate was attributed to contamination by a glutamate racemase. Later, with a purified glutamate mutase from *C. cochlearium*, it was demonstrated that D-glutamate was not a substrate for the enzyme (68).

Three possible enzymatic reactions can be involved in glutamate racemization: 1) glutamate racemase (118, 127, 128); D-amino acid transaminases (129); and 3) D- and L-glutamate dehydrogenase. The first two enzymatic activities are established for D-glutamate formation in bacteria, and recently the presence of both activities has been reported in *Staphylococcus haemolyticus* (130). However, there is no precedent on the involvement of a D-glutamate dehydrogenase in glutamate racemization.

D-Amino acid transaminase activity was not found in *F. varium*. Cell-free extract of *F. varium* incubated with 2-oxoglutarate and either D-aspartate, DL-alanine, or DL-phenylalanine did not produce any glutamate above that produced in the control incubation.

Racemization of glutamate could take place if both D- and L-glutamate dehydrogenase activities were present. A high activity of a glutamate dehydrogenase ( $20 \mu\text{mol. min.}^{-1} \text{mg protein}^{-1}$ ) in *F. varium* grown on sheep-blood agar has been reported (2), but its substrate specificity was not examined. The crude cell-free extract of *F. varium* grown on liquid peptone medium showed only

a very low glutamate dehydrogenase activity only for L-glutamate, ruling out the presence of D-glutamate dehydrogenase and its involvement in glutamate racemization.

The racemization of glutamate observed in extracts of *F. varium* (Figure 40) is most likely due to a glutamate racemase. Addition of cofactors (*i.e.*, NAD<sup>+</sup>, NADP, FMN, and pyridoxal phosphate) to the extract did not increase the rate of racemization (Figure 42). This is consistent with glutamate racemases isolated from *Pediococcus pentosaceus* (128) and *Lactobacillus fermenti* (118) which are cofactor-independent enzymes. That the racemization proceeded with a deprotonation/reprotonation mechanism at the  $\alpha$ -C of glutamate was demonstrated by disappearance of the  $\alpha$ -H signal in the <sup>1</sup>H-nmr spectrum after 48 h of incubation (Figure 43). This also excluded the involvement of other carbon atoms of glutamate in the racemization process, and is consistent with a two base mechanism for the racemization process (131). Glutamate racemase was detected after chromatography on Sephadex G-150, and the molecular mass of the enzyme was estimated as 17 kDa. Most of the glutamate racemases characterized to date have molecular masses of about 30 to 40 kDa (118, 128). The glutamate racemase encoded by the *glr* gene in *E. coli* was purified, and found to have a molecular mass of 64 kDa. SDS-PAGE electrophoresis indicated that the enzyme consisted of two identical subunits of about 31 kDa (132).

A study of glutamate racemase distribution among bacteria has reported that the enzyme exclusively occurs in lactic acid-fermenting bacteria (128), and its

role has been to provide the D-glutamate needed for cell wall biosynthesis (118). The detection of glutamate racemase activity found in a bacterium other than lactic acid bacteria (*i.e.*, *F. varium*) and its involvement in D-glutamate catabolism rather than biosynthesis, are new findings.

#### 4.6 Conclusions and Future Work

The preferential uptake of amino acid enantiomers by *F. nucleatum* and *F. varium* was demonstrated. The results indicate that stereochemistry plays an important role in amino acid metabolism, and that investigations of amino acid uptake should consider the possibility of preferential uptake of individual stereoisomers. The advantages of investigating the uptake of both isomers are evident.

1) Bacteria that assimilate only L-isomers of amino acids can be employed for the preparation of corresponding D-amino acids: it was demonstrated that *F. nucleatum* could be successfully employed for the production of D-glutamate and D-serine from their racemic mixtures. Preparation of D-arginine and D-histidine using *F. varium* was not carried out, but it is possible to obtain both D-arginine and L-ornithine from DL-arginine.

2) Although the L-amino acid uptake profile was similar for *F. nucleatum* and *F. varium*, the D-amino acids were assimilated in a more distinct fashion. For example, both *F. nucleatum* and *F. varium* utilized the L-isomers of glutamate,

histidine and serine, whereas no uptake of D-glutamate and D-serine by *F. nucleatum* and D-histidine by *F. varium* was observed. These differences in D-amino acid uptake pattern can be used for taxonomic classification of amino acid-utilizing bacteria.

3) Catabolism of both D- and L-isomers of amino acids also indicated that studies on catabolic pathways of amino acids should employ enantiomerically pure amino acids for either isotopic experiments or enzyme assays in order to generate unambiguous results.

The uptake of both isomers of lysine by *F. nucleatum* and *F. varium* and D- and L-histidine by *F. nucleatum* was demonstrated. Previous studies on the catabolism pathways of lysine in clostridia suggested two distinct pathways for D- and L-lysine. Although the occurrence of these pathways in *F. nucleatum* has been studied using isotopically labelled DL-lysine and assaying for enzymes in the L-lysine pathway, it is not certain if D-lysine degraded by a different pathway. Further isotopic investigations using enantiomerically pure lysine are needed to investigate the catabolism of D- and L-lysine in fusobacteria.

It has been reported that glutamate is an intermediate in histidine degradation, and since both D- and L-histidine are catabolized by *F. nucleatum*, it is not known if this is due to either a separate histidine-ammonia lyase or enzymatic racemization (e.g., histidine racemase). Further investigation is required to test both possibilities.

The catabolism of both D- and L-serine by *F. varium* is another finding that

has to be further investigated. The most likely possibility is the presence of both D- and L-serine dehydratases. However, the involvement of a serine racemase should not be overlooked.

Utilization of at least two isomers of diaminopimelic acid was shown, but it is not known which isomers are degraded, and the pure stereoisomers are required for further investigation.

A stable isotope approach to distinguish among the alternative pathways of glutamate catabolism by anaerobic bacteria was established and used to demonstrate that L-glutamate is degraded by the hydroxyglutarate pathway in *F. nucleatum*. Both D- and L-glutamate are degraded by the methylaspartate pathway in *F. varium* ruling out both the hydroxyglutarate pathway and the simultaneous operation of three pathways of glutamate catabolism. Also, the conversion of acetate to butyrate was demonstrated in both *F. nucleatum* and *F. varium*.

The catabolism of both D- and L-glutamate by the methylaspartate pathway in *F. varium* involves a glutamate racemase. The occurrence of glutamate racemase in *F. varium* dismissed the claim that the enzyme is exclusively present in lactic acid-fermenting bacteria. The preliminary characterization of the enzyme indicated that it is a cofactor-independent racemase. Future work requires further characterization in order to fully compare glutamate racemase from *F. varium* to those purified from other bacteria.

The formation of two isomers of 3-methylaspartate from mesaconate by methylaspartase was demonstrated by hplc, but the peaks were not assigned to

specific isomers due to unavailability of the separate stereoisomers of 3-methylaspartate. The preparation of at least two pure stereoisomers is required to identify these two products.

## Chapter 5

### Experimental

#### 5.1 Materials

All chemicals and solvents were obtained commercially and were used without further purification unless indicated. 4-Bromophenacyl bromide (Aldrich, Milwaukee, WI, USA) was recrystallized from ethanol (99%, v/v). Water was deionized (resistivity of 18.3 M $\Omega$ -cm) and filtered (0.2  $\mu$ m) using a Barnstead/Thermolyne NANOpure water system, model D4741. Methanol was distilled in glass, and hplc-grade acetonitrile was obtained from Fisher Scientific (Fair Lawn, NJ, USA). Trypticase peptone was obtained from BBL Microbiology System (Cockeysville, MD, USA). Yeast extract and proteose peptone were supplied by DIFCO Laboratories (Detroit, MI, USA). Heat inactivated calf serum was provided by GIBCO BRL (Burlington, ON, Canada). Prepared sheep-blood agar plates were purchased from the Department of Microbiology, Media Preparation Section, Victoria General Hospital, (Halifax, NS, Canada). Labelled compounds were obtained commercially: sodium [1,2-<sup>13</sup>C<sub>2</sub>]acetate and [<sup>2</sup>H<sub>3</sub>]acetate from MSD Isotopes (Montreal, QC, Canada); L-[4-<sup>13</sup>C]glutamic acid from Cambridge Isotope Laboratories (Woburn, MA, USA); L-[1-<sup>13</sup>C]glutamic acid (*F. nucleatum* experiment) from ICON Services Inc. (Summit, NJ, USA); and L-[1-<sup>13</sup>C]- (*F. varium* experiment), D-[3-<sup>13</sup>C]- and L-[5-<sup>13</sup>C]glutamic acid from C/D/N Isotopes Inc. (Vaudreuil, QC, Canada). Chiral analysis by hplc showed that the D-[3-<sup>13</sup>C]glutamate contained less than 6.5% L-glutamate.

## 5.2 General Methods

A Beckman Model  $\Phi$ 31 pH meter fitted with a Beckman combination electrode was used for pH measurements. Culture media were sterilized at 121°C for 15 min in a AMSCO model Medalist 200 autoclave. Microcentrifugations were performed using a Beckman microfuge "E" equipped with a fixed angle rotor. Large-scale centrifugations were performed on a Dupont Instruments Sorvall Model RC-5B centrifuge equipped with either a Sorvall Model GSA or SS-34 fixed angle rotor or on an International Equipment Company model IECB-22 centrifuge equipped with an 878 fixed angle rotor. Centrifugations were carried out at room temperature unless stated otherwise, and maximum centrifugal forces are reported. Sonication was performed with a Branson Sonifier, model 200 (Branson Sonic Power Co., Danbury, CT, USA). Freeze drying was performed using an Edwards Modulyo freeze dryer connected to an Edwards model E2M8 rotary vacuum pump. The Beckman hplc system consisted of two model 110B pumps, a Beckman Model 340 gradient mixer equipped with a Model 210A injector valve and a 20- $\mu$ L injection loop, and a Beckman Model 157 fluorescence detector equipped with a 9- $\mu$ L flow cell and excitation and emission filters at 305-395 nm and 420-650 nm, respectively. A CompuPartner 486 computer was interfaced to the pumps and detector for gradient control, data collection, and data analysis. The nmr spectra ( $^1\text{H}$ ,  $^{13}\text{C}$ , DEPT) were acquired on a Bruker AC 250F spectrometer using standard Bruker programs, and the chemical shifts are reported in ppm referenced to external dioxane (66.66 ppm) for carbon spectra and either HOD (4.80 ppm) or

CHCl<sub>3</sub> (7.27 ppm) for proton spectra. UV spectra were obtained in 1-cm cuvettes using a Hewlett Packard 8452A diode array spectrophotometer. The IR spectra were recorded on a Nicolet 205 FT-IR spectrometer, and optical rotations were measured on a Perkin-Elmer 141 polarimeter at 589 nm. Melting points were taken using a Gallenkamp melting point apparatus and are uncorrected.

### 5.3 Microorganisms

*Fusobacterium nucleatum* (ATCC 25586), and *Fusobacterium varium* (NCTC 10560) were provided by Dr. H.N. Shah (current address: Eastman Dental Institute, 256 Gray's Inn Road, London, WC1X 8LD, UK), and maintained as lyophilized cultures. Stock cultures were subcultured at weekly intervals on 5% (v/v) sheep-blood agar. Liquid cultures were initiated with *Fusobacterium* cells grown for 24 or 48 h on a 9-cm-diameter plate of sheep-blood agar and suspended in sterile peptone medium (3 mL). Aseptic microbial transfers were carried out in air and all cultures and cell suspensions were incubated at 37°C in anaerobic jars (Oxoid, Unipath Inc., Nepean, ON) under an atmosphere of H<sub>2</sub>/CO<sub>2</sub>/N<sub>2</sub> (5:10:85). Cells grown in liquid cultures were tested for microbial contaminants on sheep-blood agar incubated either in an anaerobic atmosphere or in air at 37°C for 48 h. Cultures which showed aerobic growth or atypical morphology for *F. nucleatum* or *F. varium* were discarded.

Lyophilized cultures of *F. nucleatum* and *F. varium* were prepared by suspending cells grown on sheep-blood agar for 48 h in a mixture of heat

inactivated calf serum (860  $\mu$ L) and peptone medium (140  $\mu$ L). Portions (100  $\mu$ L) of the cell suspension were added aseptically to the bottom of the sterile ampoules (4"  $\times$  5/16" O.D.) using a sterile pasteur pipette. The ampoules were plugged with sterile non-absorbent cotton, stored at -80°C, and freeze dried. The ampoules were sealed under vacuum using a flame, and stored at room temperature in the dark. The lyophilized cultures were tested for purity and viability by dissolving the lyophilized cells in peptone medium (300  $\mu$ L) and culturing them on a sheep-blood agar.

#### **5.4 Media**

*Sheep Blood Agar.* Sheep blood agar (5%) contained: defibrinated sheep blood, 50 mL; tryptone, 14.0 g; peptone, 4.5 g; yeast extract, 4.5 g; NaCl, 5.0 g; agar, 12.5 g; and distilled water, 1000 mL.

*Peptone Medium.* Peptone medium contained (g/L): trypticase peptone 5.0; proteose peptone, 5.0; yeast extract, 5.0; glucose, 5.0; NaCl, 5.0; and L-cysteine hydrochloride, 0.80. Peptone/2 and peptone/4 media contained, respectively, one-half and one-quarter the amounts of trypticase peptone, proteose peptone and yeast extract in the peptone medium. The components were dissolved in water, adjusted to pH 7.3-7.4 with 3 M NaOH, and autoclaved.

*Unenriched Peptone Medium.* Unenriched peptone medium was identical to peptone medium except that proteose peptone and yeast extract were omitted.

*Resuspension Buffer (133).* Phosphate buffer for resuspension experiments

contained (g/L):  $K_2HPO_4$ , 9.0;  $KH_2PO_4$ , 6.0;  $MgSO_4 \cdot 7H_2O$ , 0.2;  $CaCl_2 \cdot 2H_2O$ , 0.02; sodium acetate, 0.3; and L-cysteine-HCl, 0.4. DL-Amino acid was dissolved in freshly prepared buffer, and the pH was adjusted to 7.3-7.4 with 3 M NaOH. The solution was autoclaved and supplemented with vitamin solution 1 (10 mL/L), vitamin solution 2 (1 mL/L), and trace metal solution (1 mL/L), each autoclaved separately. Vitamin solution 1 contained *p*-aminobenzoic acid, thiamin chloride hydrochloride, riboflavin, nicotinic acid, pyridoxal hydrochloride, inositol, calcium pantothenate, each at 0.2 g/L, and was adjusted to pH 7.0 with 1 M NaOH. Vitamin solution 2 contained DL-thioctic acid, biotin, haemin, folic acid, each at 0.1 g/L. The trace metal solution contained (g/L):  $FeSO_4 \cdot 7H_2O$ , 4.0;  $MnSO_4 \cdot 2H_2O$ , 0.15; and  $Na_2MoO_4 \cdot 2H_2O$ , 0.15.

## 5.5 Analysis of Amino Acids

*Ninhydrin.* A ninhydrin spot test was routinely used to detect the presence of amino acids in fractions eluted from ion-exchange columns. The test was done using a 0.25% solution of ninhydrin (Aldrich grade) in acetone. A portion of the solution to be tested was placed on a filter paper, dried at 100°C, treated with ninhydrin solution, and heated at 100°C. The presence of an amino acid was indicated by the formation of a purple colour.

*OPA-HPLC Analysis.* Analysis of amino acids by hplc was carried out according to a published procedure (110). The precolumn derivatization was performed by mixing sample solution containing amino acid (20  $\mu$ L) with water (20  $\mu$ L) and

commercial *o*-phthalaldehyde (40  $\mu$ L) reagent (Pierce Chem. Co., Rockford, IL, USA). After 1 min at room temperature with occasional mixing, sodium acetate solution (120  $\mu$ L, 100 mM, pH 6.25) was added, and a 20- $\mu$ L portion was injected. The fluorescent isoindole-derivatives were separated on a Beckman Ultrasphere ODS column (5  $\mu$ m, 45  $\times$  4.6 mm) fitted at the inlet with an Upchurch Scientific Model C-130B guard column (2  $\times$  20 mm) containing Perisorb RP-18 (30-40  $\mu$ m) using gradient elution. Gradients were formed by mixing sodium acetate (0.1 M, pH 6.25 with 3 M HCl)-methanol-THF (900-95-5) and methanol at a total flow rate of 2.5 mL/min. The sodium acetate solution was filtered (0.45  $\mu$ m) and degassed under reduced pressure (water aspirator) prior to use. Ornithine and lysine were analyzed using a gradient of composition (min, % methanol): 0.0, 0; 0.5, 15; 3.0, 15; 3.25, 30; 4.25, 30; 4.5, 50; 6.25, 50; 6.5, 100; 7.0, 100; 7.5, 0. The following composition was used for all other amino acid determinations (min, % methanol): 0.0, 0; 0.5, 15; 3.0, 15; 3.25, 30; 5.75, 30; 6.0, 100; 6.5, 100; 7.0, 0.

When accurate measurements of amino acid concentrations were desired, the water in the derivatization mixture was replaced by a cysteic acid solution (0.118 mM) which served as an internal standard. Concentrations of glutamic acid, glutamine and 3-methylaspartic acid were calculated using standard curves constructed from injections of L-glutamic acid at 5 concentrations over a range of 0.12 to 0.27 mM, glutamine at 6 concentrations over a range of 0.05 to 0.30 mM, and 3-methylaspartic acid at 5 concentrations over a range of 0.12 to 0.72 mM. *Chiral OPA-HPLC Analysis* (111, 134). Derivatization was achieved by adding

derivatization reagent (80  $\mu\text{L}$ ), prepared by dissolving *N*-acetylcysteine (1.0 mg) in commercial incomplete *o*-phthalaldehyde reagent (1.0 mL, Sigma Chemical Co., St. Louis, MO, USA), to an amino acid solution (20  $\mu\text{L}$ ). The reaction proceeded at ambient temperature for 3 min with occasional mixing. Mobile phase used for the separation (100  $\mu\text{L}$ ) was added, and a 20- $\mu\text{L}$  portion of the resulting solution was injected. Separations of fluorescent isoindole diastereomers were achieved at a total flow rate of 2.0 mL/min on a Nucleosil 5 C18 column (4.6  $\times$  250 mm, Phenomenex, Torrance, CA, USA) using gradients formed between acetonitrile and a copper(II)-proline solution.

For glutamic acid, 3-methylaspartic acid and serine, the gradient was formed between acetonitrile and acetonitrile (2%)-copper(II) acetate (2.5 mM)-L-proline (5.0 mM) copper(II) solution, adjusted to pH 6.0 with ammonium acetate (111). Gradients of composition (min, % acetonitrile) 0.0, 0; 3.0, 4; 10.0, 4; 11.0, 7; 17.0, 7; 18.0, 0 (glutamate), 0.0, 0; 3.0, 3; 10.0, 3; 11.0, 7; 22.0, 7; 25.0, 0 (3-methylaspartate) and 0.0, 0; 3.0, 4; 9.0, 4; 10.0, 10; 14.0, 10; 16.0, 0 (serine) were used. The retention times of the D- and L-isomers of glutamic acid and serine were 14.2, 11.6, and 9.3, 8.7 min, respectively. The retention times for four stereoisomers of 3-methylaspartate were 3.8, 5.4 min for the *erythro*- and 17.2, 18.6 min for the *threo*-isomers.

The enantiomers of arginine and 3-aminobutyric acid were separated by a gradient prepared from acetonitrile and acetonitrile (5%)-copper(II) acetate (2.5 mM)-L-proline (5.0 mM)-ammonium acetate (25 mM) solution, adjusted to pH 7.0

with 5 M NaOH (134). A gradients of composition (min, % acetonitrile) 0.0, 0; 3.0, 5; 16.0, 5; 18.0, 0 (arginine) and 0.0, 0; 3.0, 8; 10.0, 8; 11.0, 12; 20.0, 12; 22.0, 0 (3-aminobutyric acid) were used. The retention times for the D- and L-isomers of arginine and 3-aminobutyric acid were 16.0, 13.5 min and 14.0, 11.2 min, respectively.

The fluorescent responses of the individual enantiomers of arginine, glutamate and serine were calibrated by triplicate injections of racemic amino acids at two different concentrations. The areas of the D-arginine, L-glutamate, and D-serine peaks were respectively 1.14, 1.10 and 1.06 times larger than the peak areas of the corresponding enantiomers. The enantiomeric excesses (% ee) were calculated from peak areas corrected for the different responses.

The four stereoisomer of 3-methylaspartate required to develop the chiral hplc conditions were prepared from DL-*threo*-3-methylaspartate (Sigma Chemical Co.) according to a literature procedure (135). DL-*threo*-3-Methylaspartic acid (100 mg, 0.68 mmol) was dissolved in HCl (6 M, 6 mL) and heated in a sealed tube at 110°C for 24 h. The reaction mixture was evaporated to dryness. The residue was twice dissolved in distilled water and evaporated to dryness to give 96 mg of white solid.

## **5.6 Stereochemical Aspects of Amino Acid Uptake**

### **5.6.1 Survey of Amino Acid Uptake from Peptone Medium by *F. nucleatum* and *F. varium***

Peptone medium was supplemented with amino acid (18 mmol/L of glutamic acid or 10 mmol/L of other amino acids), adjusted to pH 7.3-7.4, and autoclaved. Glutamine, citrulline, and asparagine were dissolved in potassium phosphate buffer (100 mmol/L, pH 7.4, 3 mL), filter sterilized (0.22  $\mu$ m), and added to sterile peptone medium; all other amino acids were added to the peptone medium prior to autoclaving.

Peptone medium (50 mL) containing an amino acid (10 mM) was inoculated with *F. nucleatum* cell suspension (150-200  $\mu$ L), and the culture was incubated under anaerobic conditions. Samples (0.5 mL) removed aseptically prior to inoculation and at various incubation times were centrifuged (15400g, 10 min); supernatant (20  $\mu$ L) was mixed with water (380  $\mu$ L) and stored at -15°C for hplc analysis. Amino acid uptake (expressed as a percentage) was calculated by comparing the chromatographic peak area of the amino acid after incubation to that obtained prior to inoculation.

### **5.6.2 Preparation of D-Glutamate by *F. nucleatum* Growing on Peptone Medium**

Peptone medium (500 mL) containing DL-glutamic acid (30 mM) was inoculated with *F. nucleatum* cell suspension (1.5 mL) and incubated under anaerobic conditions for 40 h. The culture was centrifuged (8200g, 15 min), and

a portion of the supernatant (100 mL) was lyophilized to determine the mass of residual solids. The remainder of the supernatant (ca. 400 mL) was applied to an Amberlite IR-120 column (2.5 × 48 cm). The column was washed with water (3 L) and eluted with 0.5 M ammonia (2 L). Fractions (200 mL) were collected and spot tested for amino acids with ninhydrin reagent. Fractions containing amino acids were combined and evaporated to dryness *in vacuo*. The residue was dissolved in water (3 mL) and applied to a Dowex 1-X8 column (acetate form, 2.5 × 48 cm). The column was washed with water (2 L) and eluted with 0.5 M acetic acid (2 L). Fractions (200 mL) giving a color with ninhydrin were combined and evaporated to dryness *in vacuo*. The residue (970 mg) was recrystallized from water and 95% ethanol to yield D-glutamic acid as a white solid (508 mg, 57% recovery, 97.4% ee by hplc). mp 196-198°C (lit. (136) 211-213°C);  $[\alpha]_D^{25}$  -30.1° (-31.5 for a standard sample);  $^1\text{H}$  nmr  $\delta$ : 3.79 (apparent t, 2H, splittings of 6.11 and 6.71 Hz), 2.43-2.64 (m, 2H), 2.05-2.23 (m, 2H);  $^{13}\text{C}$  nmr  $\delta$ : 179.9, 176.6, 56.6, 32.8, 28.3.

### 5.6.3 Amino Acid Uptake by Resuspensions of *F. nucleatum* and *F. varium*

Peptone medium (500 mL) inoculated with *F. nucleatum* cell suspension (1.5 mL) and incubated for 24 h was harvested aseptically in air by centrifugation (8200g, 15 min). For the development of incubation conditions, the damp cells (approximately 2.5 g) were resuspended in phosphate buffer containing DL-amino acid (50 mL). The variation in cell mass obtained in different resuspension experiments was corrected by adjusting the volume of resuspension medium so

that the ratio of 2.5 g/L of cell mass per 50 mL of resuspension medium remained constant. Samples (300  $\mu$ L) were removed at various times and centrifuged (15400g, 10 min). The supernatants were stored at  $-15^{\circ}\text{C}$  for hplc analysis.

Portions of the supernatants from glutamate and serine resuspension experiments were titrated to pH 9.5 with 5 M NaOH, lyophilized, and examined by nmr to identify the metabolic end products.

*Residue from glutamate catabolism.*  $^1\text{H}$  nmr  $\delta$ : 1.86 (s) (acetate); 1.42-1.61 (m), 0.84 (t,  $J = 7.3$  Hz) (butyrate); and 3.70 (t,  $J = 4.9$  Hz), 2.30 (apparent t, splittings of 7.3 and 7.9 Hz) (glutamate).  $^{13}\text{C}$  nmr  $\delta$ : 184.3 (s), 26.0 (q) (acetate); 42.3 (t), 22.1 (t), 16.0 (q) (butyrate); and 184.0 (s), 177.3 (s), 57.3 (d), 36.1 (t), 29.7 (t) (glutamate).

*Residue from serine catabolism.*  $^1\text{H}$  nmr  $\delta$ : 1.84 (s) (acetate); 2.07 (t,  $J = 7.3$  Hz), 1.36-1.52 (m), 0.81 (t,  $J = 7.3$  Hz) (butyrate); 4.04 (q,  $J = 6.7$  Hz), 1.25 (d,  $J = 6.7$  Hz) (lactate); 3.83 (AB part of ABX,  $J_{\text{AB}} = -12.21$  Hz,  $J_{\text{AX}} = 5.14$  Hz, and  $J_{\text{BX}} = 4.01$  Hz), and 3.7 (apparent t, splittings of 4.90 and 4.25 Hz) (serine).  $^{13}\text{C}$  nmr  $\delta$ : 184.2 (s) and 26.0 (q) (acetate); 42.3, 22.1, 16.0 (butyrate); 185.3 (s), 71.2 (d), 22.8 (q) (lactate); and 175.9 (s), 63.2 (t), 59.1 (d) (serine).

#### 5.6.4 Preparation of D-Amino Acids by Resuspensions of *F. nucleatum*

*F. nucleatum* cells (5 g damp cells/100 mL) were resuspended in phosphate buffer containing racemic amino acid and incubated anaerobically with stirring. The resuspension mixture was centrifuged (8200g, 15 min), and the supernatant was

applied to an Amberlite IR-120 column (2.5 × 48 cm) at a flow rate of 5.0 mL/min. The column was washed with water (500 mL) and eluted with 0.5 M ammonia (4 L). Fractions (200 mL) were collected and spot tested for amino acid content with ninhydrin reagent. The fractions containing amino acid were combined and evaporated to dryness *in vacuo*. The residue (approximately 3.5 g) was dissolved in hot water (100 mL), treated with decolorizing charcoal (2 g) for 30 min, and filtered through Celite. The filtrate was concentrated *in vacuo* to about 50 mL, and 95% ethanol (150-200 mL) was added. The solution was cooled to 4°C, and the white solid was collected by filtration and dried.

*D-Glutamate*. A 300-mL resuspension mixture containing 150 mM DL-glutamate incubated for 30 h yielded 2.43 g (73% recovery, >99% ee by hplc): mp 196-198°C;  $[\alpha]_D^{25}$  -33.3°.

*D-Serine*. Incubation of a 100-mL resuspension mixture containing 800 mM DL-serine for 36 h yielded 3.47 g (83% recovery, >99% ee by hplc): mp 213-215°C (lit. (9) 228°C dec.);  $[\alpha]_D^{25}$  -15.7° (-16.3° for a standard sample);  $^1\text{H}$  nmr  $\delta$ : 3.91 (AB part of ABX,  $J_{AB} = -12.21$  Hz,  $J_{AX} = 5.11$  Hz, and  $J_{BX} = 4.04$  Hz, 2H), 3.77 (apparent t, splittings of 4.28 and 4.88 Hz, 1H);  $^{13}\text{C}$  nmr  $\delta$ : 175.1, 62.8, 59.0.

## 5.7 Feeding Experiments using Isotopically Labelled Substrates

### 5.7.1 Culture Conditions

A loopful of cells grown on sheep-blood agar under anaerobic conditions at 37°C for 48 h was transferred into either peptone or unenriched peptone medium

supplemented with an isotopically labelled substrate. The culture medium was incubated under anaerobic conditions at 37°C for 48 h and centrifuged (23000g, 20 min). The pH of the supernatant was adjusted to 9.5 with 3 M NaOH, diluted to 130 mL with water, and freeze-dried.

Typically, peptone or unenriched peptone medium (50 mL) was supplemented with labelled glutamic acid (50 mg) together with unlabelled glutamic acid (75 mg) or labelled sodium acetate (42 mg in Expts. 4, 6, 42.5 mg in Expts. 13, 14, and 50 mg in Expts. 5, 7) and unlabelled glutamic acid (125 mg) prior to autoclaving. In Expt. 1, a 100 mL culture was supplemented with L-[1-<sup>13</sup>C]glutamic acid (75 mg) and unlabelled L-glutamic acid (175 mg). The details of the individual experiments are summarized in Tables 4 (*F. nucleatum*) and 7 (*F. varium*).

### 5.7.2 Formation and Isolation of 4-Bromophenacyl Acetate and Butyrate (134)

A mixture of the freeze-dried powder (2.2 g) containing sodium acetate and butyrate, 4-bromophenacyl bromide (0.70 g, 2.5 mmol), and dicyclohexano-18-crown-6 (0.045 g, 0.13 mmol) was suspended in acetonitrile (45 mL) and refluxed for 4 h. The reaction mixture was left overnight at room temperature and evaporated to dryness *in vacuo*. The solid residue was extracted with CH<sub>2</sub>Cl<sub>2</sub> (5 × 30 mL). The extracts were combined and evaporated *in vacuo* to give an oily brown residue (0.60 g). The acetate and butyrate derivatives were separated by flash chromatography (138) on silica gel (type 60, BDH, Toronto, ON, Canada) using a gradient consisting of varying proportions of CCl<sub>4</sub> and CH<sub>2</sub>Cl<sub>2</sub> starting with

pure  $\text{CCl}_4$ . Fractions (10 mL) were collected and assayed by TLC (silica,  $\text{CH}_2\text{Cl}_2$ ). Fractions containing only 4-bromophenacyl acetate ( $R_f$  0.38) or 4-bromophenacyl butyrate ( $R_f$  0.68) were combined separately and evaporated to dryness *in vacuo*. The amounts of butyrate and acetate esters isolated in individual experiments are reported in Tables 4 and 7. The following data are reported for unlabelled esters isolated from a peptone medium (50 mL) containing L-glutamate (125 mg) incubated with *F. nucleatum* for 48 h.

*p*-Bromophenacyl acetate. mp 81-83°C (lit. (139) 85°C and (140) 85-86°C); ir  $\nu_{\max}$  (KBr): 1745, 1694;  $^1\text{H}$  nmr ( $\text{CDCl}_3$ )  $\delta$ : 2.22 (s, 3H,  $-\text{CH}_3$ ), 5.28 (s, 2H,  $-\text{CH}_2-\text{O}-$ ), 7.59 and 7.74 (AB system,  $J = 8.6$  Hz, 4H, aromatic);  $^{13}\text{C}$  nmr ( $\text{CDCl}_3$ , 62.9 MHz)  $\delta$ : 20.6 ( $\text{CH}_3$ , C-2), 65.8 ( $\text{CH}_2$ ), 129.2, 129.3, 132.3, 132.9 (aromatic), 170.4 (C=O, ester, C-1), 191.5 (C=O, ketone); ms:  $m/z$  (intensity): 258 (11), 256 (11,  $\text{M}^+$ ), 185 (98), 183 (100,  $\text{M}^+-\text{C}_3\text{H}_5\text{O}_2$ ), 157 (18), 155 (19,  $\text{C}_6\text{H}_4\text{Br}^+$ ), 43 (32,  $\text{C}_2\text{H}_3\text{O}^+$ ).

*p*-Bromophenacyl butyrate. mp 62-64°C (lit. (139) 63.2°C and (140) 63.5-64°C); ir  $\nu_{\max}$  (KBr): 1741, 1704;  $^1\text{H}$  nmr ( $\text{CDCl}_3$ )  $\delta$ : 0.98 (t,  $J = 7.3$  Hz, 3H,  $-\text{CH}_3$ ), 1.70 (m, 2H,  $-\text{CH}_2-\text{CH}_3$ ), 2.50 (t,  $J = 7.3$  Hz, 2H,  $-(\text{C}=\text{O})-\text{CH}_2-$ ), 5.30 (s, 2H,  $-\text{CH}_2-\text{O}-$ ), 7.61 and 7.75 (AB system,  $J = 7.9$  Hz, 4H, aromatic);  $^{13}\text{C}$  nmr ( $\text{CDCl}_3$ )  $\delta$ : 13.6 ( $\text{CH}_3$ , C-4), 18.7 ( $\text{CH}_2-\text{CH}_3$ , C-3), 35.7 ( $\text{CH}_2-\text{C}=\text{O}$ , C-2), 65.6 ( $\text{CH}_2-\text{O}$ ), 129.1, 129.3, 132.2, 132.9 (aromatic), 173.0 (C=O, ester, C-1), 191.5 (C=O, ketone); ms:  $m/z$  (intensity): 286 (9), 284 (9,  $\text{M}^+$ ), 185 (98), 183 (100,  $\text{M}^+-\text{C}_5\text{H}_9\text{O}_2$ ), 157 (17), 155 (17,  $\text{C}_6\text{H}_4\text{Br}^+$ ), 71 (28,  $\text{C}_4\text{H}_7\text{O}^+$ ), 43 (31,  $\text{C}_3\text{H}_7^+$ ).

### 5.7.3 Isotopic Analysis

The  $^{13}\text{C}$ -nmr spectra were obtained on a Bruker AC 250F spectrometer at 62.9 MHz using 16000 data points in a 10 kHz spectral window and a delay time in the range of 5-15 s. The number of scans ranged from 600 to 2000, depending on the amount of sample available, and free-induction data were processed using a line broadening of 0.6-1 Hz. Spectra for  $^{13}\text{C}$ -enriched samples and natural-abundance reference samples were acquired under identical conditions. The percentage  $^{13}\text{C}$  enrichment was calculated for each individual carbon atom (111) by normalizing peak intensities to the average peak intensity of the five carbon atoms in the phenacyl moiety provided by the derivatization reagent. An enrichment factor was obtained by dividing the normalized intensity for each peak observed in the labelled compound by the normalized intensity for the corresponding peak in a reference sample containing  $^{13}\text{C}$  at natural abundance. Percentage enrichments (Tables 5 and 8) were calculated as follows: 1.1 (enrichment factor)-1.1. For coupled systems, the enrichment factor was calculated from the sum of the intensities of the doublet signals and multiplied by the natural abundance of  $^{13}\text{C}$  (1.1%) to give the percentage enrichment (Tables 6 and 10).

The  $^2\text{H}$ -nmr spectra were acquired in chloroform (10 mm tube) on a Bruker AMX-400 spectrometer at 61.4 MHz using 4000 data points in a 2454 Hz spectral window, a 15- $\mu\text{s}$   $90^\circ$  pulse, and a 1-s recycle time. Typically, 200-2000 scans were acquired, and chemical shifts referenced to  $[\text{}^2\text{H}]\text{chloroform}$  (7.27 ppm) are reported relative to tetramethylsilane. The  $^2\text{H}$  enrichments (Tables 6 and 10) were

calculated from the relative molar amounts of sample and solvent and the area of a sample peak relative to the natural abundance peak of chloroform in the solvent (141).

Mass spectra were obtained by electron impact on a CEC 21-104 mass spectrometer at 70 eV for routine spectra and 15 eV for precise isotopic measurements. The relative peak-intensity values for the molecular ion and its isotope peaks were calculated. The amount of each isotopic species present (*i.e.*,  $I_1$ ,  $I_2$ ,  $I_3$ , ...) was calculated by subtracting the contributions from natural abundance isotopes ( $^2\text{H}$ ,  $^{13}\text{C}$ ,  $^{15}\text{N}$ ,  $^{17}\text{O}$ ,  $^{18}\text{O}$ , and  $^{81}\text{Br}$ ) from the corresponding peaks (*i.e.*, M+1, M+2, M+3, ...) in the mass spectrum (142).

### **5.8 Preparation and Partial Purification of *F. varium* Cell-free Extracts**

Peptone medium (4L) supplemented with L-glutamic acid (0.5 g/L) was inoculated with *F. varium* grown on sheep-blood agar for 24 h (3 9-cm plates/L), and after 8.5 h of incubation the culture was harvested centrifugation (8200g, 20 min). The pelleted cells were washed twice with potassium phosphate buffer (50 mM, pH 7.4) containing dithiothreitol (2 mM) and stored at -78°C. The thawed pelleted cells (10 g) were suspended in cold potassium phosphate buffer (23 mL, 50 mM, pH 7.4) containing dithiothreitol (5 mM) and sonicated for 3 min in 15 s intervals with cooling in an ice-sodium chloride bath. The sonicated suspension (27 mL) was centrifuged (38700g, 20 min), and the supernatant was used as the crude cell-free extract. In some experiments, crude cell-free extract (15 mL) was stirred

with charcoal (100 mg) for 30 min under a nitrogen atmosphere and centrifuged (38700g, 20 min).

All subsequent steps were performed at 4°C, and centrifugations were done at 30,000g for 20 min. Protamine sulfate (8 mL, 1% solution, Sigma Chemical Co.) was added dropwise over 15 min to supernatant (15 mL) stirred under a nitrogen atmosphere. Stirring was continued for 10 min, and the mixture was centrifuged. Solid ammonium sulfate was added to the supernatant (19.5 mL). The precipitate that formed between 45 and 80% saturation was collected by centrifugation, resuspended in potassium phosphate buffer (4 mL, 50 mM, pH 7.4) containing dithiothreitol (5 mM), and stored at -15°C.

The ammonium sulfate precipitate dissolved in potassium phosphate buffer as prepared above (4 mL) was applied to a Sephadex G-150 column (2.5 × 50 cm) preequilibrated in potassium phosphate buffer (50 mM, pH 7.4) containing dithiothreitol (2 mM) and DL-glutamate (1 mM). Fractions (3.8 mL) eluted from the column with the same buffer were collected at 0.4 mL/min flow rate, and their uv absorbance was measured at 254 and 280 nm. The data for construction of the standard curve for molecular mass calculations was collected under identical conditions except that the ammonium sulfate precipitate was replaced with a mixture of either blue dextran (0.3 mg), alcohol dehydrogenase (4.4 mg), and carbonic anhydrase (3.0 mg) or blue dextran (2.0 mg), bovine serum albumin (1.8 mg), and cytochrome C (1.1 mg) dissolved in the same buffer (1 mL).

## **5.9 Enzyme Assays**

### **5.9.1 General Conditions**

Crude or partially purified cell-free extract supplemented with substrate and cofactors was incubated at 30°C. Samples (100 µL) taken from the incubation mixture were heated for 30 s at 130°C in a sand bath to inactivate enzymes and centrifuged (15,400g, 10 min). The supernatant was diluted with water and stored at -15°C for hplc analysis.

### **5.9.2 Catabolism of D- and L-Glutamate**

A mixture of crude cell-free extract (1.2 mL), potassium phosphate buffer (50 mM, pH 7.4), and either D- or L-glutamate (10 mM) in a total volume of 1.5 mL was incubated under a nitrogen atmosphere, and samples were analyzed by hplc. <sup>13</sup>C nmr spectroscopy was used to monitor a mixture of crude cell-free extract (700 µL), L-[4-<sup>13</sup>C]glutamate (7.6 mM), o-phenanthroline (0.5 mM), and deuteriated water (100 µL, Stohler Isotope Chemicals, Waltham, MA, USA) in a total volume of 950 µL. The <sup>13</sup>C nmr spectra were acquired over a period of 4 h on a Bruker AC 250F spectrometer operating at 62.9 MHz using 16k data points in a 10 kHz spectral window. The number of scans ranged from 120 to 240, and the FID data were processed using a line broadening of 1 Hz.

### **5.9.3 Glutamate Mutase and 3-Methylaspartase**

Mesaconate was incubated with ammonium sulfate precipitate prepared

either from crude or charcoal-treated, partially purified cell-free extract (480  $\mu$ L) was incubated with non-intrinsic factor (300 units, Sigma Chemical Co.), *o*-phenanthroline (0.5 mM),  $\text{NH}_4\text{Cl}$  (25 mM), mesaconate (10 mM), and potassium phosphate buffer (pH 7.4, 50 mM) to a total volume of 1.2 mL. Samples were removed periodically to monitor the formation of methylaspartate and glutamate by hplc.

An increase in absorbance at 240 nm corresponding to the formation of mesaconate from *L-threo*-3-methylaspartate (143) was used to measure 3-methylaspartase activity eluted from the Sephadex G-150 column. The reaction mixture (1.0 mL) contained *DL-threo*-3-methylaspartate (10.8 mM), KCl (10 mM),  $\text{MgCl}_2$  (1 mM), ethanolamine (50 mM, pH 9.7), and partially purified cell-free extract (100  $\mu$ L).

#### 5.9.4 Glutamate Racemase

A reaction mixture (0.5 mL) containing charcoal-treated, partially purified cell-free extract (200  $\mu$ L), *o*-phenanthroline (0.5 mM), either D- or L-glutamate (11.0 and 10.8 mM, respectively), and potassium phosphate buffer (50 mM, pH 7.4) was incubated under a nitrogen atmosphere. Samples were removed periodically for normal and chiral hplc analysis. To test the effect of cofactors on racemase activity, the above incubation was repeated with the addition of either FMN,  $\text{NAD}^+$ ,  $\text{NADP}^+$ , or pyridoxal phosphate (1 mM each) to a reaction mixture containing D-glutamate (10 mM), ammonium sulfate precipitate (200  $\mu$ l), non-intrinsic factor (50

unit), *o*-phenanthroline (0.5 mM), and potassium phosphate buffer (pH 7.4, 50 mM).

The racemase activity in cells grown on peptone medium containing either D- or L-glutamate was assessed in the reaction mixture as described above except that the ammonium sulfate precipitate was replaced by the one obtained from its respective liquid culture. Samples were removed at 0.5, 1, 2, and 3.25 h after incubation at 32°C under nitrogen. A blank containing all components except glutamate was also included.

To monitor the racemase reaction by  $^1\text{H}$  NMR spectroscopy, potassium phosphate buffer (71 mM, pH 7.4, 1 mL), containing DTT (1.2 mM), *o*-phenanthroline (0.7 mM), and D-glutamate (14 mM) was dried *in vacuo*. The residue was redissolved in  $\text{D}_2\text{O}$  (1 mL) and dried three times. The final residue was dissolved in  $\text{D}_2\text{O}$  (1 mL). Ammonium sulfate precipitate dissolved in deuteriated buffer (200  $\mu\text{L}$ ) was added to a portion of this solution (0.5 mL) and the mixture was incubated in the nmr tube at ambient temperature.  $^1\text{H}$  nmr spectra were recorded after 0, 15, and 48 h with a Bruker AC 250F spectrometer operating at 250 MHz.

#### **5.9.5 Glutamate Dehydrogenase (2)**

Glutamate dehydrogenase activity was assayed by following the changes in absorbance at 340 nm (14). The reaction mixture (1.0 mL) contained either D- or L-glutamate (4 mM),  $\text{NAD}^+$  (1 mM), Tris-HCl (pH 8.5, 100 mM), and either crude

(200  $\mu$ L) or partially purified (100  $\mu$ L) cell-free extract.

#### **5.9.6 D-Amino Acid Transaminase**

A reaction mixture (0.5 mL) containing DL-alanine (25 mM), 2-oxoglutarate (4 mM), o-phenanthroline (0.5 mM), and crude cell-free extract (375  $\mu$ L) was incubated for 1 h, heated in boiling water (3 min), centrifuged and the supernatant was used for hplc analysis. Under identical conditions, DL-alanine was replaced with either D-aspartate, L-aspartate, or DL-phenylalanine. Two blanks either lacking the amino acid or both the amino acid and 2-oxoglutarate were also included.

## References

1. P.N. Levett. *Anaerobic Bacteria, A Functional Biology*, Open University Press, Milton Keynes, Philadelphia. **1990**.
2. S.E. Gharbia, and H.N. Shah. *J. Gen. Microbiol.*, **1991**, *137*, 1201-1206.
3. M.J. McInerney. Anaerobic hydrolysis and fermentation of fats and proteins. *In Biology of Anaerobic Microorganisms. Edited by A.J.B. Zehnder*. John Wiley and Sons, New York. **1988**. pp. 373-445.
4. K. Ring. *Angew. Chem. Int. Ed. Engl.*, **1970**, *9*, 345-356.
5. P. Truffa-Bachi and G.N. Cohen. *Annu. Rev. Biochem.*, **1973**, *42*, 113-134.
6. M. Iaccarino, J. Guardilo, and M. De Felice. *In Microorganisms and Nitrogen Sources, Edited by J.W. Payne*, John Wiley and Sons Ltd., **1980**, p. 136.
7. A.I. Bolstad, H.B. Jensen, and V. Bakken. *Clin. Microbiol. Rev.*, **1996**, *9*, 55-71.
8. H.C. Jackins and H.A. Barker. *J. Bacteriol.*, **1951**, *16*, 101-114.
9. W.J. Loesche and R.J. Gibbons. *Archs. Oral Biol.*, **1968**, *13*, 191-201.
10. V. Bakken, B.T. Høgh, and H.B. Jensen. *Scand. J. Dent. Res.*, **1989**, *97*, 43-53.
11. S.E. Gharbia and H.N. Shah. *Curr. Microbiol.*, **1989**, *18*, 189-193.
12. J.L. Zink, and S.S. Socransky. *Oral Microbiol. Immunol.*, **1990**, *5*, 172-174.
13. A.H. Rogers, P.S. Zlim, N.J. Gully, A.L. Pfenning, and P.D. Marsh. *Oral Microbiol. Immunol.*, **1991**, *6*, 250-255.
14. S.E. Gharbia, H.N. Shah, and S.G. Welch. *Curr. Microbiol.*, **1989**, *19*, 231-235.
15. S.E. Gharbia and H.N. Shah. *Oral Microbiol. Immunol.*, **1991**, *6*, 264-269.

16. Y. Izumi, I. Chibata, and T. Itoh. *Angew. Chem. Int. Ed. Engl.*, **1978**, *17*, 176-183.
17. J. Crosby. Chirality in Industry, An Overview. The Commercial Manufacture and Application of Optically Active Compounds. *In Chirality in Industry. Edited by A.N. Collins, G.N. Sheldrake, and J. Crosby.* John Wiley and Sons, Chichester, West Sussex, England. **1992**. pp. 1-66.
18. R.M. Williams. Synthesis of Optically Active  $\alpha$ -Amino Acids, Pergamon Press, Oxford, England. **1989**.
19. I. Ojima, N. Clos, and C. Bastos. *Tetrahedron*, **1989**, *45*, 6901-6939.
20. A.N. Glazer and H. Nikaido. Microbiology Biotechnology, Fundamentals of Applied Microbiology. W.H. Freeman and Company, New York, **1995**, p. 397.
21. L. Eggeling. *Amino Acids*, **1994**, *6*, 261-272.
22. T. Tosa and T. Shibatani. *Ann. N.Y. Acad. Sci.*, **1995**, *750*, 364-375.
23. S. Yamada, H. Maeshima, M. Wada, and I. Chibata. *Appl. Microbiol.*, **1973**, *25*, 636-640.
24. N. Nakajima, K. Tanizawa, H. Tanaka, and K. Soda. *J. Biotechnol.*, **1988**, *80*, 243-248.
25. F. Hasumi, K. Fukuoka, S. Adachi, Y. Miyamoto, and I. Okura. *Appl. Biochem. Biotechnol.*, **1996**, *56*, 341-344.
26. L. Pasteur. *C.R. Hebd. Seances Acad. Sci.*, **1858**, *46*, 615-618.
27. M. Senuma, O. Otsuki, N. Sakata, M. Furui, and T. Tosa. *J. Ferment. Bioeng.*, **1989**, *67* (4), 233-237.
28. I. Umemura, K. Yanagiya, S. Komatsubara, T. Sato, and T. Tosa. *Appl. Microbiol. Biotechnol.*, **1992**, *36*, 722-726.
29. Y. Chang and S.C. Massey. *Prep. Biochem.*, **1980**, *10* (2), 215-217.
30. M. Yagasaki, A. Ozaki, and Y. Hashimoto. *Biosci. Biotech. Biochem.*, **1993**, *57*, 1499-1502.

31. M. Yagasaki, M. Azuma, S. Ishino, and A. Ozaki. *J. Ferment. Bioeng.*, **1995**, 79, 70-72.
32. M.E. Foppen, F. van Rantwijk, L. Maat, and A.P.G. Kieboom. *Recl. Trav. Chim. Pays-Bas*, **1989**, 108, 424-425.
33. N. Nakajima, N. Esaki, and K. Soda. *J. Chem. Soc., Chem. Commun.*, **1990**, 947-948.
34. Meeting Briefs from New Orleans. *C&EN*, **1996**, p. 32.
35. C.M. Rosell, R. Fernandez-Lafunte, and J.M. Guisan. *Ann. N.Y. Acad. Sci.*, **1995**, 750, 425-428.
36. A. Ozaki, H. Kawasaki, M. Yagasaki, and Y. Hashimoto. *Biosci. Biotech. Biochem.*, **1992**, 56, 1980-1984.
37. R. Grifantini, G. Frascotti, G. Galli, and G. Grandi. *Eur. Pat. Appl. EP 677,585*, **1995**; *Chem. Abst.*, **1996**, 124, 7179c.
38. G. Kim and H. Kim. *Ann. N.Y. Acad. Sci.*, **1995**, 750, 185-189.
39. D. Volkel and F. Wagner. *Ann. N.Y. Acad. Sci.*, **1995**, 750, 1-9.
40. K. Drauz, M. Kottenhahn, K. Makryaleas, H. Klenk, and M. Bernd. *Angew. Chem. Int. Ed. Engl.*, **1991**, 30 (6), 712-714.
41. O. Keil, M.P. Schneider, and J.P. Rasor. *Tetrahedron: Asymmetry*, **1995**, 6, 1257-1260.
42. H.A. Barker. Fermentation of Nitrogenous Compounds. *In The Bacteria. Edited by I.C. Gunsalus and R.Y. Stanier*, 2nd ed., New York, Academic Press, **1961**, pp. 151-207.
43. L. Pine and H.A. Barker. *J. Bacteriol.*, **1954**, 68, 216.
44. H.A. Barker. Bacterial Fermentations. CIBA Lectures in Microbiology and Biochemistry. John Wiley and Sons, Inc., NY, **1956**.
45. G.M. Smith, B.W. Kim, A.A. Franke, and J.D. Roberts. *J. Biol. Chem.*, **1985**, 260, 13509-13512.
46. R.A. Wolff, G.W. Urben, S.M. O'Herrin, and W.R. Keneary. *Appl. Environ. Microbiol.*, **1993**, 59, 1876-1882.

47. G. Wohlfarth and W. Buckel. *Arch. Microbiol.*, **1985**, *142*, 128-135.
48. H.A. Barker, J.M. Kahn, and L. Hendrick. *J. Bacteriol.*, **1982**, *152* (1), 201-207.
49. G.N. Bennett and F.B. Rudolph. *FEMS Microbiol. Rev.*, **1995**, *17*, 241-249.
50. J.T. Wachsman and H.A. Barker. *J. Biol. Chem.*, **1955**, *217*, 695-702.
51. J.T. Wachsman. *J. Biol. Chem.*, **1956**, *223*, 19-27.
52. A. Munch-Petersen and H.A. Barker. *J. Biol. Chem.*, **1958**, *230*, 649-653.
53. C.C. Wang and H.A. Barker. *J. Biol. Chem.*, **1969**, *244*, 2516-2526.
54. A.H. Blair and H.A. Barker. *J. Biol. Chem.*, **1966**, *241*, 400-408.
55. C.C. Wang and H.A. Barker. *Meth. Enzymol.*, **1969**, *13*, 331-344.
56. H.A. Barker. *Meth. Enzymol.*, **1969**, *13*, 344-346.
57. W. Buckel and A. Bobi. *Eur. J. Biochem.*, **1976**, *64*, 255-262.
58. H.A. Barker, R.D. Smyth, E.J. Wawaszkievicz, M.N. Lee, and R.M. Wilson. *Arch. Biochem. Biophys.*, **1958**, *78*, 468-476.
59. H.A. Barker, R.D. Smith, R.M. Wilson, and H.W. Weissbach. *J. Biol. Chem.*, **1959**, *234*, 320-328.
60. N.P. Botting, M. Akhtar, M.A. Cohen, and D. Gani. *Biochemistry*, **1988**, *27*, 2953-2955.
61. N.P. Botting, M.A. Cohen, M. Akhtar, and D. Gani. *Biochemistry*, **1988**, *27*, 2956-2959.
62. N.P. Botting and D. Gani. *Biochemistry*, **1992**, *31*, 1509-1520.
63. S.K. Goda, N.P. Minton, N.P. Botting, and D. Gani. *Biochemistry*, **1992**, *31*, 10747-10756.
64. H.J. Bright and L.L. Ingraham. *Biochim. Biophys. Acta*, **1960**, *44*, 586-588.

65. Y. Asano and Y. Kato. *FEMS Microbiol. Lett.*, **1994**, *118*, 255-258.
66. H.A. Barker, H. Weissbach, and R.D. Smyth. *Proc. Natl. Acad. Sci.*, **1958**, *44*, 1093-1097.
67. F. Suzuki, and H.A. Barker. *J. Biol. Chem.*, **1966**, *241*, 878-888.
68. U. Leutbecher, R. Bocher, D. Linder, and W. Buckel. *Eur. J. Biochem.*, **1992**, *205*, 759-765.
69. D.E. Holloway and E.N.G. Marsh. *J. Biol. Chem.*, **1994**, *39*, 20425-20430.
70. D.E. Holloway and E.N.G. Marsh. *FEBS Lett.*, **1993**, *317*, 44-48.
71. M. Brecht, J. Kellermann, and A. Plucktham. *FEBS Lett.*, **1993**, *319*, 84-89.
72. O. Zelder, B. Beatrix, and W. Buckel. *FEMS Microbiol. Lett.*, **1994**, *118*, 15-22.
73. H.R. Whiteley. *J. Bacteriol.*, **1957**, *74*, 324-330.
74. D.F. Horler, D.W.S. Westlake, and W.B. McConnell. *Can. J. Microbiol.*, **1966**, *12*, 47-52.
75. W. Buckel and H.A. Barker. *J. Bacteriol.*, **1974**, *117*, 1248-1260.
76. M.A. Foglesong, D.L. Cruden, and A.J. Markovetz. *J. Bacteriol.*, **1984**, *158*, 474-480.
77. D.F. Horler, W.B. McConnell, and D.W.S. Westlake. *Can. J. Microbiol.*, **1966**, *12*, 1247-1252.
78. W.M. Johnson and D.W.S. Westlake. *Can. J. Microbiol.*, **1969**, *47*, 1103-1107.
79. W.M. Johnson and D.W.S. Westlake. *Bacteriol. Proc.*, **1970**, *P196*, p. 153.
80. R. Lerud and H.R. Whiteley. *Bacteriol. Proc.*, **1970**, *P197*, p. 153

81. O.M. Kew and C.A. Woolfolk. *Biochem. Biophys. Res. Comm.*, **1970**, *39*, 1129-1133.
82. R.F. Lerud and H.R. Whiteley. *J. Bacteriol.*, **1971**, *106*, 571-577.
83. S.E. Gharbia and H.N. Shah. *FEMS Microbiol. Lett.*, **1991**, *80*, 283-288.
84. D.W. Rice, D.P. Hornby, and P.C. Engel. *J. Mol. Biol.*, **1985**, *181*, 147-149.
85. W. Buckel. *Eur. J. Biochem.*, **1980**, *106*, 439-447.
86. G. Schweiger and W. Buckel. *Arch. Microbiol.*, **1984**, *137*, 302-307.
87. A. Klees, D. Linder, and W. Buckel. *Arch. Microbiol.*, **1992**, *158*, 294-301.
88. W. Buckel, U. Dorn, and R. Semmler. *Eur. J. Biochem.*, **1981**, *118*, 315-321.
89. W. Buckel and R. Semmler. *Eur. J. Biochem.*, **1983**, *136*, 427-434.
90. W. Buckel. *Eur. J. Biochem.*, **1986**, *156*, 259-263.
91. B. Beatrix, K. Bendrat, S. Rospert, and W. Buckel. *Arch. Microbiol.*, **1990**, *154*, 362-369.
92. K. Bendrat and W. Buckel. *Eur. J. Biochem.*, **1993**, *211*, 697-702.
93. J.K. Hardman and T.C. Stadtman. *J. Biol. Chem.*, **1963**, *238*, 2081-2087.
94. J.K. Hardman and T.C. Stadtman. *J. Biol. Chem.*, **1963**, *238*, 2088-2093.
95. J. Hardman. *Meth. Enzymol.*, **1962**, *5*, 778-783.
96. U. Scherf and W. Buckel. *Appl. Environ. Microbiol.*, **1991**, *57*, 2699-2702.
97. R.G. Bartsch and H.A. Barker. *Arch. Biochem. Biophys.*, **1961**, *92*, 122-132.
98. P. Willadsen and W. Buckel. *FEMS Microbiol. Lett.*, **1990**, *70*, 187-192.
99. G.C. Mead. *J. Gen. Microbiol.*, **1971**, *67*, 47-56.
100. W. Buckel. *Arch. Microbiol.*, **1980**, *127*, 167-169.

101. H.A. Barker, R.M. Wilson, and A. Munch-Petersen. *Federation Proceeding*, **1957**, 16, 151.
102. W.E.C. Moore, L.V. Holdeman, and R.W. Kelley. *In Bergey's Manual of Systematic Bacteriology*, 9th edn., Edited by N.R. Krieg, and J.C. Holt. William and Wilkins, Baltimore, USA. 1984. pp. 631-637.
103. H.L. Ritz. *Archs. Oral Biol.*, **1967**, 12, 1561-1568.
104. D.J. Hentges. *In Anaerobic Infections in Humans*, Edited by S.M. Finegold, and W.L. George, Academic Press, Inc., San Diego, California. **1989**. p. 43.
105. P.E. Kolenbrander and J. London. *J. Bacteriol.*, **1993**, 175, 3247-3252.
106. P.M. Bartold, N.J. Gully, P.S. Zilm, and A.H. Rogers. *J. Periodont. Res.*, **1991**, 26, 314-322.
107. R.E. Singer and B.A. Buckner. *Infect. Immun.*, **1981**, 32, 458-463.
108. S.A. Robrish, C. Oliver, and J. Thompson. *J. Bacteriol.*, **1987**, 169, 3891-3897.
109. D.L. Singer and I. Kleinberg. *Arch. Oral Biol.*, **1983**, 28, 873-878.
110. R.L. White, A.C. DeMarco, and K.C. Smith. *J. Chromatogr.*, **1989**, 483, 437-442.
111. R.L. White, K.C. Smith, and A.C. DeMarco. *Can. J. Chem.*, **1934**, 72, 1645-1655.
112. E. Grushka, H.D. Durst, and E.J. Kikta. *J. Chromatogr.*, **1975**, 112, 673-678.
113. A.L. Stockburn and C.W. Thomas. *Org. Mass Spectrom.*, **1974**, 9, 1027-1038.
114. H.N. Shah. Private communication.
115. H.A. Barker, F. Suzuki, A. Iodice, and V. Rooze. *Ann. N.Y. Acad. Sci.*, **1964**, 112, 644-660.
116. F.D. Warren, J.J. Scholz, and R.B. Johnston. *Biochim. Biophys. Acta*, **1963**, 85, 322-332.

117. G.J. Cardinale and R.H. Abeles. *Biochemistry*, **1968**, *7*, 3970-3978.
118. K.A. Gallo and J.R. Knowles. *Biochemistry*, **1993**, *32*, 3981-3990.
119. A.H. Roger, W.J. Gully, A.L. Pfennig, and P.S. Zilm. *Oral Microbiol. Immunol.*, 1992, *7*, 299-303.
120. T.C. Stadtman. In *Advances in Enzymology*. Edited by A. Meister. An Interscience Publication. **1973**, *38*, pp. 413-449.
121. D. Dupourque, W.A. Newton, and E.E. Snell. *J. Biol. Chem.*, **1966**, *241*, 1233-1238.
122. J.E. Carter and R.D. Sagers. *J. Bacteriol.*, **1972**, *109*, 757-763.
123. E. Takahashi, K. Nakamichi, M. Furui, and T. Mori. *J. Ferment. Bioeng.*, **1995**, *79*, 439-442.
124. C.I. Pogson and R.G. Wolfe. *Biochem. Biophys. Res. Commun.*, **1972**, *46*, 1048-1054.
125. C.H. Archer and D. Gani. *J. Chem. Soc., Chem. Commun.*, **1993**, 140-142.
126. H.A. Barker, V. Rooze, F. Suzuki, and A.A. Iodice. *J. Biol. Chem.*, **1964**, *239*, 3260-3266.
127. L. Glaser. *J. Biol. Chem.*, **1960**, *235*, 2095-2098.
128. N. Nakajima, K. Tanizawa, H. Tanaka, and K. Soda. *Agric. Biol. Chem.*, **1988**, *52*, 3099-3104.
129. M. Martinez-Carrion and W.T. Jenkins. *J. Biol. Chem.*, **1965**, *240*, 3538-3546.
130. M.J. Pucci, J.A. Thanassi, H.T. Ho, P.J. Falk, and T.J. Dougherty. *J. Bactriol.*, **1995**, *177*, 336-342.
131. K.A. Gallo, M.E. Tanner, and J.R. Knowles. *Biochemistry*, **1993**, *32*, 3991-3997.
132. T. Yoshimura, M. Ashiuchi, N. Esaki, C. Hobatake, S-Y. Choi, and K. Soda. *J. Biol. Chem.*, **1993**, *268*, 24242-24246.

133. Y.H. Li and G.H. Bowden. *Oral Microbiol. Immunol.*, **1994**, 9, 1-11.
134. S. Lam. *J. Chromatogr.*, **1986**, 355, 157-164.
135. M. Bodanszky and G.G. Marconi. *J. Antibiotics*, **1970**, 23, 238-241.
136. H. King. *Org. Synth., Collect. Vol. 1*, **1941**, 286-288.
137. R.L. White, M. Ramezani, S.E. Gharbia, R. Seth, A.L. Doherty-Kirby, and H.N. Shah. *Biotechnol. Appl. Biochem.*, **1995**, 22, 385-396.
138. L.M. Harwood. *Aldrichim. Acta*. **1985**, 18, 25.
139. W.L. Judofind and E.E. Reid. *J. Am. Chem. Soc.*, **1920**, 42, 1043-1055.
140. J.L.E. Erickson, J.M. Dechary, and M.R. Kesling. *J. Am. Chem. Soc.*, **1951**, 73, 5301-5302.
141. C.R. Hutchinson, A.H. Heckendrof, J.L. Straughn, P.E. Daddona, and D.E. Cane. *J. Am. Chem. Soc.*, **1979**, 101, 3358-3369.
142. J.H. Beynon and A.E. Williams. *Mass and Abundance Tables for Use in Mass Spectrometry*, Elsevier, Amsterdam, **1963**.
143. M.W. Hsiang and H.J. Bright. *Methods in Enzymol.*, **1969**, 13, 347-353.